MOLECULAR SPECTROSCOPIC PROPERTIES IN THE RELATIVISTIC COUPLED CLUSTER FRAMEWORK

Thesis submitted to AcSIR for the award of
the degree of
DOCTOR OF PHILOSOPHY
in Chemical Sciences

By

Sudip Sasmal
Registration Number: 10CC12A26012

Under the guidance of

Dr. Nayana Vaval
(Research Supervisor)

&

Prof. Sourav Pal
(Research Co-supervisor)

Physical and Materials Chemistry Division
CSIR-National Chemical Laboratory
Pune 411 008

December 2016

सीएसआयआर–राष्ट्रीय रासायनिक प्रयोगशाला
(वैज्ञानिक तथा औद्योगिक अनुसंधान परिषद)
डॉ. होमी भाभा मार्ग, पुणे – 411 008. भारत
CSIR-NATIONAL CHEMICAL LABORATORY
(Council of Scientific & Industrial Research)
Dr. Homi Bhabha Road, Pune - 411008. India

Certificate

This is to certify that the work incorporated in this Ph.D. thesis entitled **"Molecular Spectroscopic Properties in the Relativistic Coupled Cluster Framework"** submitted by **Sudip Sasmal** to Academy of Science and Innovative Research (AcSIR) in fulfillment of the requirements for the award of the degree of **Doctor of Philosophy in Chemical Sciences**, embodies original research work under my supervision. I further certify that this work has not been submitted to any other University or Institution in part or full for the award of any degree or diploma. Research material obtained from other sources has been duly acknowledged in the thesis. Any text, illustration, table, etc., used in the thesis from other sources, have been duly cited and acknowledged.

Sudip Sasmal
Sudip Sasmal
(Student)

N. Vaval
Dr. Nayana Vaval
(Supervisor)

Prof. Sourav Pal
(Co-supervisor)

Date: 21.12.2016

Place: CSIR-NCL, Pune

Communications Channels
NCL Level DID : 2590
NCL Board No. : +91-20-25902000
Four PRI Lines : +91-20-25902000
FAX
Director's Office : +91-20-25902601
COA's Office : +91-20-25902660
SPO's Office : +91 20 25902664
WEBSITE
www.ncl-india.org

DECLARATION

I hereby declare that the thesis entitled **"Molecular Spectroscopic Properties in the Relativistic Coupled Cluster Framework"** submitted for the degree of Doctor of Philosophy in Chemical Sciences to the Academy of Scientific & Innovative Research (AcSIR), has been carried out by me at the Physical Chemistry Division of CSIR-National Chemical Laboratory, Pune under the supervision of Dr. Nayana Vaval and Prof. Sourav Pal. Such material as has been obtained by other sources has been duly acknowledged in the thesis. The work is original and has not been submitted in part or full by me for any other degree or diploma to any other Institution or University.

Date: 21·12·2016

Place: CSIR-NCL, Pune

Sudip Sasmal.

Sudip Sasmal
Ph. D candidate

To
my family

Acknowledgements

Knowledge is in the end based on acknowledgement.

Ludwig Wittgenstein

A great number of distinguished personalities, directly or indirectly, have contributed and extended their valuable support in this study. They, thankfully, have also made me realize that it is the journey that is important, not the end result. It is indeed a pleasure to convey my sincere gratitude and thanks to all of them, and a few are enumerated.

First of all, I am extremely grateful to my research supervisor, Dr. Nayana Vaval for her valuable guidance, scholarly inputs and continuous encouragement I received throughout my research carrier. I believe that the real education makes a person simple, polite and respectful and she is the reason I believe that.

I specially want to acknowledge my co-supervisor, Prof. Sourav Pal, for giving me the opportunity to be a part of his group. With other so many qualities, he has been an excellent teacher. I wish to be a teacher like him; at least a few percentage would be enough. I also want to thank him for his academic freedom to promote independent thinking, without putting any obligation to my work.

No words can express my appreciation to Dr. Malaya K. Nayak. I was worried about my decision to join an alien field, where things were new to me. Dr. Nayak came to my rescue with his intelligent ideas, thought provoking discussions and comprehensive understanding to help me sail through the initial fumbling. His collaboration made it possible to extend the coupled cluster method in the relativistic domain which is the cornerstone of this thesis.

I deeply acknowledge Himadri da for his contribution in this thesis and also in my life. He is my senior but I never feel it that way. I have done all of my thesis work with him. Without his correlating ideas, serendipitous observations and converting them into new possibilities, this thesis would not have seen the light of the day. He transformed an average M. Sc. student to an almost independent researcher. I'll never find words to tell what I owe to him, and if I start doing it, I would not know where to stop ... thanks for everything Himu da. I wouldn't wish you "best

of luck" for your future as I don't believe in luck. And I know you don't need luck for that; you already have all the ingredients to become successful in your life.

I want to acknowledge my DAC members Dr. Debashree Ghosh, Dr. Kumar Vanka and Dr. Pankaj Poddar for helping me throughout my Ph. D. carrier. I want to thank Dr. Ashish Orpe, Dr. T. G. Ajithkumar, Dr. Nayana Vaval, Dr. Kumar Vanka, Dr. Durba Sengupta and Dr. Kavita Joshi for their teaching in the course work.

I will take delight in recognizing all my past and present lab-mates Sumantra da, Deepti di, Gupta ji, Achintya da, Mudit da, Debarati di, Aryya da, Kamalika di, Susanta da, Manzoor, Madhulita di, Vidhika di, Saba di, Anagha, Turbasu, Deepak, Samik, Kaushik, and other theoretical group members Ashish da, Tiwari ji, Prathit da, Amrita di, Shantanu da, Sneha, Jaya, Nisha, Manoj (Mamu), Jugal, Yuvraj, Subhrashis, Tamal, Vipin, Shailja, Baljinder, Rahul, Paulami, Mukunda, Collins, Amit, Neharika, Vrushali, Pragati, Santu da, Subhadip da, Prithvi da, Chandan da, Swagata di, Souvik da, Anil, Sujit da, Manoj da, Atreyee di, Sayantan, Ujjwal for creating a nice working environment.

I specially want to acknowledge Turbasu for helping me throughout this journey. Whenever I found any technical difficulty, I knew whom to approach and he never disappointed me.

My stay in the campus has been pleasant with the association of all the research scholars at CSIR-NCL. I am thankful to Partha da, Mrinmoy da, Tamas da, Arpan da, Kanak da, Anjan da, Saikat da, Pravat da, Pati da, Binay da, Shyam da, Sajal da, Munmun di, Abhik da, Souvik da, Doss da, Prithvi da, Ramkrishna da, Sujit da, Garai da, Basab da, Prathit da, Anup da, Soumen da, Santu da, Sudhangsu da, Satya da, Prasenjit da, Arunava da, Hridesh da, Arijit da, Bikash, Shantigopal, Shiba, Abhijit, Subhrashis, Tamal, Debu, Tapas, Bilu, Manzoor, Mohitosh, Suvendu, Anirban, Sutanu, Piyali, Rupa. I want to acknowledge Mrinmoy da and Anup da for helping me to settle down in Pune at the initial stage of my Ph. D. I want to thank Sumantra da for teaching me to ride bike and also at the same time to appreciate the environmental beauty while riding it.

I'll always cherish the fun time with the "Weekend Party Group". My staying in the New Hostel (not so brand!) is one of the best thing happened in Pune; it minimized my homesickness feeling. For this, I am thankful to Santanu, Atanu, Suman, Manojit, Suman, Manik, Atreyee di, Manoj da, Monalisa di, Chayanika di, Sujit da, Bittu, Gablu da, Sayantan, Surajit (Meso), Chanchal (Vaipo).

I am going to miss all the “bawal”, gossips, discussions we used to do in our special seating place beside the mess. I specially want to acknowledge Atreyee di for understanding my stress, frustration, and anger and for being so kind, helpful and motivating to me. For the last two years, she has always been there for me with her sisterly hand whenever I needed it the most. I thank you for taking care of me as your little brother and wish you all the success in your life.

I would like to acknowledge my other friends for their moral support and motivation, which drive me to give my best. Sourav, Saptarshi, Atanu (Lama), Arnab, Ashta da, Atin, Tuhin, Ipsita, Kalyan, Kousik, Suman, ... the list is endless ... thanks to one and all. I want to specially thank Atanu (Acharya) da. He is one of the reason I chose quantum mechanics as my carrier path. I would like to acknowledge Soumitra and Nibedita for staying by my side in all the highs and lows of my life. Any words of appreciation will be less to describe your influence for shaping my life the way it is now. And I know that I’ll need you more than ever in the next and all the following states of my life.

Of course, many names were missed in the process, some by mistake and some by deliberation! It does not necessarily mean that they did not play any part in this journey. Let them occupy the space in my mind.

My acknowledgement will never be complete without the special mention of my teachers who shaped my academic life. Arunava Bera is the first teacher who introduced me to the modern science in the very early stage of my study life. Dr. Arun Maity is not only a good teacher but also a great human being. Without his help, I cannot become what I am now. He not only shows confidence in me but also broadens my academic visualization. I thank Prof. N. Chandrakumar for his inspiration as a researcher and as a teacher.

I acknowledge the Council of Scientific and Industrial Research (CSIR), Government of India for providing me with the necessary funding and fellowship to pursue research at NCL.

Finally, I would like to acknowledge the people who mean the world to me, my parents. I deeply acknowledge for their prayerful wishes for my well being and their sacrifices for me. Although they do not perceive what precisely I do, they are much more satisfied than me with the fruitful exploration of my work. I want to acknowledge my sister, brother-in-law and niece for their love, affection and encouragement in my professional and personal life. I want to acknowledge my

uncle (Kaku), aunt (Masi) and cousins (Pupu and Rupu) for their sacrifice, love and encouragement in my life. I want to thank my grand father, uncle (Jethu), aunt (Jethima), cousins (Borda and Chorda) sister-in-law (Boudi), and niece (Piklu and Mimi) for their love and good wishes. I specially want to acknowledge Bula da, Boudi and their family for their influence in my life. I want to acknowledge all other family members for their support.

I conclude by few lines from C. P. Cavafy's "Ithaka"

As you set out for Ithaka
hope your road is a long one,
full of adventure, full of discovery.
...
Arriving there is what you're destined for.
But don't hurry the journey at all.
Better if it lasts for years,
so you're old by the time you reach the island,
wealthy with all you've gained on the way,
not expecting Ithaka to make you rich.
...
And if you find her poor, Ithaka won't have fooled you.
Wise as you will have become, so full of experience,
you'll have understood by then what these Ithakas mean.

Sudip

Contents

List of Tables

Abstract

The shape of electron or to be more specific, the electric dipole moment of electron (eEDM) has a great importance in physics as it can explain some of the well known mysteries of fundamental physics like matter-antimatter asymmetry in our universe. The best known theory till date [standard model (SM) of elementary particles] is unable to explain this asymmetry as it treats both particle and antiparticle exactly in the same way. Therefore, the search for eEDM can explore the physics beyond the SM. However, the deviation of the shape of the electron from perfect roundness or the value of eEDM has to be very small. This smallness restricts us to do experiments with single electron as the highest electric field generated by today's technology is not large enough to observe any eEDM effect. So, we are bound to do experiments with atoms or molecules where we can use the internal electric filed generated by the heavy nucleus. Heavy hetero-diatomic molecules are very promising candidate for the eEDM experiment as they offers very high internal effective electric field (E_{eff}). However, E_{eff} cannot be measured by any experimental technique. So, one has to rely on a very accurate theoretical method to calculate E_{eff}, precisely. So, the accuracy of the theoretically estimated E_{eff} cannot assessed from experiments. However, the accuracy of theoretically obtained E_{eff} can be estimated by comparing theoretically obtained hyperfine structure (HFS) constants with the experimental values, because the calculation of both requires an accurate wave function in the nuclear region. However, the computation of an accurate wavefunction in the nuclear region of a heavy diatomic molecule is not a trivial task as it requires simultaneous inclusion of both the effect of special relativity and electron correlation due to the intertwined nature of these two effects. The relativistic coupled-cluster method using four-component wavefunction meets these requirements to fulfill the purpose.

The thesis deals with the implementation of various coupled-cluster methods in the relativistic framework to generate an accurate ground state wavefunction in the nuclear region and finally the calculation of various parity ($\mathcal{P}$) and time reversal invariance ($\mathcal{T}$) violating ($\mathcal{P},\mathcal{T}$-odd) properties of different heavy diatomic molecules in their ground state configuration. The thesis is organized as follows:

CHAPTER 1: The question, why the precise value of eEDM is so important, how it can explore the physics beyond standard model is being addressed in subsequent sections of the chapter. The importance of electronic structure theory in the eEDM experiment is also discussed here. In the

electronic structure theory, we have chosen the relativistic domain for the calculations and the reasons are explained here. We have also discussed the advantage of coupled-cluster method over the other various many-body method for the correlation calculation.

CHAPTER 2: As in the previous chapter, we have shown the importance of *ab initio* method for the calculation of various $\mathcal{P},\mathcal{T}$-odd interaction constants, in this chapter, we have opted for the implementation of the extended coupled-cluster (ECC) method in the relativistic framework to generate an accurate wavefunction in the nuclear region of atoms and molecules. The implemented ECC method is applied to calculate the magnetic HFS constant of alkali metals (Li, Na, K, Rb, and Cs), singly charged alkaline-earth-metals (Be^+, Mg^+, Ca^+, and Sr^+) along with parallel and perpendicular magnetic HFS constants of BeH, MgF, and CaH molecules. We have compared our ECC results with the calculations based on the restricted active space configuration interaction (RAS-CI) method. Our results are in better agreement with the available experimental values than those of the RAS-CI values.

CHAPTER 3: Although the implemented ECC method yields relatively good results for the HFS constant of atoms and molecules, it is not good enough for our purpose as the generated wavefunction is not that much accurate in the nuclear region what we need for the calculation of various $\mathcal{P},\mathcal{T}$-odd interaction constants. Further, this method is computationally very expensive to do a calculation of the relevant heavy diatomic molecules with a reasonable basis set. So, in this chapter, we opted for the implementation of Z-vector method in the relativistic coupled-cluster framework to generate an accurate wavefunction in the nuclear region as well as outer region. The implemented method is applied to calculate the molecular dipole moment and parallel component of the magnetic hyperfine-structure constant of the SrF molecule. The results of our calculation are compared with the experimental and other available theoretically calculated values. We are successful in achieving good accordance with the experimental results. We also compared the Z vector results of the HFS constants of alkali metals and singly charged alkaline-earth-metals with the results using the ECC method calculated in the previous chapter using the same basis and cutoff. The comparison shows that the Z-vector method can yields more accurate results than the ECC method. Thus, these results show that the Z-vector method can yield an accurate wave function in both the far and near nuclear region.

CHAPTER 4: In this chapter, we have employed both the Z-vector method and the expectation-value approach in the relativistic coupled-cluster framework to calculate the effective electric field (E_{eff}) experienced by the unpaired electron and the scalar-pseudoscalar (S-PS) $\mathcal{P},\mathcal{T}$-odd interaction constant (W_{s}) in the ground electronic state of RaF. As the experimental magnetic HFS constants of RaF are not available, we have calculated the magnetic HFS constants of $^{223}Ra^{+}$ and compared with the experimental values. The outcome shows that the Z-vector method is superior to the expectation-value approach. The Z-vector calculation shows that RaF has a high E_{eff} (52.5 GV/cm) and W_{s} (141.2 kHz). This makes it a potential candidate for the eEDM experiment.

CHAPTER 5: The chapter considers the calculation of E_{eff} and parallel component of HFS constant ($A_{\parallel}$) of PbF as it has some interesting characteristics, which make it a strong candidate in the search of electron EDM. We have achieved a very accurate wavefunction in the near nuclear region which is evident from our $A_{\parallel}$ values. This shows that our calculated E_{eff} value (38.1 GV/cm) is the most reliable one. The outcome of our calculations also clearly suggests that the core electrons have significant contribution to the "atom in compound" properties.

CHAPTER 6: Here, we have applied the Z-vector method in the relativistic coupled-cluster framework to calculate various $\mathcal{P},\mathcal{T}$-odd interaction constants of HgH and found that it has a very large E_{eff} (123.2 GV/cm) and W_{s} (284.2 kHz). This makes HgH a potential candidate for the next generation eEDM experiment. Our calculated parallel and perpendicular magnetic HFS constants of HgH are also in good agreement with the experiment. This shows the reliability of our final E_{eff} and W_{s} values. Further, We have derived the relationship between these quantities and the ratio which will help us to get model independent value of eEDM and S-PS interaction constant.

List of Publications

1. **S. Sasmal***, H. Pathak, M. K. Nayak, N. Vaval and S. Pal*, *Relativistic extended-coupled-cluster method for the magnetic hyperfine structure constant*, Phys. Rev. A **91**, 022512 (2015).

2. **S. Sasmal***, H. Pathak, M. K. Nayak, N. Vaval and S. Pal, *Implementation of the Z-vector method in the relativistic-coupled-cluster framework to calculate first-order energy derivatives: Application to the SrF molecule*, Phys. Rev. A **91**, 030503(R) (2015).

3. **S. Sasmal***, H. Pathak*, M. K. Nayak*, N. Vaval and S. Pal, *Calculation of P,T-odd interaction constant of PbF using Z-vector method in the relativistic coupled-cluster framework*, J. Chem. Phys. **143**, 084119 (2015).

4. **S. Sasmal***, H. Pathak*, M. K. Nayak*, N. Vaval and S. Pal, *Search for parity and time reversal violating effects in HgH: Relativistic coupled-cluster study*, J. Chem. Phys. **144**, 124307 (2016).

5. **S. Sasmal**, H. Pathak, M. K. Nayak, N. Vaval and S. Pal, *Relativistic coupled-cluster study of RaF as a candidate for parity and time reversal violating interaction*, Phys. Rev. A **93**, 062506 (2016).

6. **S. Sasmal**, K. Talukdar, M. K. Nayak, N. Vaval and S. Pal*, *Calculation of hyperfine structure constants of small molecules using Z-vector method in the relativistic coupled-cluster framework*, J. Chem. Sci. **128**, 1671 (2016).

7. H. Pathak*, **S. Sasmal**, M. K. Nayak, N. Vaval and S. Pal, *Relativistic equation-of-motion coupled-cluster method for the ionization problem: Application to molecules*, Phys. Rev. A **90**, 062501 (2014).

8. H. Pathak*, **S. Sasmal***, M. K. Nayak, N. Vaval and S. Pal, *Relativistic equation-of-motion coupled-cluster method for the electron attachment problem*, Computational and Theoretical Chemistry, **1076**, 94 (2016).

9. H. Pathak*, **S. Sasmal***, M. K. Nayak, N. Vaval and S. Pal, *Relativistic equation-of-motion coupled-cluster method using open-shell reference wavefunction: Application to ionization spectra*, J. Chem. Phys. **145**, 074110 (2016).

10. **S. Sasmal***, K. Talukdar, M. K. Nayak*, N. Vaval and S. Pal*, *Electron-nucleus scalar-pseudoscalar interaction in PbF: Z-vector study in the relativistic coupled-cluster framework*, 2016. Submitted to Molecular Physics as a special issue in honour of Prof. Debashis Mukherjee on the occasion of his 70th birthday.

CHAPTER 1

The Scope of Electronic Structure Theory in the Electric Dipole Moment Experiment of Electron

> No problem can be solved from the same level of consciousness that created it.
>
> Albert Einstein

The question, why the precise value of eEDM is so important, how it can explore the physics beyond standard model is being addressed in subsequent sections of the chapter. The importance of electronic structure theory in the eEDM experiment is also discussed here. In the electronic structure theory, we have chosen the relativistic domain for the calculations and the reasons are explained here. We have also discussed the advantage of coupled-cluster method over the other various many-body method for the correlation calculation.

1.1 Introduction

Our universe, thankfully, imparts a continuous source of mysteries, which at first give excitement and somewhat entertainment but then put us in an enigmatic state to solve those mysteries. Despite the success of the standard models (SM) of elementary particle physics and cosmology, there are a 'cosmic gaps' in our understanding of the way of our universe works. The characteristic of dark matter and dark energy, which together form almost 96% mass and energy of our universe, remains an absolute mystery. Yet there is a bewildering puzzle even within the 4% of the universe which we do claim to understand. The puzzle is about the paradox of matter-antimatter asymmetry. Equal amounts of matter and antimatter were created out of the energy after the Big Bang, but at the present time, any considerable amount of antimatter does not seem to be naturally exist anywhere in our universe [1]. So, the million dollar question remains as where all the antimatter has gone. The combination of charge conjugation ($\mathcal{C}$) and parity ($\mathcal{P}$) symmetries ($\mathcal{CP}$) violating interaction along with other factors can explain this matter-antimatter asymmetry [2]. However, the $\mathcal{CP}$ violation within the SM of electroweak and strong interaction (arising from complex quark mixing Kobayashi-Maskawa matrix) is not strong enough to explain this asymmetry [3]. Despite the fact that the SM has some well known unresolved problems and drawbacks, there is very little experimental data available which directly contradict the SM. On the other hand, there are many extensions of the SM which can resolve the flaws of the SM but the validation of the correct theory or the right step towards a "theory of everything" can only be resolve through extensive experimental findings [4–6]. Thus, the search for the violation of fundamental symmetries can explore 'beyond standard model physics' and in turn can help us to test various unification theories of particle physics [7].

1.2 The three fundamental discrete symmetries of physics: $\mathcal{C}$, $\mathcal{P}$ and $\mathcal{T}$

For a long time, it was considered that the laws of physics would be the same if we invert the space. Thus, the conservation of space inversion symmetry, parity ($\mathcal{P}$), was believed to be the symmetry

of nature. However, in 1957, the surprised discovery reveals that the $\mathcal{P}$ symmetry is violated in the radioactive β decay process [8]. Wu and co-workers found that when a particular nucleus was located in a magnetic field, emitted electrons from the β decay were preferentially radiated in the opposite direction of the angular momentum of the nucleus [8]. This situation is illustrated in

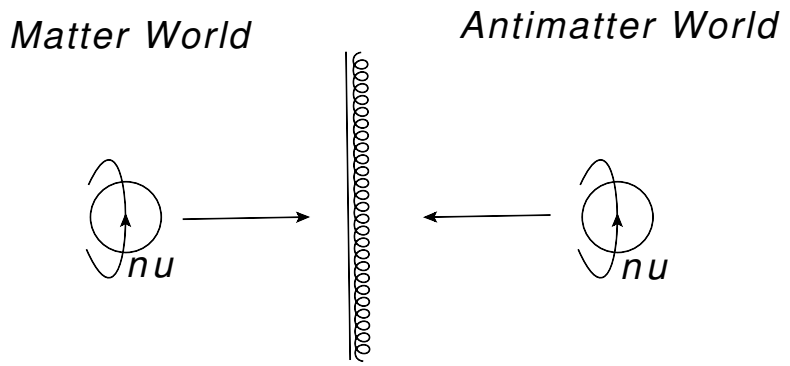

Figure 1.1: Violation of $\mathcal{P}$ symmetry

Figure 1.1. On reflection, the emitted electron (arrow) reverses its direction but the direction of rotation or the angular momentum does not change. The left hand side of the mirror represents the actual directional preferences, while its mirror image represents a directional preference that is not observed in this world. So, when an experiment can identify an object from its mirror image, $\mathcal{P}$ is not conserved. However, if somehow we can make a nucleus out of antimatter, its β decay would occur same way, except the right hand side of the mirror would represent the directional preference of the outgoing electron. In that antimatter world, the left hand side image would represent the directional preference that would not be found in nature.

So, if the mirror represents $\mathcal{CP}$ operation i.e., it not only reverses spatial direction ($\mathcal{P}$) but also transforms matter to antimatter ($\mathcal{C}$), then the image and its mirror image would look like identical. The individual violation of $\mathcal{C}$ and $\mathcal{P}$ mutually cancels each other and preserves $\mathcal{CP}$ symmetry. Another fundamental symmetry is the time-reversal $\mathcal{T}$ symmetry. This symmetry deals with the question of whether a system behaves same way or different way when the direction of time is reversed i.e., run backwards instead of forward.

It is now well known that the combination of $\mathcal{C}$, $\mathcal{P}$ and $\mathcal{T}$ which is also known as $\mathcal{CPT}$ symmetry is a symmetry of the nature [9, 10]. Lorentz invariance, locality and quantum field theory (QFT)

ensure the $\mathcal{CPT}$ symmetry. So, an experimental observation of $\mathcal{CPT}$ violation implies either one or any combination of QFT, principle of locality or Lorentz symmetry is broken but so far there are no such experimental indication. Therefore, $\mathcal{CP}$ symmetry refers $\mathcal{T}$ symmetry also. There are no direct experimental confirmation of $\mathcal{T}$ violation but our everyday "arrow of time" experience suggests that there must be a counterpart of $\mathcal{T}$ asymmetry in the microscopic world; a mystery for which physicists currently have no answer.

Until 1964, the $\mathcal{CP}$ symmetry was thought to be the symmetry of nature but in that year, Christenson, *et al* [11] observed that the long lived K meson, K_L^ν decayed into two pions, π^+ and π^-. For the decay of K meson, $\mathcal{CP} = -1$ if $\mathcal{CP}$ were a good symmetry and K_L^ν should decay into three pions not two. Since, only two pions were observed experimentally, it means, $\mathcal{CP}$ symmetry is violated. In the light of $\mathcal{CPT}$ theorem, $\mathcal{CP}$ violation means $\mathcal{T}$ violation also. Despite so many attempts, no direct $\mathcal{T}$ violation has been observed yet [12].

The $\mathcal{T}$ violation can help us to understand the matter-antimatter asymmetry of our universe. One plausible solution to this mystery involves the $\mathcal{T}$ asymmetry in the early phase of the universe; the theory is that the rate of certain processes that turn antimatter to matter is faster than the inverse processes that convert matter to antimatter [2]. But this idea does not quite work as the known (indirect) $\mathcal{T}$-violation in particle physics is too weak to explain the observed size of the matter-antimatter asymmetry [3]. This makes us to believe that there must be other $\mathcal{T}$ violation interaction out there in physics that is unknown as of now. The permanent electric dipole moment of electron (eEDM) might play a part in the search for such new sources of $\mathcal{T}$ violation [13].

1.3 Permanent electric dipole moment of electron and its particle physics implication

The electric dipole moment (EDM) of any elementary particle in an eigenstate of angular momenta is a consequence of violation of both $\mathcal{T}$ and $\mathcal{P}$ as dipole moment (D) is odd under $\mathcal{P}$ [$\mathcal{P}(D) = -D$] and even under $\mathcal{T}$ [$\mathcal{T}(D) = D$] but spin (S) is even under $\mathcal{P}$ [$\mathcal{P}(S) = S$] and odd under $\mathcal{T}$ [$\mathcal{T}(S) = -S$] [4, 5]. In the SM of electroweak and strong interaction, the $\mathcal{CP}$ violation originates itself by a complex quark mixing matrix, the Kobayashi-Maskawa matrix (this matrix maps the mismatch

Table 1.1: Predicted eEDM in different model of particle physics

Name of Model	$\lvert d_e \rvert$ (e.cm)
Standard Model	$< 10^{-38}$
Lepton flavor-changing	$10^{-29} - 10^{-26}$
Left-right symmetry	$10^{-28} - 10^{-26}$
Multi-Higgs	$10^{-28} - 10^{-27}$
Supersymmetry (SUSY)	$\leq 10^{-25}$
Experimental bound	$< 8.7 \times 10^{-29}$

of quark's quantum states when they propagate freely and participate in the weak interaction), which arises from complex Yukawa coupling [14]. Kobayashi-Maskawa model can explain the $\mathcal{CP}$ violation found in the decay of neutral K and B meson [15], which is the only place where $\mathcal{CP}$ violation is observed so far. This $\mathcal{CP}$ violation within the SM is inadequate to explain the matter-antimatter asymmetry. If the additional $\mathcal{CP}$ violation required to explain this asymmetry is present in the lepton sector, it is predicted to show up as an observable eEDM. According to the SM, the eEDM is too small ($d_e < 10^{-38}$ e cm) to be observed experimentally [16]. On the other hand, many extensions of the SM suggest that it would lie in the range of current experimental sensitivity (see Table 1.1 [5, 17]). Therefore, the discovery of an EDM or an improved limit on its size can give information about new sources of $\mathcal{CP}$ or $\mathcal{T}$ violation. The limit on the eEDM has already prohibited a significant section of the parameter space of supersymmetry (SUSY) [18], a theoretical extension of the SM that is often believed to be true.

Till date, the best limit of electron EDM in an atomic system is achieved from the Tl atom experiment ($|d_e| < 1.6 \times 10^{-27}$ e cm) [19]. However, the discovery of Sandars [20] reveals that the effective internal electric field experienced by an electron is profoundly enhanced in heavy-atom containing polar molecule which makes these polar diatomics very promising candidate in the search of the $\mathcal{P}$- and$\mathcal{P}, \mathcal{T}$ -violating experiments [21, 22]. The latest best upper limit of electron EDM is set from the ThO experiment ($|d_e| < 8.7 \times 10^{-29}$ e cm) by ACME collaboration [23]. This limit is one order lower in magnitude than the previous best limit ($|d_e| < 10.5 \times 10^{-28}$ e cm), which is obtained from the molecular YbF experiment [24].

1.4 General principle for the measurement of eEDM

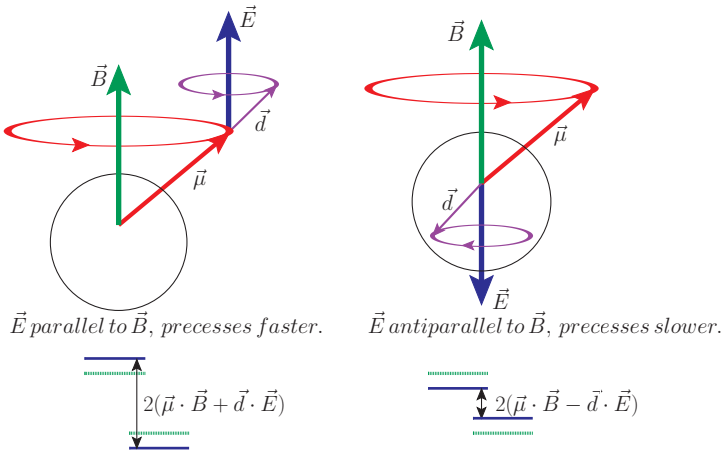

Figure 1.2: Basic sketch of the EDM experiment

Now that we understand precise value of the eEDM is a very important quantity, the next question is how to measure it. The basic principle for the measurement of eEDM is same as the measurement of EDM of any neutral system (see Figure 1.2). If the system of interest has a magnetic moment, $\vec{\mu}$, and is placed in a magnetic field $\vec{B}$, the interaction Hamiltonian is

$$H_{\text{mag}} = -\vec{\mu}\cdot\vec{B}. \tag{1.1}$$

From the point of view of a classical theory, the magnetic moment $\vec{\mu}$ experiences a torque due to the magnetic field $\vec{B}$, and precesses around it. The precessional frequency for the system having an energy separation of $2\vec{\mu}\cdot\vec{B}$ between $|J,+m\rangle$ and $|J,-m\rangle$ (where J and m are total angular momentum and its component along z axis, respectively) states are given as

$$\omega = \frac{2(\vec{\mu}\cdot\vec{B})}{\hbar}. \tag{1.2}$$

If the system under consideration has an EDM ($\vec{d}$) and we apply an electric field ($\vec{E}$), the electric field will exert a torque on the dipole moment. So, the interaction of the EDM with the electric field will change the precessional frequency depending on the orientation of $\vec{E}$ with respect to $\vec{B}$. Now, from the projection theorem [25], we know that in the eigenstate of angular momentum, the

expectation value of the operator $\vec{d}$ is proportional to the expectation value of $\vec{J}$. This means that if $\vec{E}$ is parallel to $\vec{B}$, the precessional frequency will be

$$\Delta\omega_+ = \frac{2(\vec{\mu}\cdot\vec{B} + \vec{d}\cdot\vec{E})}{\hbar}. \tag{1.3}$$

Now, if $\vec{E}$ is anti-parallel to $\vec{B}$, the precessional frequency will be

$$\Delta\omega_- = \frac{2(\vec{\mu}\cdot\vec{B} - \vec{d}\cdot\vec{E})}{\hbar}. \tag{1.4}$$

The purpose of the EDM experiment is to measure the change of precessional frequency, $\delta\omega$ ($= \Delta\omega_+ - \Delta\omega_-$) when $\vec{E}$ is flipped with respect to $\vec{B}$. So, the change of frequency is given by

$$\delta\omega = \Delta\omega_+ - \Delta\omega_- = \frac{4\vec{d}\cdot\vec{E}}{\hbar}. \tag{1.5}$$

The Eq. (1.5) can be used to obtain the value of permanent EDM of the system of consideration.

1.5 The scope of relativistic electronic structure theory

The Eq. (1.5) of the previous section shows that the observed quantity (i.e., the $\mathcal{P},\mathcal{T}$-odd frequency change) in the eEDM experiment is directly proportional to the value of the permanent EDM of the system and the electric field it is experiencing. The smallness of the value of eEDM restricts us to do experiment with single electron as the highest external electric field generated in the laboratory is not large enough to observe any eEDM effect. On the other hand, atoms and molecules have been proposed and experimented as it offers very high sensitivity of the EDM effect [16, 21, 22, 26]. The interaction Hamiltonian of the eEDM with the electric field in an atom or molecule can be given in the relativistic theory as [27]

$$H_{\text{EDM}} = -\sum_i d_e \beta \vec{\Sigma}_i \cdot \vec{E}_i, \tag{1.6}$$

where β is a Dirac matrix and $\vec{\Sigma}$ are Dirac spin vectors. The sum is over all the electrons, but only the unpaired electrons will contribute to the above summation. $\vec{E}_i$ is the total electric field acting on the i^{th} electron. Near the nuclear region, $\vec{E}_i$ is governed by the electric field of the nucleus which is given by

$$\vec{E}_i \approx \frac{Z\vec{r}_i}{r_i^2}, \tag{1.7}$$

where Z is the atomic number.

In a non-relativistic theory where the point particles (both electron and nucleus) are held together by the classical electrostatic forces, the expectation value of H_{EDM} is always zero; a consequence of the Schiff's theorem [28, 29]. This result is surprising as it states that although individual electron has EDM, the net effects in an atomic or molecular system is always zero if we treat it non-relativistically. On the other hand, Salpeter [27] pointed out that when a particular electronic configuration allow electrons to approach close enough to the nucleus to experience relativistic effects, H_{EDM} can have a non-zero expectation value in that particular electronic state. Sandars [20, 30–33] also pointed out that in the appropriately chosen situation, the interaction can also become much larger than achieved in the laboratory field ($\sim d_e E_{\text{lab}}$). The expectation value of H_{EDM} in an atomic state can be written as

$$\langle\Psi|H_{\text{EDM}}|\Psi\rangle \equiv -d_e\langle\Psi|\vec{J}|\Psi\rangle \cdot \vec{E}_{\text{atom}}, \tag{1.8}$$

where, $|\Psi\rangle$ is the four component electronic wavefunction of the atomic state, $\vec{J}$ is the total angular momentum and $\vec{E}_{\text{atom}}$ is the "internal electric field" of the atom. It is parallel to the $\vec{E}_{\text{lab}}$ and its magnitude is dependent on the extent of polarization of the atom in the laboratory electric filed $\vec{E}_{\text{lab}}$ [16]. The magnitude of $\vec{E}_{\text{atom}}$ is also dependent on the amplitude of the electronic wavefunction ($|\Psi\rangle$) in the nuclear region where the electrons are accelerated to achieve relativistic speed and the Sanders effect is most enhanced. This means that the effect is strongest for the s electrons. E_{atom} scales with Z as $\propto Z^3$ [16, 33].

The polarizability of an atom is $\sim a_0^3$ [34]. So, even in the largest applied electric fields, the atomic polarization and the E_{atom} are linear with respect to the polarizing electric field E_{lab}. So, for atoms, the Eq. (1.8) can be alternatively written as

$$\langle\Psi|H_{\text{EDM}}|\Psi\rangle \equiv -\vec{D}_a \cdot \vec{E}_{\text{lab}} \equiv -Rd_e\frac{\vec{J}}{|J|} \cdot \vec{E}_{\text{lab}}, \tag{1.9}$$

where, $\vec{D}_a$ is the permanent atomic EDM resulting from EDMs of individual electrons. R is called the "enhanced factor" which is defined as $R = \frac{D_a}{d_e}$. This enhancement factor, which is a very important quantity to derive the limit on d_e from an atomic EDM experiment cannot be measured experimentally and thus has to be calculated from a relativistic electronic structure theory. A number of heavy atoms were experimented and eventually improved the upper limit on the

eEDM value. The best upper bound limit from an atomic experiment comes from the Tl beam spectroscopy where the obtained limit is $|d_e| \leq 1.6 \times 10^{-27}$ e cm [19].

Polar diatomic molecules are generally more polarizable than the atoms. It can be easily understood in terms of the following picture. Consider a polar molecule MX, where the heavy M^{y+} ion is bound to the small X^{y-} ion. We also consider that in the molecular-fixed frame, the atomic cores are not rotating about their center of mass. The presence of $\sim ye$ units of charge, located only a small distance a_0 (where a_0 is bond length) away from the X^{y-} ion, generates an electric field $E_{\text{mol}} \sim \frac{y}{a_0^2} \sim$ 10s of GV/cm (depending on the molecule) that polarizes the heavy M^{y+} ion. However, in the laboratory frame, where the state of the collection of all particles (i.e., nuclei, core and valance electrons) is an eigenstate of the total angular momentum (J), the polarization of the M atom by the X atom averages out and the static polarization vanishes. When a laboratory field $\vec{E}_{\text{lab}}$ is applied, the eigenstates of the molecule have polarization oriented either along or against $\vec{E}_{\text{lab}}$. When this happen, the polarization of M atom by the X atom that existed in the molecular-fixed frame (or some fraction of it depending on the orientation of the molecule) gets oriented either along or against $\vec{E}_{\text{lab}}$. The laboratory electric field only orients the molecule-fixed dipole, while the strong electronic interaction between two oppositely charged nuclei polarizes the M atom.

The large polarizability of diatomic molecules can also be understood as originating from the presence of closely spaced opposite parity labels in the molecules. The opposite parity states are typically spaced by around $2\pi \times$ 10s of GHz (for rotational states) or even as small as $2\pi \times$ 10s of kHz (for Ω-doublets), even though the dipole matrix elements between these states are still in the order of an atomic unit ($D \sim ea_0$). Larger internal electric field can be obtained by the larger polarization of diatomic molecules in a laboratory scale electric field. However, this also means that the $\vec{E}_{\text{mol}}$, which is the internal electric field analogue of $\vec{E}_{\text{atom}}$ for a molecule, is no longer linear to the polarizing electric field $\vec{E}_{\text{lab}}$ when the molecule is strongly polarized. Therefore, the parametrization in terms of enhancement factor R is meaningless, and thus, we need to describe the enhancement due to Sandars effect in term of internal electric field of molecule.

In heavy diatomic molecules, the relativistic effects that lead to large E_{mol} are very important. The spin-orbit effects, which also originates due to special relativity, strongly couple the spin $\vec{S}$ of

the electrons to their orbital angular momentum $\vec{L}$ to result the total angular momentum $\vec{J} = \vec{L}+\vec{S}$. Thus, for such systems, the $\vec{d_e}$ lies along $\vec{J}$. The projection of $\vec{J}$ onto the internuclear axis of the molecule ($\hat{n}$) is called $\hat{\Omega}$ ($\equiv \vec{J}\cdot\hat{n}$). The electronic states of diatomic molecules are eigenstates of the operator $\hat{\Omega}$ [35–37]. In the laboratory frame, the expectation value of $\hat{\Omega}$ is zero ($\langle\Psi|\hat{\Omega}|\Psi\rangle = 0$) in any eigenstate of the parity operator or the square of the total angular momentum operator J^2. In a diatomic molecule the relativistic eEDM Hamiltonian can be parametrized as [38]

$$\langle\Psi|H_{\text{EDM}}|\Psi\rangle \equiv -d_e\langle\Psi|\vec{J}|\Psi\rangle\cdot\vec{E}_{\text{mol}} = -d_e\Omega E_{\text{mol}}, \tag{1.10}$$

where, $\Omega = \langle\Psi|\hat{\Omega}|\Psi\rangle$ is determined by the degree of polarization of $|\Psi\rangle$ state by the laboratory electric field $\vec{E}_{\text{lab}}$. The internal electric field $\vec{E}_{\text{mol}}$ ($= \hat{n}E_{\text{mol}}$) is directed along the internuclear axis. The quantity ΩE_{mol}, also known as effective internal electric field (E_{eff}) is a property of a specific molecular electronic state. Just like the enhancement factor R in atomic case, there are no experimental observable for the E_{eff} of diatomic molecule. So, it has to be calculated by a very reliable relativistic electronic structure theory [39, 40].

1.6 eEDM in Dirac theory

In a many electron molecular system, the Dirac Hamiltonian is given by

$$H_{DC} = \sum_i \Big(c\vec{\alpha}_i\cdot\vec{p}_i + \beta mc^2 + \sum_n V_n(r_i)\Big) + \sum_{j\neq i}\frac{e^2}{r_{ij}}, \tag{1.11}$$

where, c is the speed of light, α and β are the usual Dirac matrices and $V^{nuc}(r_i)$ is the nuclear potential function. The above Hamiltonian is also known as Dirac-Coulomb (DC) Hamiltonian as the two-electron interaction is approximated as Coulomb interaction, which treats electron-electron repulsion non-relativistically. From the above expression it is clear that the internal electric field ($\vec{E}_i^{\text{int}}$), which the i^{th} electron experiences due to the presence of other nuclei and electrons of the molecule can be parametrized as

$$e\vec{E}_i^{\text{int}} = -\vec{\nabla}_i\Big(\sum_n V_n(r_i) + \sum_{j\neq i}\frac{e^2}{r_{ij}}\Big). \tag{1.12}$$

The permanent molecular EDM resulting from EDMs of individual electrons is given as

$$H_{\text{EDM}} = -d_e\beta\sum_i \vec{\Sigma}_i\cdot\vec{E}_i^{\text{int}}. \tag{1.13}$$

However, from Schiff's theorem [28, 29], we know that the expectation value of the above Hamiltonian vanishes in the non-relativistic limit ($\beta = 1$). So, we can replace β by $\beta - 1$ and thus, the residual EDM interaction Hamiltonian becomes [41]

$$H_{\text{EDM}} = -d_e(\beta - 1)\sum_i \vec{\Sigma}_i \cdot \vec{E}_i^{\text{int}}. \tag{1.14}$$

The expectation value of the effective internal electric field (E_{eff}) can be obtained by evaluating the following matrix element

$$E_{\text{eff}} = \frac{1}{d_e}\langle \Psi_\Omega | H_{\text{EDM}} | \Psi_\Omega \rangle, \tag{1.15}$$

where, Ψ_Ω is the electronic wavefunction of the Ω state where Ω is the projected value of the total angular momentum along the molecular axis of a diatomic molecule.

1.7 Scalar-pseudoscalar interaction in atoms or molecules

Experimentally, only the net molecular EDM effects induced by various $\mathcal{P}, \mathcal{T}$-odd interactions (not only just eEDM) can be observed. There are two main sources of permanent molecular EDM (arises only when both $\mathcal{T}$ and $\mathcal{P}$ symmetries are broken and the Stark shift induced by this EDM increases linearly with external electric field [42, 43]) of a paramagnetic molecule: the eEDM and the scalar-pseudoscalar (S-PS) interaction of nucleon and electron. The former has been described extensively in the previous sections and in this section, we'll briefly describe about the latter one.

The S-PS electron-nucleon interaction arises from the coupling interaction between the scalar-hadronic current and the pseudoscalar electronic current. The scalar and pseudoscalar components of neutral Higgs boson (H) particle can mediate this interaction (see Figure 1.3) [44]. There is only one Higgs particle in the SM which forbids such interaction but a number of various multi Higgs models [including the minimal supersymmetric standard model (MSSM)] predicts such interaction [44]. An interesting characteristics of these models is that they also predict the baryon number violation originating from the exchange of neutral Higgs particle which is one of the other conditions to solve the matter-antimatter asymmetry of our universe [45].

The Hamiltonian of the S-PS interaction of nucleons and electrons are given as [43]

$$H_{\text{SP}} = i\frac{G_F}{\sqrt{2}} Z k_s \gamma^0 \gamma^5 \rho_N(r), \tag{1.16}$$

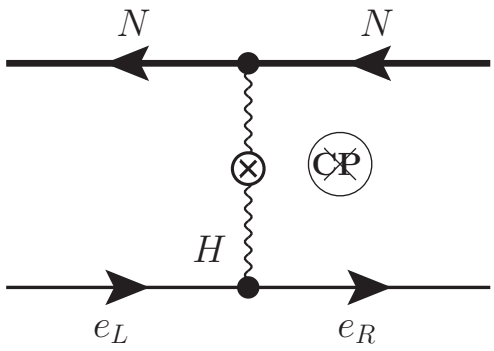

Figure 1.3: Scalar-pseudoscalar interaction of nucleon (N) and electron mediated by an exchange of Higgs (H) particle. Here, e_R and e_L are right and left handed electrons, respectively.

where G_F is the Fermi constant, γ matrices are the usual Dirac matrices and $\rho_N(r)$ is the nuclear charge density normalized to unity. The matrix element of $\mathcal{P},\mathcal{T}$-odd S-PS interaction constant, W_s, can be parametrized as

$$W_s = \frac{1}{\Omega k_s}\langle\Psi_\Omega|\sum_j^n H_{SP}(j)|\Psi_\Omega\rangle. \tag{1.17}$$

Here k_s is the dimensionless S-PS electron-nucleus coupling constant. k_s can be expressed as $k_s = k_{s,p}+(\frac{N}{Z})k_{s,n}$, where $k_{s,n}$ and $k_{s,p}$ are electron-neutron and electron-proton coupling constant, respectively. Z and N are the number of proton and neutron in the nucleus, respectively. It is worth to remember that just like d_e, the value (or upper bound limit) of k_s is very important to explore "new physics" beyond the standard model. The quantity W_s is a very important quantity to set upper bound limit on k_s from the experimentally measured $\mathcal{P},\mathcal{T}$-odd frequency change. However, W_s cannot be measured experimentally and thus it has to be calculated by a very reliable *ab initio* theory.

1.8 Importance of the ratio of E_{eff} to W_s

As both eEDM and S-PS interactions of electrons and nuclei give rise to the permanent molecular dipole moment of a diatomic molecule, it is impossible to decouple these two contribution from a single experiment. That's why in most of the calculation, either eEDM or the S-PS interaction

is considered as the only possible source of permanent molecular EDM. For example, the best upper bound limit of eEDM (d_e) and S-PS interaction constant (k_s) is obtained from the ThO experiment by ACME collaboration [23] where they have used the theoretically calculated value of effective electric field (E_{eff}) and S-PS $\mathcal{P},\mathcal{T}$-odd interaction constant (W_{s}) [46, 47]. In the calculation of d_e, the S-PS coupling constant k_s, is assumed to be zero and vice versa, although both of these contribute to the $\mathcal{P},\mathcal{T}$-odd frequency shift in the experiment. However, it is possible to get independent limit of d_e and k_s by using the results from two different experiments [48] and for this the accurate value of the ratio of E_{eff} to W_{s} is very important.

Since, the dominant contribution of $\mathcal{P},\mathcal{T}$-odd frequency shift comes from the eEDM and S-PS interaction, considering only those two effects we can get the following relation [23]

$$d_e E_{\text{eff}} + \frac{W_{\text{s}} k_s}{2} = \hbar\omega_{_{P,T}}, \tag{1.18}$$

where $\hbar$ is the Planck's constant and $\omega_{_{P,T}}$ is the experimentally measured $\mathcal{P},\mathcal{T}$-odd frequency shift.

$$\implies d_e + \frac{W_{\text{s}} k_s}{2E_{\text{eff}}} = \frac{\hbar\omega_{_{P,T}}}{E_{\text{eff}}}, \tag{1.19}$$

or,

$$d_e + \frac{k_s}{2R} = d_e^{\text{expt}}\big|_{k_s=0}. \tag{1.20}$$

Here, $d_e^{\text{expt}}\big|_{k_s=0}$ is the eEDM limit derived from the experimentally measured P,T-odd frequency shift where k_s is assumed to be 0 and R is defined as

$$R = \frac{E_{\text{eff}}}{W_{\text{s}}}. \tag{1.21}$$

Eq. (1.20) defines the interrelation of the independent limit of d_e, k_s and experimentally determined $d_e^{\text{expt}}\big|_{k_s=0}$. In experiment, the only measured quantity is the $\mathcal{P},\mathcal{T}$-odd frequency shift ($\omega_{_{P,T}}$). As both d_e and k_s are responsible for the $\mathcal{P},\mathcal{T}$-odd frequency shift, we cannot get independent limit of d_e and k_s since there are two unknowns (d_e and k_s) and one equation (Eq. 1.18). However, the experimentalists extract the upper bound limit of d_e by assuming only d_e contribution, i.e., they put $k_s = 0$ in the Eq. 1.18.

1.9 Magnetic hyperfine structure interaction in atoms and diatomic molecules

The accuracy of the theoretically estimated $\mathcal{P},\mathcal{T}$-odd interaction constants described in Eq. (1.15) and (1.17) cannot be mapped with the experiment as there are no corresponding experimental observables. However, the accuracy of theoretically obtained $\mathcal{P},\mathcal{T}$-odd interaction constants can be assessed by comparing theoretically obtained magnetic hyperfine structure (HFS) constants with the experimental values, because the calculation of both requires an accurate wave function in the nuclear region.

The interaction of nuclear moment with the internally generated electromagnetic field by electrons causes small shift and splitting in the energy levels of atom, molecule or ion. This interaction is known as magnetic hyperfine structure (HFS) interaction [49]. Thus, it can be viewed as a one body interaction from the electronic structure point of view. The magnetic vector potential $(\vec{A})$ at a distance $\vec{r}$ due to a nucleus K of an atom can be parametrized as

$$\vec{A} = \frac{\vec{\mu}_k \times \vec{r}}{r^3}, \tag{1.22}$$

where $\vec{\mu}_k$ is the magnetic moment of nucleus K. The perturbed HFS Hamiltonian of an atom due to $\vec{A}$ in the Dirac theory is given by $H_{hyp} = \sum_i^n \vec{\alpha}_i \cdot \vec{A}_i$, where n is the total no of electrons and α_i denotes the Dirac α matrices for the i^{th} electron. Now the magnetic hyperfine constant (A_J) of the J^{th} electronic state of an atom is given by

$$A_J = \frac{1}{IJ}\langle\Psi_J|H_{hyp}|\Psi_J\rangle = \frac{\vec{\mu}_k}{IJ} \cdot \langle\Psi_J| \sum_i^n \left(\frac{\vec{\alpha}_i \times \vec{r}_i}{r_i^3}\right) |\Psi_J\rangle, \tag{1.23}$$

where $|\Psi_J\rangle$ is the wavefunction of the J^{th} electronic state and I is the nuclear spin quantum number.

For a diatomic molecule, the parallel $(A_\parallel)$ and perpendicular $(A_\perp)$ magnetic HFS constant can be written as

$$A_{\parallel(\perp)} = \frac{\vec{\mu}_k}{I\Omega} \cdot \langle\Psi_\Omega| \sum_i^n \left(\frac{\vec{\alpha}_i \times \vec{r}_i}{r_i^3}\right)_{z(x/y)} |\Psi_{\Omega(-\Omega)}\rangle. \tag{1.24}$$

It is clear from the above equation that the $A_\parallel$ is proportional to the diagonal matrix elements of $\left(\frac{\vec{\alpha}\times\vec{r}}{r^3}\right)_z$ but $A_\perp$ is proportional to the non-diagonal matrix elements of $\left(\frac{\vec{\alpha}\times\vec{r}}{r^3}\right)_{x/y}$ between two different states ($+\Omega$ and $-\Omega$). However, $+\Omega$ and $-\Omega$ states are degenerate and their corresponding

determinants differ by only one spin up or spin down electron (for a single unpaired electron systems). Thus, the cluster amplitudes are of same magnitude for both $+\Omega$ and $-\Omega$ states. So, for each system, cluster amplitudes can be evaluated once and they can be used to calculate both $A_{\parallel}$ and $A_{\perp}$ with their corresponding property integrals. However, the rearrangement of the one electron property matrix of $A_{\perp}$ is necessary in the contraction between individual matrix element and proper cluster amplitude.

1.10 Importance of hyperfine structure constant

The best way to know the quality of the electronic wavefunction in the nuclear region is to check the theoretically obtained hyperfine structure (HFS) constant with the available experimental value. The interaction of nuclear moment with the internally generated electromagnetic field by electrons causes small shift and splitting in the energy levels of atom, molecule or ion. This interaction is known as hyperfine structure [49], which plays a key role in atomic clock and laser experiments. A variety of applications including telecommunications, global positioning system, very-long-baseline interferometry telescopes [50] and test of fundamental concepts of physics [51] demand very precise measurement of time, which can be given by an atomic clock, where the unit of time is defined in terms of frequency at which an atom absorbs or emits photon during a particular transition. The laser cooling and atom trapping experiments require the knowledge of HFS as it influences the optical selection rule and the transfer of momentum from photon to the atom. In particular, as the line width of transition of laser is much smaller than the energy difference between two hyperfine labels, the frequency of repumping laser depends on the separation of hyperfine labels [52].

The standard model (SM) of particle physics predicts either a zero or a very small (less than 10^{-38} e.cm) electric dipole moment (EDM) of an electron. Therefore, a measurable non-zero EDM of an electron can explore the physics beyond SM. The violation of time reversal ($\mathcal{T}$) or equivalently charge conjugation ($\mathcal{C}$) and spatial parity ($\mathcal{P}$) symmetry of an atomic/molecular system is responsible for the non zero EDM of an electron. Unfortunately, the accuracy of the theoretically estimated $\mathcal{P},\mathcal{T}$-odd interaction constants cannot be mapped with the experiment as there are no

corresponding experimental observables. However, the accuracy of theoretically obtained $\mathcal{P},\mathcal{T}$-odd interaction constants can be estimated by comparing theoretically obtained HFS constants with the experimental values as the calculation of both requires an accurate wave function in the nuclear region and the operator forms are more or less similar.

1.11 Dirac-Hartree-Fock method

Now that we have known the importance of the electronic structure theory, our aim is to implement a many-body theory in the relativistic framework that can produce an accurate wavefunction in the nuclear region of the heavy diatomic molecules. The many-electron relativistic Hamiltonian is given in Eq. (1.11), where the two-body interaction is incorporated as Coulomb approximation. However, it is not possible to solve this Hamiltonian exactly due to the presence of two-electron term. So, in search for an approximate solution, at the first attempt, independent particle approximation is incorporated where the complex two-body interaction is approximated as summation of one-body potential terms. Within a single determinant theory, the best solution of Dirac-Coulomb Hamiltonian can be obtained by using Dirac-Hartree-Fock (DHF) method. The DHF Hamiltonian can be written as

$$\begin{aligned} H_{DHF} &= \sum_i [-ic\,\vec{\alpha}\cdot\vec{\nabla} + (\beta - I)c^2 + V^{nuc}(r_i) + v^{DHF}(r_i)], \\ &= \sum_i f(r_i), \end{aligned} \tag{1.25}$$

where f is the Fock operator with DHF potential

$$v^{DHF}|\chi_i\rangle = \sum_{a=1}^{occ} \langle\chi_a|\frac{1}{r_{ij}}|\chi_a\rangle|\chi_i\rangle - \langle\chi_a|\frac{1}{r_{ij}}|\chi_i\rangle|\chi_a\rangle. \tag{1.26}$$

Here χ are the single particle wavefunction and summation is over all occupied occ orbitals. The single particle wavefunction can be obtained by solving the following equation

$$f(r_i)|\chi_i\rangle = \varepsilon_i|\chi_i\rangle, \tag{1.27}$$

where ε_i is the energy of the i^{th} orbital.

So, the DHF Hamiltonian approximates the electron-electron repulsion in an average way such that the complicated many electron problem becomes the sum of one electron problems. The residual interaction is given as

$$V_{res}(ij) = \sum_{j<i} \frac{1}{r_{ij}} - \sum_{j} v^{DF}(r_j). \tag{1.28}$$

This residual interaction can be incorporated by the treatment of electron correlation.

1.12 Electron correlation

The DHF method takes care most of the part of the energy calculation but the missing instantaneous electron-electron interaction is very important for the $\mathcal{P},\mathcal{T}$-odd properties we discussed above. The energy difference between the DHF energy and the exact energy of a state in complete basis limit is defined as the correlation energy of the state [53]. There are various method that can treat electron correlation of opposite spin electrons. These methods can be based on perturbation theory or variational theorem , or both or even can be neither of them. Among various post Hartree-Fock methods, many body perturbation theory (MBPT), configuration interaction (CI) or coupled-cluster (CC) methods are the most familiar one. In this thesis, we have used the CC method to treat the dynamic part of the electron correlation.

1.13 Why coupled-cluster?

Among the three correlation methods stated above, the CI [53–55] is the simplest one and the corresponding wavefunction can be parametrized as

$$|\Psi\rangle = |\Phi_0\rangle + \sum_{i,a} C_i^a |\Phi_i^a\rangle + \sum_{\substack{j<i \\ b<a}} C_{ij}^{ab} |\Phi_{ij}^{ab}\rangle + \ldots, \tag{1.29}$$

where i, j are the hole indices (or occupied orbital indices in DHF wavefunction) and a, b represent the particle or virtual orbital indices. $|\Phi_0\rangle$ is the DHF wavefinction and Φ_i^a is the excited determinant where the i^{th} occupied orbital of $|\Phi_0\rangle$ is replaced by a^{th} virtual orbital and so on. $C_{i..}^{a..}$ is the expansion coefficient corresponding to the determinant $\Phi_{i..}^{a..}$. The expansion coefficients can be

achieved either by method of variation or by method of projection. However, as the above expression is linear, both the method lead to the identical equation which is nothing but an eigenvalue problem and thus, the solution of the coefficients can be achieved by diagonalizing the Hamiltonian in an appropriate determinantal space. If we include all the terms in the above expression, it is called the full CI (FCI) method, which leads to the exact solution of the system in that particular basis set. However, the calculation of FCI in a reasonable basis is practically impossible and thus, one need to use a truncation scheme to do CI calculation. Some of the popular CI methods are CI with single and double approximation (CISD) or restricted active space CI (RAS-CI). However, the truncated CI is neither size consistent nor size extensive [56–58]. Size extensivity ensures that the energy scales properly (i.e., linearly) with the particle number and size consistency deals with the fact that energy is properly described at the dissociation limit. So, truncated CI fails to live up the expectation of fulfilling two important criteria of the many-body theory.

Another alternative choice to include electron correlation effect is the perturbation theory [49, 59–62]. In this method, the Hamiltonian is divided into two parts

$$H = H_0 + H', \tag{1.30}$$

where H_0 is the perturbation independent zeroth order Hamiltonian whose solution is already known. H' is any extra interaction that we want to include. The wave function can be parametrized as

$$|\Psi_0\rangle = |\Phi_0\rangle + |\Psi_0^{(1)}\rangle + |\Psi_0^{(2)}\rangle + |\Psi_0^{(3)}\rangle + \cdots + |\Psi_0^{(n)}\rangle, \tag{1.31}$$

where $|\Phi_0\rangle$ is the solution of H_0 and $|\Psi_0^{(n)}\rangle$ is the n^{th} order correction to the ground state wave function. The difference between the exact ground state energy, ϵ_0, and the zeroth-ordered ground state E_0 can be expressed as

$$\epsilon_0 - E_0 = \Delta\epsilon_0 = \langle\Phi_0|\hat{H}'|\Psi_0\rangle, \tag{1.32}$$

where intermediate normalization between the zeroth-order ground state and the corresponding exact state is assumed. $\Delta\epsilon_0$ can be written as

$$\Delta\epsilon_0 = \Delta\epsilon_0^{(1)} + \Delta\epsilon_0^{(2)} + \Delta\epsilon_0^{(3)} + \cdots + \Delta\epsilon_0^{(n)}, \tag{1.33}$$

with

$$\Delta\epsilon_0^{(n)} = \langle\Phi_0|\hat{H}'|\Psi_0^{(n-1)}\rangle, \tag{1.34}$$

where, $\Delta\epsilon_0^{(n)}$ is the n^{th} order correction to the ground state energy. The computational problem of perturbation theory is that it converges very slowly. With the addition of higher terms (and thus, with the expense of more computational cost), the convergence becomes relatively better. The addition of higher terms through the conventional technique becomes enigmatic from a technical point of view and thus, one needs to adopt diagrammatic technique.

The most popular among the various many-body theories is the coupled-cluster method as it can incorporate the electron correlation effects very elegantly. It fulfills both the criteria of the many-body theory i.e., size-extensivity and size-consistency, provided that the reference state is size-extensive and size-consistence.

1.14 Coupled-cluster method

Cöester and Kümmel first proposed the concept of CC to solve problems in the area of nuclear physics [63, 64]. However, in the electronic structure theory, the pair correlation method of Sinanoğlu [65, 66] and Nesbet [67] constituted the CC method. Hubbard [68], by applying diagrammatic techniques of many-body perturbation theory, showed that the exact form of the wavefunction of the ground state can be parametrized as an exponential form. Cizek and Paldus are the pioneer of the CC theory to apply it for the quantum-chemical problems [69–72].

The exact wavefunction can be generated by operating a wave operator to the DHF wavefunction. The wave operator adds the orthogonal space (or correlation space) to the Dirac-Fock space. The exact wavefunction is given by

$$|\Psi_{exact}\rangle = \Omega|\Phi_0\rangle, \tag{1.35}$$

where Ω is the wave operator and $|\Phi_0\rangle$ is the DHF ground state. The form of wave operator and wave function in CC approximation can be parametrized as

$$\Omega = e^T, \tag{1.36}$$

$$|\Psi_{cc}\rangle = e^T|\Phi_0\rangle, \tag{1.37}$$

where T is the cluster operator which is the sum of one-electron excitation, two-electron excitation and so on upto N electron-excitation operators. The second quantized form of the coupled-cluster excitation operator, T, is given as

$$T = T_1 + T_2 + \cdots + T_N = \sum_n^N T_n, \tag{1.38}$$

with

$$T_m = \frac{1}{(m!)^2} \sum_{ij\ldots ab\ldots} t_{ij\ldots}^{ab\cdots} a_a^\dagger a_b^\dagger \ldots a_j a_i, \tag{1.39}$$

where i, j are the hole and a, b are the particle indices and $t_{ij..}^{ab..}$ are the cluster amplitudes corresponding to the cluster operator T_m. Intermediate normalization scheme is generally used which is given by

$$\langle \Phi_0 | \Phi_0 \rangle = \langle \Psi_{cc} | \Phi_0 \rangle = 1. \tag{1.40}$$

Using normal-ordered Hamiltonian we can write

$$H_N e^T |\Phi_0\rangle = E^{corr} e^T |\Phi_0\rangle, \tag{1.41}$$

where normal-ordered Hamiltonian and E^{corr} is given by

$$H_N = H - \langle \Phi_0 | H | \Phi_0 \rangle, \tag{1.42}$$

$$E^{corr} = E_{cc} - E_{HF}. \tag{1.43}$$

The Eq. (1.41) can be solved by either variational or non-variational way. A traditional CC method, also known as normal CC (NCC) is a non-variational type and can be achieved in two ways: method of projection or similarity transformation. In the method of projection, we project the ground state DHF determinant and excited determinants from the left to obtain the expressions for energy and cluster amplitudes, respectively. We can get a set of equations by applying generalized Wick's theorem for both the energy and the amplitudes where H_N and Ts are connected. Similarity transformation procedure also leads to the same set of equations. In this method, we pre-multiply the Eq. (1.41) by e^{-T} to get

$$e^{-T} H_N e^T |\Phi_0\rangle = E^{corr} |\Phi_0\rangle. \tag{1.44}$$

According to Campbell-Baker-Hausdorff formula, one can expand the term $e^{-T}H_N e^T$ as

$$e^{-T}H_N e^T = H + [H,T] + \frac{1}{2!}[[H,T],T] + \frac{1}{3!}[[[H,T],T,T] + \frac{1}{4!}[[[[H,T],T],T],T] + \ldots \quad (1.45)$$

The consequence of Wick's theorem and the fact that different cluster operators commute with each other produce two types of terms. One is of connected types, i.e., in diagrammatic representation, no vertex is isolated from the rest of the vertex. Another type is the disconnected terms where one part is disconnected from the other part of the diagram. However, in the above commutation formula, the disconnected terms mutually cancels each other leading to a set of connected diagrams only. Thus it follows that

$$e^{-T}H_N e^T = (H_N e^T)_c, \quad (1.46)$$

where the subscript c indicates only the connected terms in the contraction between H_N and T. The connectedness ensures the size-extensivity. Due to maximum two-body nature of Hamiltonian, H_N can connect at most four different T vertex. This is called the natural truncation of CC ansatz. Hamiltonian of the left hand side of Eq. (1.44) may be considered as a similarity transformed Hamiltonian

$$\tilde{H} = e^{-T}H_N e^T = (H_N e^T)_c. \quad (1.47)$$

This similarity transformed Hamiltonian is non-Hermitian and in principle, can have complex eigenvalues. The equations for correlation energy and n-body cluster amplitudes are obtained by projecting $\langle\Phi_0|$ and n-tuply excited determinants from the left to the equation (1.44), respectively

$$\langle\Phi_0|(H_N e^T)_c|\Phi_0\rangle = E^{corr}, \quad (1.48)$$

$$\langle\Phi^{a\cdots}_{i\cdots}|(H_N e^T)_c|\Phi_0\rangle = 0. \quad (1.49)$$

The Eq. (1.49) leads to a coupled set of nonlinear equations which have to be solved iteratively to obtain the cluster amplitudes. Once the cluster amplitude equations are solved, one can get the correlation energy from Eq. (1.48). The most commonly used CC ansatz is the singles and doubles approximation where T is truncated as $T = T_1 + T_2$.

References

[1] M. Dine and A. Kusenko, Reviews of Modern Physics **76**, 1 (2003).

[2] A. D. Sakharov, JETP lett. **5**, 24 (1967).

[3] M. B. Gavela, P. Hernández, J. Orloff, O. Pène, and C. Quimbay, Nuclear Physics B **430**, 382 (1994).

[4] E. D. Commins, Advances In Atomic, Molecular, and Optical Physics **40**, 1 (1999).

[5] W. Bernreuther and M. Suzuki, Rev. Mod. Phys. **63**, 313 (1991).

[6] A. Zichichi, *Theory and experiment heading for new physics* (World Scientific, 2002).

[7] J. Ginges and V. Flambaum, Physics Reports **397**, 63 (2004).

[8] C.-S. Wu, E. Ambler, R. Hayward, D. Hoppes, and R. P. Hudson, Physical review **105**, 1413 (1957).

[9] W. Pauli, L. Rosenfeld, and V. Weisskopf, *Niels Bohr and the development of physics* (Mc Graw-Hill, New York, 1957).

[10] G. Lüders, Annals of Physics **2**, 1 (1957).

[11] J. H. Christenson, J. W. Cronin, V. L. Fitch, and R. Turlay, Physical Review Letters **13**, 138 (1964).

[12] R. F. Streater and A. S. Wightman, *PCT, spin and statistics, and all that* (Princeton University Press, 2000).

[13] N. Fortson, P. Sandars, and S. Barr, Physics Today **56**, 33 (2003).

[14] H. Yukawa, Nippon Sugaku-Buturigakkwai Kizi Dai 3 Ki **17**, 48 (1935).

[15] W.-M. Y. etal, Journal of Physics G: Nuclear and Particle Physics **33**, 1 (2006).

[16] I. B. Khriplovich and S. K. Lamoreaux, *CP Violation without Strangeness: The Electric Dipole Moments of Particles, Atoms, and Molecules* (Springer, London, 2011).

[17] M. K. Nayak and R. K. Chaudhuri, Advances in Chemical Physics **140**, 239 (2008).

[18] K. A. Olive, M. Pospelov, A. Ritz, and Y. Santoso, Physical Review D **72**, 075001 (2005).

[19] B. C. Regan, E. D. Commins, C. J. Schmidt, and D. DeMille, Phys. Rev. Lett. **88**, 071805 (2002).

[20] P. G. H. Sandars, Phys. Rev. Lett. **19**, 1396 (1967).

[21] O. Sushkov and V. Flambaum, Journal of Experimental and Theoretical Physics **48**, 608 (1978).

[22] V. V. Flambaum, Sov. J. Nucl. Phys. **24**, 199 (1976).

[23] J. Baron *et al.*, Science **343**, 269 (2014).

[24] J. Hudson *et al.*, Nature **473**, 493 (2011).

[25] J. J. Sakurai, *Modern Quantum Mechanics* (Addison Wesley Publishing Company Inc., New York, 1985).

[26] B. L. Roberts and W. J. Marciano, *Lepton dipole moments* (World Scientific, 2010).

[27] E. Salpeter, Physical Review **112**, 1642 (1958).

[28] E. Purcell and N. Ramsey, Physical Review **78**, 807 (1950).

[29] L. Schiff, Physical Review **132**, 2194 (1963).

[30] P. Sandars, Physics Letters **14**, 194 (1965).

[31] P. Sandars, Physics Letters **22**, 290 (1966).

[32] P. Sandars, Journal of Physics B: Atomic and Molecular Physics **1**, 499 (1968).

[33] P. Sandars, Journal of Physics B: Atomic and Molecular Physics **1**, 511 (1968).

[34] E. Purcell, *Electricity and Magnetism (Berkeley Physics Course, Vol. 2)* (Mc Graw-Hill Book Company, New York, 1965).

[35] N. Stepanov and B. Zhilinskii, Journal of Molecular Spectroscopy **52**, 277 (1974).

[36] J. T. Hougen, The calculation of rotational energy levels and rotational line intensities in diatomic molecules, 1970.

[37] J. M. Brown and A. Carrington, *Rotational spectroscopy of diatomic molecules* (Cambridge University Press, 2003).

[38] E. R. Meyer, J. L. Bohn, and M. P. Deskevich, Physical Review A **73**, 062108 (2006).

[39] H. S. Nataraj. Electric Dipole Moment of the Electron and its Implications on Matter-Antimatter Asymmetry in the Universe. PhD thesis, Mangalore University, 2009.

[40] Edmund R. Meyer. Structure and spectroscopy of candidates for an electron electric dipole moment experiment. PhD thesis, University of Colorado, 2010.

[41] M. G. Kozlov and L. N. Labzowsky, Journal of Physics B: Atomic, Molecular and Optical Physics **28**, 1933 (1995).

[42] The EDM of a polar diatomics due to the different number of proton in two nucleus and uneven distribution of electron density is not really be called as permanent molecular EDM. This is because the Stark shift induced by this EDM in an external laboratory field does not increase linearly rather quadratically with the electric field in the weak field limit. Thus strictly speaking, a polar diatomic molecule cannot have a permanent molecular EDM unless there is a violation of both P and T. [43].

[43] L. R. Hunter, Science **252**, 73 (1991).

[44] S. M. Barr, Physical review letters **68**, 1822 (1992).

[45] A. Kazarian, S. Kuzmin, and M. Shaposhnikov, Physics Letters B **276**, 131 (1992).

[46] L. Skripnikov, A. Petrov, and A. Titov, Journal of Chemical Physics **139**, 221103 (2013).

[47] L. Skripnikov and A. Titov, Journal of Chemical Physics **142**, 024301 (2015).

[48] V. A. Dzuba, V. V. Flambaum, and C. Harabati, Phys. Rev. A **84**, 052108 (2011).

[49] I. Lindgren and J. Morrison, *Atomic Many-Body Theory* (Springer-Verlag, New York, 1985).

[50] D. Normile and D. Clery, Science **333**, 1820 (2011).

[51] T. Rosenband *et al.*, Science **319**, 1808 (2008).

[52] W. D. Phillips, Reviews of Modern Physics **70**, 721 (1998).

[53] P. Lowdin, Advances in Chemical Physics **2**, 207 (1959).

[54] I. Shavitt, *Methods of Electronic Structure Theory, Edited by H. F. Schaefer III* (Plenum, New York, 1977).

[55] J. Karwowski, *Methods in Computational Molecular Physics, Edited by S.Wilson and G. H. F. Dierksen* (NATO ASI Series B: Physics, Volume 293, Plenum, New York, 1992).

[56] J. A. Pople, J. S. Binkley, and R. Seeger, International Journal of Quantum Chemistry **10**, 1 (1976).

[57] R. Chaudhary, D. Mukherjee, and M. D. Prasad, *Aspects of Many-Body Effects in Molecules and Extended Systems, Edited by D. Mukherjee, Lecture Notes in Chemistry, Vol. 50* (Springer-Verlag, Heidelberg, 1989).

[58] M. Nooijen, K. Shamasundar, and D. Mukherjee, Molecular Physics **103**, 2277 (2005).

[59] I. N. Levine, *Quantum Chemistry* (IV Edition, Prentice Hall, New Delhi, 1995).

[60] A. Szabo and N. S. Ostlund, *Modern Quantum Chemistry* (McGraw-Hill, New York, 1989).

[61] S. Raimes, *Many-Electron Theory* (North-Holland, Amsterdam, 1972).

[62] S. A. Kucharski and R. J. Bartlett, Advances in quantum chemistry **18**, 281 (1986).

[63] F. Coester, Nuclear Physics **7**, 421 (1958).

[64] F. Coester and H. Kümmel, Nuclear Physics **17**, 477 (1960).

[65] O. Sinanoğlu, Journal of Chemical Physics **36**, 706 (1962).

[66] O. Sinanoğlu, *Many-Electron Theory of Atoms, Molecules and Their Interactions* (John Wiley & Sons, Inc., 2007), pp. 315–412.

[67] R. K. Nesbet, *Electronic Correlation in Atoms and Molecules* (John Wiley & Sons, Inc., 2007), pp. 321–363.

[68] J. Hubbard, Proceedings of the Royal Society of London A: Mathematical, Physical and Engineering Sciences **240**, 539 (1957).

[69] J. Čížek, Journal of Chemical Physics **45**, 4256 (1966).

[70] J. Čížek, *On the Use of the Cluster Expansion and the Technique of Diagrams in Calculations of Correlation Effects in Atoms and Molecules* (John Wiley & Sons, Inc., 2007), pp. 35–89.

[71] J. Čížek and J. Paldus, International Journal of Quantum Chemistry **5**, 359 (1971).

[72] J. Paldus, J. Čížek, and I. Shavitt, Phys. Rev. A **5**, 50 (1972).

CHAPTER 2

Is Extended Coupled-Cluster Method in the Relativistic Framework Good Enough for an Accurate Wavefunction in the Nuclear Region?

All theories are legitimate, no matter.
What matters is what you do with them.

Jorge Luis Borges

As in the previous chapter, we have shown the importance of *ab initio* method for the calculation of various $\mathcal{P},\mathcal{T}$-odd interaction constants, in this chapter, we have opted for the implementation of the extended coupled-cluster (ECC) method in the relativistic framework to generate an accurate wavefunction in the nuclear region of atoms and molecules. The implemented ECC method is applied to calculate the magnetic HFS constant of alkali metals (Li, Na, K, Rb, and Cs), singly charged alkaline-earth-metals (Be^+, Mg^+, Ca^+, and Sr^+) along with parallel and perpendicular magnetic HFS constants of BeH, MgF, and CaH molecules. We have compared our ECC results with the calculations based on the restricted active space configuration interaction (RAS-CI) method. Our results are in better agreement with the available experimental values than those of the RAS-CI values.

2.1 Introduction

In the previous chapter, we have seen that it is very important to implement a many-body theory which can produce very good wavefunction in the nuclear region of heavy nucleus. To do so, we need to incorporate both relativistic and electron correlation effects simultaneously as these two effects are intertwined in nature. The best way to include relativistic effect in a single determinant theory is to solve the Dirac-Hartree-Fock (DHF) Hamiltonian, whereas single reference coupled cluster (SRCC) method is known to be the most efficient to include the dynamic part of the electron correlation [1–5]. The SRCC method can be solved either by method of variation or by non-variation. The non-variational solution of SRCC method is the most familiar, known as normal CC (NCC). The NCC, being non-variational, does not have the upper bound property of energy. The generalized Hellmann-Feynman (GHF) theorem and (2n+1) rule, which states that $(2n+1)^{th}$ order energy derivative can be obtained with the knowledge up to n^{th} order amplitude derivatives, are not satisfied [6, 7]. The implication of these theorems save enormous computational effort for the calculation of higher order properties, which clearly a lack in the NCC. However, the energy derivatives within the NCC can be obtained by Z-vector approach [8] or Lagrange multiplier method of Helgaker *et al* [9]. However, the GHF theorem and the (2n+1) rule are automatically satisfied in the variational CC (VCC). Among the various VCC methods, expectation value CC (XCC), unitary CC (UCC) and extended CC (ECC) are the most familiar in literature. The XCC and UCC use Euler type of functional where the left vector is complex conjugate of the right vector. The detailed discussion on various variational coupled cluster methods can be found in reference [10]. The ECC functional proposed by Arponen and coworkers [11, 12] can bypass all the problems associated with the Euler type of functional by assuming an energy functional which deals with the dual space of both right and left vector in a double linked form. This double linking ensures that the energy and its all order derivatives are size extensive. As the left and right vectors of the ECC functional are not complex conjugates, it contains relatively large variational space as compared to corresponding Euler type functional.

The linearized version of ECC, in which the left vector is linear, leads to the equations of NCC [13]. Thus, it can be inferred that ECC wavefunction, which spans more correlated determinantal space than the NCC, eventually improves the correlation energy as well as energy derivatives.

2.2 ECC functional

The ECC functional can be derived by parameterizing both bra and ket states. The parametrization is done by a double similarity transformation that leads to an alternative approach of many body problem where the functional is biorthogonal in nature. It is pertinent to note that the double similarity transformed Hamiltonian is no longer Hermitian as the similarity transformations are not unitary. The ECC functional of an arbitrary operator (A) is given by

$$\langle A\rangle = \frac{\langle\Phi_0|e^{\Sigma'}Ae^{\Sigma}|\Phi_0\rangle}{\langle\Phi_0|e^{\Sigma'}e^{\Sigma}|\Phi_0\rangle}, \tag{2.1}$$

where $|\Phi_0\rangle$ is the DHF reference determinant and Σ', Σ are hole-particle (h-p) destruction and creation operators respectively. Arponen proved that $\langle\Phi_0|e^{\Sigma'}e^{\Sigma}/\langle\Phi_0|e^{\Sigma'}e^{\Sigma}|\Phi_0\rangle$ can be written as $\langle\Phi_0|e^{\Sigma''}$, where Σ'' is h-p destruction operator [11]. Therefore, the ECC functional for the operator becomes

$$\langle A\rangle = \langle\Phi_0|e^{\Sigma''}e^{-\Sigma}Ae^{\Sigma}|\Phi_0\rangle. \tag{2.2}$$

The diagrammatic structure of $e^{-\Sigma}Ae^{\Sigma}$, which can also be written as $(Ae^{\Sigma})_c$ (where c stands for connected), leads to a terminating series. However, the diagrams in which Σ'' is solely connected to a single Σ leads to disconnected term in the amplitude equation. To avoid this problem, Arponen has defined two sets of amplitudes, s and t, with which the functional can be written as

$$\langle A\rangle = \langle\Phi_0|e^{S}(Ae^{T})_L|\Phi_0\rangle_{DL}, \tag{2.3}$$

where L means that the T operators right side of A are linked to A vertex and DL denotes that a S operator must be connected to either A or at least two T operators. The form of the S and T operators are given by

$$X = \sum_{\substack{q_1<q_2\cdots\\ p_1<p_2\cdots}} t^{q_1q_2\cdots}_{p_1p_2\ldots} a^{\dagger}_{q_1}a^{\dagger}_{q_2}\ldots a_{p_2}a_{p_1}, \tag{2.4}$$

where X is T when $p(q)$ are hole(particle) index and X is S when $p(q)$ are particle(hole) index.

The analytic energy derivatives can be calculated by using the ECC functional given in equation 2.3 where the operator is replaced by a perturbed Hamiltonian. The field dependent perturbed Hamiltonian is given by

$$H(\lambda) = H + \lambda O = f + v + \lambda O, \tag{2.5}$$

where H is the field independent Hamiltonian, O is the interaction Hamiltonian due to external field and λ indicates the strength of the interaction. f and v are one electron and two electron part of the field independent Hamiltonian respectively. Vaval *et al* [14] have shown that the ECC analytic derivatives can be obtained by expanding the ECC functional as a power series of λ and making the functional stationary with respect to cluster amplitudes in progressive orders of λ. The zeroth order k-body cluster amplitudes, which are sufficient to get the first order derivative of energy (which is nothing but the expectation value in the light of GHF theorem), can be obtained by using the following conditions

$$\frac{\delta E^{(0)}}{\delta t_k^{(0)}} = 0, \qquad \frac{\delta E^{(0)}}{\delta s_k^{(0)}} = 0. \tag{2.6}$$

Although ECC functional is a terminating series, the natural truncation in the single and double model leads to computationally very costly terms. To avoid the costly terms, we have used the truncation scheme as proposed by Joshi *et al,* [15] where the right exponential of the functional is full within the coupled cluster single and double (CCSD) approximation and all the higher order double linked terms within the CCSD approximation are taken in left exponent. The detailed algebraic expression and diagrammatic of the amplitude equations and first order energy derivative are given in Appendix A and Appendix B, respectively

2.3 Computational details

The DIRAC10 program package [16] is used to solve the DHF equation and to generate one-, and two-body matrix elements. The magnetic hyperfine integrals are constructed by using locally modified version of DIRAC10 program package. Finite size of nucleus with Gaussian charge distribution is considered as the nuclear model. The nuclear parameters for the Gaussian charge distribution are taken as default values in DIRAC10. Aug-cc-pCVQZ basis [17, 18] is used for Li, Be, Na, Mg, F atoms and aug-cc-pCV5Z [17] is used for H atom. We have used dyall.cv4z [19] basis for K, Ca and Cs atoms and dyall.cv3z [19] basis for Rb and Sr atoms. All the occupied orbitals are taken in our calculations. The virtual orbitals whose energy exceed a certain threshold (see Table 2.1) are not taken into account in our calculations as the contribution of high energy virtual orbitals is negligible in the correlation calculation. Restricted active space configuration

interaction (RAS-CI) calculations are done using a locally modified version of DIRAC10 package and the detailed description of RAS configuration is compiled in Table 2.1. The nuclear magnetic

Table 2.1: RAS-CI configuration and threshold energy of atoms and molecules

Atom/Molecule	RAS Configuration[a]		Threshold energy[b]
	RAS I	RAS II	(a.u.)
Li	2, 1	3, 4	∞
Na	6, 5	3, 4	∞
K	10, 9	3, 4	500
Rb	19, 18	3, 4	500
Cs			60
Be^+	2, 1	3, 4	∞
Mg^+	6, 5	3, 4	∞
Ca^+	10, 9	3, 4	500
Sr^+	19, 18	3, 4	100
BeH	3, 2	3, 4	∞
MgF	11, 10	3, 4	10
CaH	11, 10	5, 6	15

[a] In each RAS configuration spin up and spin down spinors are separated by comma. Maximum number of holes in RAS I is 2. Maximum number of electrons in RAS III is 2.
[b] ∞ value means all the spinors are considered in the correlation calculation.

Table 2.2: Nuclear magnetic moment (μ) and nuclear spin quantum no (I) of atoms

Atom	^{1}H	^{2}D	^{6}Li	^{7}Li	^{9}Be	^{19}F	^{23}Na	^{25}Mg	^{39}K	^{40}K	^{41}K	^{43}Ca	^{85}Rb	^{87}Rb	^{87}Sr
I [20]	1/2	1	1	3/2	3/2	1/2	3/2	5/2	3/2	4	3/2	7/2	5/2	3/2	9/2
μ/μ_N [20]	2.7928	0.8574	0.8220	3.2564	-1.1779	2.6288	2.2175	-0.8554	0.3914	-1.2981	0.2149	-1.3172	1.3530	2.7512	-1.0928

moment (μ) and spin quantum number (I) of the atoms are given in Table 2.2. The experimental bond length of molecules used in our calculation are presented in Table 2.3.

2.4 Results and discussion

The numerical results of our calculations of HFS constant using 4-component spinor ECC method, capable of treating ground state open-shell configuration are presented. We also present results using RAS-CI method.

Table 2.3: Bond length of the molecules in Å

Molecule	Bond length [21]
BeH	1.343
MgF	1.750
CaH	2.003

Table 2.4: Magnetic hyperfine structure constant (A) of ground state ($^2S_{1/2}$) of atoms in MHz

Atom	This work		Others	Experiment	$\delta\%$
	RAS-CI	ECC			
^{6}Li	148.5	149.3	152.1 [22]	152.1 [23]	1.9
^{7}Li	392.1	394.3	401.7 [22]	401.7 [23]	1.9
^{23}Na	812.1	861.8	888.3 [24]	885.8 [23]	2.8
^{39}K	188.8	223.5	228.6 [24]	230.8 [23]	3.3
^{40}K	-234.7	-277.9		-285.7 [25]	2.8
^{41}K	103.6	122.7		127.0 [23]	3.5
^{85}Rb	782.3	972.5	1011.1 [24]	1011.9 [26]	4.0
^{87}Rb	2651.0	3295.7		3417.3 [27]	3.7
^{133}Cs		2179.1	2278.5 [24]	2298.1 [28]	5.5
^{9}Be$^+$	-613.7	-614.6	-625.4 [22]	-625.0 [29]	1.7
^{25}Mg$^+$	-568.7	-581.6	-593.0 [30]	-596.2 [31]	2.5
^{43}Ca$^+$	-733.3	-794.9	-805.3 [32]	-806.4 [33]	1.4
^{87}Sr$^+$	-872.1	-969.9	-1003.2 [32]	-1000.5(1.0) [34]	3.1

In Table 2.4, we present the HFS constant values of alkali metal atoms starting from Li to Cs and singly charged alkaline earth metal atoms (Be$^+$ to Sr$^+$). Our results are compared with the available experimental values and the values calculated using RAS-CI method. The deviation of our ECC values from the experimental values are presented as $\delta\%$. Our ECC results are in good agreement with the experimental results ($\delta\% < 6\%$). It is observed that the deviations increase as we go down both in the alkali metal and in alkaline earth metal group of the periodic table except for the Ca$^+$ ion in the series. The deviations of RAS-CI and ECC values with the experimental values are presented in Figure 2.1. It is clear that the deviations of RAC-CI are always greater than ECC and it is expected as the coupled cluster is a better correlated theory than the truncated CI theory. It is interesting to note that the deviations in RAS-CI increase much faster rate compared

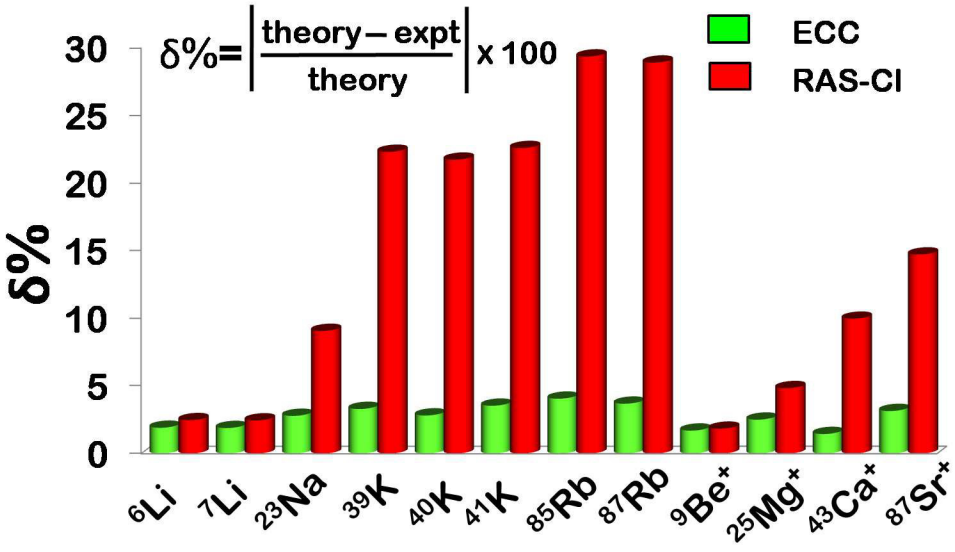

Figure 2.1: Comparison of relative deviations between ECC and RAS-CI values of our calculations.

to ECC as we go down the groups. This reflects the fact that truncated CI is not size extensive and thus it does not scale properly with the increasing number of electrons. It should be noted that the ratio of theoretically estimated HFS constant of different isotopes must be the ratio of their nuclear g factor for point nuclear model. Different isotopes are treated by changing the nuclear magnetic moment (μ) of the atom but nuclear parameters for each isotope are same which is by default of the most stable isotopes in DIRAC10. This causes difference in $\delta\%$ of different isotopes.

Table 2.5: Parallel ($A_{\parallel}$) and perpendicular ($A_{\perp}$) magnetic HFS constant of molecules in MHz

		$A_{\parallel}$					$A_{\perp}$				
Molecule	Atom	This work			Experiment	$\delta\%$	This work			Experiment	$\delta\%$
		SCF	RAS-CI	ECC	[35]		SCF	RAS-CI	ECC	[35]	
BeH	^{1}H	84.2	177.2	204.1	201(1) [36]	1.5	65.8	158.7	185.6	190.8(3) [36]	2.8
	^{9}Be	-182.7	-203.3	-200.6	-208(1) [36]	3.7	-169.4	-188.9	-186.0	-194.8(3) [36]	4.7
MgF	^{19}F	168.0	255.4	320.9	331(3) [37]	3.1	99.8	139.4	153.3	143(3) [37]	6.7
	^{25}Mg	-249.2	-272.4	-282.6			-239.4	-260.3	-270.4		
CaH	^{1}H	41.1	74.6	146.4	138(1) [38]	5.7	37.5	70.9	141.9	134(1) [38]	5.6
	^{43}Ca	-259.5	-307.9	-321.6			-242.7	-284.6	-295.7		

In Table 2.5, we present the parallel and perpendicular HFS constant of ground state of BeH,

MgF and CaH molecules obtained from RAS-CI and ECC theory. We have compared our ECC results with the available experimental values and the deviations are reported as $\delta\%$. Our calculated results within the ECC framework show good agreement with the experimental values. The highest deviation for parallel HFS constant is in the case of ^{1}H of CaH where the ECC value differs only $\sim$ 8.5 MHz. This is also better than the RAS-CI values where the deviation is too off ($\sim$ 63.5 MHz) from the experimental values. However, $A_{\parallel}$ value for ^{9}Be in BeH and ^{19}F in MgF, RAS-CI yields marginally better results ($\sim$ 10 MHz) as compared to ECC.

Table 2.6: Magnetic HFS constant of ^1H of CaH molecule in RAS-CI method

Basis		$A_{\parallel}$ (MHz)					$A_{\perp}$ (MHz)			
Ca	H	Spinor	SCF	Correlation	Total	Experiment	SCF	Correlation	Total	Experiment
dyall.v3z	cc-pVTZ	192	38.9	35.3	74.2		35.3	35.4	70.7	
dyall.cv3z	aug-cc-pCV5Z	274	41.2	33.4	74.6	138(1) [35, 38]	37.5	33.4	70.9	134(1) [35, 38]
dyall.cv3z	aug-cc-pCV5Z	318	41.2	34.0	75.2		37.5	34.1	71.6	

Like the RAS-CI parallel HFS constant values of ^{1}H of CaH, the perpendicular HFS constant is very off from the experimental values. To investigate this, we have calculated the HFS of CaH with more number of virtual orbitals in the same as well as with a different basis. The results are presented in table 2.6. It is clear from the Table that for this system RAS-CI gives very bad estimation of HFS constant. A possible explanation is as follows, according to Kutzelnigg's error analysis [39] the comparative error in CI energy can be written as [O(δ + O(S^2))]^2 where e^S is the wave operator of NCC method and δ is the error of the wave operator. Although the comparative error analysis of CI by Kutzelnigg is with respect to NCC but we expect a similar expression will be hold for ECC also. From Table 2.6, it is clear that the DHF (SCF) contribution to the energy derivative is significantly less whereas the correlation contribution for ECC to the energy derivative is very large as compared to SCF contribution which is evident from table 2.5. Therefore, the DHF ground state is very poor reference for this system and for ECC, the wave operator must be large enough. Thus, it associates considerably large error in the CI energy as the error in CI energy is proportional to the quartic of wave operator of CC wave function.

It is interesting to see that both the parallel and perpendicular HFS of ^{1}H decrease as we go from BeH to CaH. This indicates that the spin density near ^{1}H nucleus of CaH is less than that of

BeH. This explains the ionicity of the bond in CaH is greater than the bond in BeH.

Table 2.7: Comparison of full CI and ECC HFS values (in MHz) of ^{7}Li

Basis	Full CI	ECC
aug-cc-pCVDZ	384.1	383.9
aug-cc-pCVTZ	402.0	401.5
aug-cc-pCVQZ[a]	386.0	385.5

[a] Considering 3 electrons and 189 virtual orbitals

Table 2.8: Comparison of full CI and ECC HFS values (in MHz) of $^{9}Be^{+}$

Basis	Full CI	ECC
aug-cc-pCVDZ	-586.6	-586.5
aug-cc-pCVTZ	-615.7	-615.6
aug-cc-pCVQZ[a]	-613.0	-612.8

[a] Considering 3 electrons and 183 virtual orbitals

Table 2.9: Comparison of full CI and ECC HFS values (in MHz) of BeH

Basis	Atom	$A_{\parallel}$		$A_{\perp}$	
		Full CI	ECC	Full CI	ECC
cc-pVDZ	^{9}Be	-158.7	-159.3	-145.9	-146.6
	^{1}H	189.9	187.6	174.5	172.2
aug-cc-pVDZ	^{9}Be	-165.5	-166.1	-152.6	-153.2
	^{1}H	188.7	186.2	172.1	169.7

We have done series of calculations to estimate uncertainty in our calculations by comparing our ECC results with FCI results taking example of ^{7}Li, ^{9}Be and BeH. The comparison of full CI and ECC HFS constant values of ^{7}Li and $^{9}Be^{+}$ is presented in table 2.7 and table 2.8 respectively. The comparison of parallel and perpendicular component of full CI and ECC HFS constant values of BeH is compiled in table 2.9. We believe that the uncertainty in our calculations with respect to full CI results for the atomic systems are well within 5% and 10% for the molecular systems considering all possible sources of error in our calculations.

2.5 Conclusion

We have successfully implemented the relativistic ECC method using 4-component Dirac spinors to calculate first order energy derivatives of atoms and molecules in their open-shell ground state configuration. We applied this method to calculate the magnetic HFS constant of Li, Na, K, Rb, Cs, Be^{+}, Mg^{+}, Ca^{+} and Sr^{+} along with parallel and perpendicular magnetic HFS constant of BeH,

MgF and CaH molecules. We also present RAS-CI results to show the effect of correlation in the calculation of HFS constant. Our ECC results are in good agreement with the experiment. We have found some anomalies in RAS-CI results of CaH and given a possible explanation.

Although the implemented ECC method yields relatively good results for the HFS constant of light and moderately heavy atoms and small diatomic molecules, it is not good enough for our purpose as the generated wavefunction is not that much accurate in the nuclear region what we need for the calculation of various $\mathcal{P},\mathcal{T}$-odd interaction constants. The worse part is that as the amplitude equations for both excitation and deexcitation operators are coupled in the ECC method, it takes too much time to solve the amplitude equations with our truncation scheme. So, it is very difficult, if not impossible to calculate the $\mathcal{P},\mathcal{T}$-odd interaction constants of the relevant systems with a reasonable basis set using the ECC method with the truncation scheme stated above.

References

[1] J. Čížek, Journal of Chemical Physics **45**, 4256 (1966).

[2] J. Čížek, *On the Use of the Cluster Expansion and the Technique of Diagrams in Calculations of Correlation Effects in Atoms and Molecules* (John Wiley & Sons, Inc., 2007), pp. 35–89.

[3] R. J. Bartlett and G. D. Purvis, International Journal of Quantum Chemistry **14**, 561 (1978).

[4] R. J. Bartlett and M. Musiał, Reviews of Modern Physics **79**, 291 (2007).

[5] D. Mukherjee and S. Pal, Advances in Quantum Chemistry **20**, 291 (1989).

[6] H. J. Monkhorst, Int. J. Quantum Chem. **12**, 421 (1977).

[7] H. Sekino and R. J. Bartlett, International Journal of Quantum Chemistry **26**, 255 (1984).

[8] E. A. Salter, G. W. Trucks, and R. J. Bartlett, Journal of Chemical Physics **90**, 1752 (1989).

[9] H. Koch *et al.*, Journal of Chemical Physics **92**, 4924 (1990).

[10] P. G. Szalay, M. Nooijen, and R. J. Bartlett, Journal of Chemical Physics **103**, 281 (1995).

[11] J. Arponen, Annals of Physics **151**, 311 (1983).

[12] R. Bishop, J. Arponen, and P. Pajanne, *Aspects of Many-body Effects in Molecules and Extended Systems, Lecture Notes in Chemistry Vol. 50* (Springer-Verlag, Berlin, 1989).

[13] S. Pal, Physical Review A **39**, 2712 (1989).

[14] N. Vaval, K. B. Ghose, and S. Pal, Journal of Chemical Physics **101**, 4914 (1994).

[15] S. P. Joshi and N. Vaval, Chemical Physics Letters **568**, 170 (2013).

[16] DIRAC, a relativistic ab initio electronic structure program, Release DIRAC10 (2010), written by T. Saue, L. Visscher and H. J. Aa. Jensen, with contributions from R. Bast, K. G. Dyall, U. Ekström, E. Eliav, T. Enevoldsen, T. Fleig, A. S. P. Gomes, J. Henriksson, M. Iliaš, Ch. R. Jacob, S. Knecht, H. S. Nataraj, P. Norman, J. Olsen, M. Pernpointner, K. Ruud, B. Schimmelpfennig, J. Sikkema, A. Thorvaldsen, J. Thyssen, S. Villaume, and S. Yamamoto (see http://www.diracprogram.org).

[17] T. H. Dunning, Journal of Chemical Physics **90**, 1007 (1989).

[18] D. E. Woon and T. H. Dunning Jr. (unpublished).

[19] K. G. Dyall, The Journal of Physical Chemistry A **113**, 12638 (2009).

[20] http://www.webelements.com/isotopes.html.

[21] http://ccbdb.nist.gov/.

[22] V. Yerokhin, Physical Review A **78**, 012513 (2008).

[23] A. Beckmann, K. Böklen, and D. Elke, Zeitschrift für Physik **270**, 173 (1974).

[24] M. Safronova, W. Johnson, and A. Derevianko, Physical Review A **60**, 4476 (1999).

[25] J. Eisinger, B. Bederson, and B. Feld, Physical Review **86**, 73 (1952).

[26] J. Vanier, J.-F. Simard, and J.-S. Boulanger, Physical Review A **9**, 1031 (1974).

[27] L. Essen, E. Hope, and D. Sutcliffe, Nature **189**, 298 (1961).

[28] E. Arimondo, M. Inguscio, and P. Violino, Reviews of Modern Physics **49**, 31 (1977).

[29] D. Wineland, J. Bollinger, and W. M. Itano, Physical Review Letters **50**, 628 (1983).

[30] C. Sur, B. K. Sahoo, R. K. Chaudhuri, B. Das, and D. Mukherjee, The European Physical Journal D-Atomic, Molecular, Optical and Plasma Physics **32**, 25 (2005).

[31] W. M. Itano and D. Wineland, Physical Review A **24**, 1364 (1981).

[32] K.-z. Yu, L.-j. Wu, B.-c. Gou, and T.-y. Shi, Physical Review A **70**, 012506 (2004).

[33] F. Arbes, M. Benzing, T. Gudjons, F. Kurth, and G. Werth, Zeitschrift für Physik D Atoms, Molecules and Clusters **31**, 27 (1994).

[34] F. Buchinger *et al.*, Physical Review C **41**, 2883 (1990).

[35] W.Weltner, *Magnetic Atoms and Molecules* (Dover, New York, 1983).

[36] L. Knight Jr, J. Brom Jr, and W. Weltner Jr, Journal of Chemical Physics **56**, 1152 (1972).

[37] L. Knight Jr, W. Easley, W. Weltner Jr, and M. Wilson, Journal of Chemical Physics **54**, 322 (1971).

[38] L. B. Knight Jr and W. Weltner Jr, Journal of Chemical Physics **54**, 3875 (1971).

[39] W. Kutzelnigg, Theoretica chimica acta **80**, 349 (1991).

CHAPTER 3

Implementation of the Z-vector Method in the Relativistic Coupled-Cluster Framework to Generate an Accurate Wavefunction in the Near Nuclear as well as Outer Region

> The essence of science is that it is always willing to abandon a given idea for a better one; the essence of theology is that it holds its truths to be eternal and immutable.
>
> H.L. Mencken

As the ECC method, implemented in the previous chapter is not good enough to fulfill our purpose, in this chapter, we opted for the implementation of Z-vector method in the relativistic coupled-cluster framework to generate an accurate wavefunction in the nuclear region as well as outer region. The implemented method is applied to calculate the molecular dipole moment and parallel component of the magnetic hyperfine-structure constant of the SrF molecule. The results of our calculation are compared with the experimental and other available theoretically calculated values. We are successful in achieving good accordance with the experimental results. We also compared the Z vector results of the HFS constants of alkali metals and singly charged alkaline-earth-metals with the results using the ECC method calculated in the previous chapter using the same basis and cutoff. The comparison shows that the Z-vector method can yields more accurate results than the ECC method. Thus, these results show that the Z-vector method can yield an accurate wave function in both the far and near nuclear region.

3.1 Introduction

In the previous chapter, we have tried to solve the coupled cluster method in a variational way. Although we were quite successful to implement the extended coupled cluster (ECC) method and to calculate the magnetic hyperfine structure constant of atoms and molecules, the ECC method is not good enough for our purpose. So, in this chapter, we have tried to solve the coupled cluster method in a non-variational or in other word, a traditional way. The normal coupled cluster (NCC) [1–5] method is known to be the most elegant many-body theory to effectuate the dynamic part of the electron correlation. The calculations of one electron response properties in the NCC framework, can either be done by taking expectation value of the desired property operator or as a derivative of energy. These two approaches are not same as the NCC is by nature non-variational. In fact, the first order derivative of energy is the corresponding expectation value plus some additional terms, which makes the derivative approach closer to the full configuration interaction (FCI) property value. It is worth to mention that the expectation value approach in the NCC leads to a nonterminating series and any truncation scheme introduces an additional error [6].

In general, the energy is a function of both the determinantal coefficients (C_D) in the expansion of the many electron correlated wavefunction and the molecular orbital coefficients (C_M) for a fixed nuclear geometry [7]. The first order energy derivative in NCC can be written as

$$\frac{\delta E[C_D(\lambda), C_M(\lambda)]}{\delta \lambda} = \frac{\delta E}{\delta C_D}\frac{\delta C_D}{\delta \lambda} + \frac{\delta E}{\delta C_M}\frac{\delta C_M}{\delta \lambda}.$$

Thus, for the calculation of energy derivative in NCC framework, it is, therefore, necessary to calculate the derivative of energy with respect the determinantal coefficients as well as the molecular orbital coefficients. It further requires the derivative of the determinantal coefficients and molecular orbital coefficients with respect to the external field of perturbation. However, Bartlett and co-workers [8] have shown that these derivative terms can be transformed into a single linear equation by using Z-vector method. The advantage of the Z-vector method [9, 10] is that for the calculation of several properties, one needs to solve a single linear equation instead of solving equations for each external perturbation field of interest. The detailed diagrammatic of Z-vector method in NCC framework is given in Ref. [10].

we have shown that the Z-vector method in the NCC framework within its four component description can generate an accurate wavefunction in the near nuclear region as well as in the region far from the nucleus. To justify our argument, we have compared magnetic hyperfine structure constant (HFS) and molecular dipole moment of SrF with the experimental values as the calculation of these properties need an accurate wavefunction in the near nuclear region and the region far from the nucleus, respectively.

3.2 Why SrF?

The knowledge of long range dipole-dipole interaction is very important to produce ultra cold molecules in optical lattice [11]. SrF molecule can be cooled by laser spectroscopy [12] and thus, it can be used for high precession spectroscopy [13, 14]. Currently an experimental search for parity violation using SrF molecule is in progress [15]. Therefore, detailed knowledge of the spectroscopic properties like dipole moment and magnetic HFS is very important to interpret the experimental findings.

3.3 Z-vector method

The dynamic part of the electron correlation is included using the coupled cluster method. The details about the single reference coupled-cluster method is discussed in Section 1.14

The coupled cluster energy is a function of both the determinantal coefficients (C_D) and the molecular orbital coefficients (C_M). Therefore, the calculation of coupled cluster energy derivative need both the derivative of C_Ds and C_Ms with respect to external field of perturbation. However, the equations involving derivative of C_Ds and C_Ms are linear equations. Thus, one needs to solve the linear equations for each external field perturbation of interest. However, the derivative of energy with respect to determinantal coefficients, C_D, and the derivative of C_D with respect to external perturbation field can be included with the introduction of a perturbation independent linear operator (Λ) whose solution yields the Z-vector [10]. Therefore, the solution of one linear equation is required instead of solving for each external perturbation. The second quantized form

of the perturbation independent operator, Λ is given by

$$\Lambda = \Lambda_1 + \Lambda_2 + ... + \Lambda_N = \sum_n^N \Lambda_n \tag{3.1}$$

where

$$\Lambda_m = \frac{1}{(m!)^2} \sum_{ij..ab..} \lambda_{ab..}^{ij..} a_i^\dagger a_j^\dagger ....a_b a_a \tag{3.2}$$

where i,j(a,b) are the hole(particle) indices and $\lambda_{ab..}^{ij..}$ are the cluster amplitudes corresponding to the cluster operator Λ_m. The detailed description of Λ operator and corresponding amplitude equation is given in Ref. [10].

$$\langle\Phi_0|[\Lambda(H_N e^T)_c]_c|\Phi_{i..}^{a..}\rangle + \langle\Phi_0|(H_N e^T)_c|\Phi_{i..}^{a..}\rangle + \langle\Phi_0|(H_N e^T)_c|\Phi_{int}\rangle\langle\Phi_{int}|\Lambda|\Phi_{i..}^{a..}\rangle = 0. \tag{3.3}$$

where Φ_{int} is the determinant corresponding to the intermediate excitation between Φ_0 and $\Phi_{i..}^{a..}$. In the coupled cluster single and double (CCSD) model, Λ becomes, $\Lambda = \Lambda_1 + \Lambda_2$. The explicit equations for the amplitudes of Λ_1 and Λ_2 operators are

$$\langle\Phi_0|[\Lambda(H_N e^T)_c]_c|\Phi_i^a\rangle + \langle\Phi_0|(H_N e^T)_c|\Phi_i^a\rangle = 0, \tag{3.4}$$

$$\langle\Phi_0|[\Lambda(H_N e^T)_c]_c|\Phi_{ij}^{ab}\rangle + \langle\Phi_0|(H_N e^T)_c|\Phi_{ij}^{ab}\rangle + \langle\Phi_0|(H_N e^T)_c|\Phi_i^a\rangle\langle\Phi_i^a|\Lambda|\Phi_{ij}^{ab}\rangle = 0. \tag{3.5}$$

It is interesting to note that the term $\langle\Phi_0|(H_N e^T)_c|\Phi_i^a\rangle\langle\Phi_i^a|\Lambda|\Phi_{ij}^{ab}\rangle$ of Eq. (3.5) yields one disconnected diagram, which is given in Figure 3.1. The said diagram is not of the type of closed with disconnected part. This ensures that the energy derivative is linked and thus size extensive. The energy derivative can be given as

$$\Delta E' = \langle\Phi_0|(O_N e^T)_c|\Phi_0\rangle + \langle\Phi_0|[\Lambda(O_N e^T)_c]_c|\Phi_0\rangle \tag{3.6}$$

where, O_N is the derivative of normal ordered perturbed Hamiltonian with respect to external field of perturbation. The detailed diagrammatic expression is given in Figure 3.2 and the corresponding algebraic equation is given in the following Eq. 3.7,

$$\begin{aligned}\Delta E' \;=\; & O(i,a)\cdot t_i^a + \lambda_a^i \cdot O(a,i) + \lambda_a^i \cdot O(a,b)\cdot t_i^b + \lambda_a^i \cdot O(j,i)\cdot t_j^a + \lambda_a^i \cdot O(j,b)\cdot t_{ij}^{ab} \\ & -\lambda_a^i \cdot O(j,b)\cdot t_i^b \cdot t_j^a - \frac{1}{2}\lambda_{ab}^{ij}\cdot O(k,j)\cdot t_{ik}^{ab} + \frac{1}{2}\lambda_{ab}^{ij}\cdot O(b,c)\cdot t_{ij}^{ac} \\ & -\frac{1}{2}\lambda_{bc}^{ik}\cdot O(j,a)\cdot t_i^a \cdot t_{jk}^{bc} - \frac{1}{2}\lambda_{ac}^{jk}\cdot O(i,b)\cdot t_i^a \cdot t_{jk}^{bc}.\end{aligned} \tag{3.7}$$

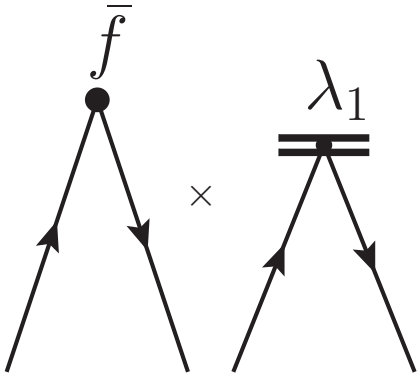

Figure 3.1: Disconnected yet linked diagram in Λ_2 equation.

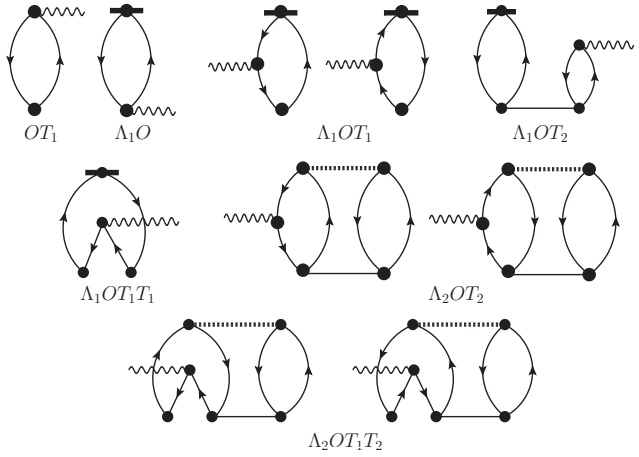

Figure 3.2: Diagrams for the energy derivative in Z-vector method

Here, we have used Einstein summation convention in the expression. The rules to generate algebraic expression are given in Ref. [16].

3.4 Computational details

The N electron ground and excited determinants are constructed with the one electron spinors, which are the solutions of Dirac-Hartree-Fock equation. The DIRAC10 [17] program package is used to solve the Dirac-Fock equation and to obtain the matrix elements required for property

calculations. Gaussian charge distribution is considered as the nuclear model where the nuclear parameters [18] are taken as default values in DIRAC10. Large and small component basis functions are generated by applying restricted kinetic balance (RKB) [19] in which basis functions are represented in scalar basis and unphysical solutions are removed by diagonalizing the free particle Hamiltonian. This generates the electronic and positronic solution in 1:1 manner. We have done five different sets of calculation using five different basis sets for Sr and F. These are cc-pVDZ, aug-cc-pVTZ, aug-cc-pCVTZ, d-aug-cc-pCVTZ and aug-cc-pCVQZ for F atom [20] and dyall.v2z, dyall.v3z, dyall.cv3z, d-aug-dyall.cv3z and dyall.cv4z for Sr atom [21]. Both large and small component basis are taken in uncontracted form. None of the electrons are frozen in our correlation calculation and the virtual orbitals whose energies are greater than a certain threshold are not considered as the high energy virtual orbitals contribute less in correlation calculation.

We have taken the following strategies to code the Z-vector method. First, the one electron and two electron matrix elements are obtained from DIRAC10 package [17]. Then we have solved the NCC part i.e., the T_1 and T_2 amplitude equations. This is followed by the construction of different types of $\bar{H}$ ($\bar{H} = (He^T)_c$). After that $\bar{H}$ vertices are contracted with one Λ_1 or Λ_2 vertex to construct the Λ_1 and Λ_2 amplitude equations. At the end T_1, T_2, Λ_1 and Λ_2 amplitudes are contracted with property integrals to get corresponding property value. To solve the T_1 and T_2 amplitudes and to construct the $\bar{H}$, we have used a recursive intermediate factorization of diagrams as described by Bartlett and coworkers [22]. This saves enormous computational cost.

Table 3.1: Cutoff used and correlation energy of the ground state of SrF in different basis sets

Basis			Cutoff	Spinor	Correlation Energy
Name	Sr	F	(a.u.)		CCSD (a.u.)
A	dyall.v2z	cc-pVDZ		298	-1.474175309
B	dyall.v3z	aug-cc-pVTZ	500	366	-1.256789931
C	dyall.cv3z	aug-cc-pCVTZ	500	436	-1.775710294
D	d-aug-dyall.cv3z	d-aug-cc-pCVTZ	100	596	-1.621603448
E	dyall.cv4z	aug-cc-pCVQZ	50	520	-1.402836367

To debug this code, we benchmarked our correlation energy with the results obtained from

DIRAC10 with same basis, same convergence criteria and using same direct inversion in the iterative subspace (DIIS). We have achieved 7 to 8 decimal place agreement with DIRAC10 program package for correlation energy independent of the choice of molecules as well as of the basis sets. The discrepancy beyond this limit could be due to the use of cutoff in storing of the intermediate diagrams or the use of different convergence algorithm. The H and $\bar{H}$ matrix elements are stored by setting a cutoff of 10^{-12} to save storage requirement as the contribution of the two body matrix elements beyond that limit is negligible. The tolerance used for the convergence of both T and Λ amplitudes is 10^{-9}. We have used the experimental bond length (2.075 Å) of SrF [23] in all the calculations.

3.5 Results and discussion

3.5.1 Molecular dipole moment and magnetic hyperfine structure constant of SrF

In Table 3.1, we present the basis sets used in our calculations and each combination is denoted by an English alphabet letter. The fourth and fifth column of Table 3.1 represent the cutoff used and the number of spinor generated using that cutoff for correlation calculation, respectively. We also compiled the correlation energy of SrF obtained from CCSD and second-order many body perturbation theory (MBPT(2)), which uses a first-order perturbed wavefunction.

Table 3.2: Molecular dipole moment (μ) (in Debye) of the ground state of SrF

Basis	Z-vector	Experiment [24]
A	3.0158	
B	3.3898	
C	3.4023	3.4676(10)
D	3.4376	
E	3.4504	

In Table 3.2, we present the molecular dipole moment in units of Debye of the ground state of SrF molecule in five different basis sets. The experimental value [24] is also presented in

the same table for comparison. It is clear from the table that with increase in the number of basis function the dipole moment converges towards the experimental value. This is expected as more basis functions generate more correlation space and thereby improve the dipole moment. In particular, our calculated dipole moment in basis E is very close ($\sim$ 0.5 %) to the experimental value. The results obtained for the dipole moment of the ground state of SrF by other methods and

Table 3.3: Comparison of molecular dipole moment (μ) of the ground state of SrF in different methods

Method	Reference	μ (D)
Ionic model	Torring *et al.* [25]	3.67
SCF	Langhoff *et al.* [26]	2.579
CPF	Langhoff *et al.* [26]	3.199
CISD	Langhoff *et al.* [26]	2.523
EPM	Mestdagh *et al.* [27]	3.6
HF (finite difference)	Kobus *et al.* [28]	2.5759
CCSD	Prasannaa *et al.* [29]	3.41
Z-vector	This work(E)	3.4504
Expt.	Ernst *et al.* [24]	3.4676(10)

experiment are compiled in Table 3.3. The dipole moment of SrF was first calculated by Torring *et al,* [25] by using an ionic model and they got a value of 3.67 D. Langhoff *et al,* [26] performed the first *ab initio* calculation of the dipole moment of SrF by using Slater type of basis function. They reported the dipole moment using three different methods, i.e., self consistent field (SCF), configuration interaction in single and double approximation (CISD) and the coupled pair function (CPF) method. Among them, CISD method is not size extensive while CPF is, thus CPF approach gives better agreement with experiment. However, Langhoff *et al,* did not consider the relativistic motion of electrons. Mestdagh *et al,* [27] used electrostatic polarization model and got 3.6 D as a molecular dipole moment of SrF. Kobus *et al,* [28] obtained a dipole moment of 2.5759 D by using finite difference method in the Hartree-Fock (HF) level. The first relativistic calculation of dipole moment of SrF in the CCSD model was calculated by Prasannaa *et al,* [29] by taking expectation value of the corresponding operator. The expectation value framework leads to a connected yet nonterminating series. Prasannaa *et al,* took only the linear terms in the property calculations using CCSD wavefunction and got 3.41 D as a result. Our four component Z-vector calculation

gives a result of 3.4504 D by using dyall.cv4z basis for Sr [21] and aug-cc-pCVQZ basis for F [20] (basis E) and this result shows the best agreement with the experiment so far.

Table 3.4: Parallel ($A_{\parallel}$) magnetic hyperfine structure constant of the ground state of SrF in MHz

	^{87}Sr		^{19}F	
Basis	Z-vector	Experiment	Z-vector	Experiment
A	546.08		121.93	
B	558.96		118.70	
C	566.62	591(3) [30]	119.64	126(3) [30]
D	561.25	576.27(2) [31]	116.35	127.49(2) [31]
E	559.65		117.74	

In Table 3.4, we present the parallel component of the magnetic HFS constant of ^{87}Sr and ^{19}F of the ground state of SrF molecule. We also present the experimental value [30, 31] of those in the same table for comparison.

Our calculated result using Z-vector method show good agreement with the experimental result. The highest and lowest deviation from the latest experimental values [31] for parallel magnetic HFS constant of ^{87}Sr atom are for the basis A ($\sim$ 30 MHz) and C ($\sim$ 10 MHz) respectively. For the parallel magnetic HFS constant of ^{19}F, the maximum and minimum deviation occur for the basis D ($\sim$ 11 MHz) and A ($\sim$ 6 MHz) basis.

The calculated magnetic HFS constant values are in good agreement with the sophisticated experiment but the extent of accuracy is not so in comparison to that of the calculated dipole moment values. This could possibly be due to the fact that as we proceed from basis A to E, we have added extra Gaussian type orbitals (GTOs) of higher angular momentum in addition to lower angular momentum. As the higher angular momentum GTO shifts the electron density towards the outer region, the addition of higher angular momentum GTO improves the outer region much better than the inner region of the molecular wavefunction. This is why as we go from basis A to E, our molecular dipole moment value matches more closely than the magnetic HFS values with the experimental results.

3.5.2 Magnetic hyperfine structure constant of atoms

Although the Z-vector results of molecular dipole moment of SrF are quite impressive, the parallel component of the magnetic HFS constants of SrF are not quite good as compared to molecular dipole moment. So, the wavefunction produced by the Z-vector method is more accurate in the outer region than the nuclear region of SrF. To check whether the Z-vector method can produce more impressive wavefunction in the nuclear region or not and how good is the near nuclear wavefunction of Z-vector compared to the extended coupled cluster (ECC) method, we have calculated and compared the magnetic HFS constant of alkali metals and mono-positive alkaline earth metals. We have used the same basis and cutoff for the atoms as used in the ECC calculation of the previous chapter (for more details see Section 2.3 of Chapter 2).

Table 3.5: Hyperfine coupling constant (in MHz) of ground state of atoms

Atom	SCF	ECC [32]	Z-vector	Expt.	δ%	
					ECC	Z-vector
^{6}Li	107.2	149.3	148.3	152.1 [33]	1.9	2.6
^{7}Li	283.2	394.3	391.6	401.7 [33]	1.9	2.6
^{23}Na	630.6	861.8	859.8	885.8 [33]	2.8	3.0
^{39}K	151.0	223.5	226.6	230.8 [33]	3.3	1.9
^{40}K	-187.7	-277.9	-281.8	-285.7 [34]	2.8	1.4
^{41}K	82.9	122.7	124.4	127.0 [33]	3.5	2.1
^{85}Rb	666.9	972.5	986.5	1011.9 [35]	4.1	2.6
^{87}Rb	2260.1	3295.7	3343.3	3417.3 [36]	3.7	2.2
^{133}Cs	1495.5	2179.1	2218.4	2298.1 [37]	5.5	3.6
^{223}Fr	5518.0		7512.2	7654(2) [38]		1.9
^{9}Be^{+}	-498.8	-614.6	-612.9	-625.0 [39]	1.7	2.0
^{25}Mg^{+}	-466.7	-581.6	-584.8	-596.2 [40]	2.5	1.9
^{43}Ca^{+}	-606.2	-794.9	-801.5	-806.4 [41]	1.4	0.6
^{87}Sr^{+}	-761.0	-969.9	-977.9	-1000.5(1.0) [42]	3.2	2.3
^{135}Ba^{+}	2737.4		3513.3	3591.7 [43]		2.2
^{137}Ba^{+}	3062.1		3930.2	4018.9 [43]		2.3
^{223}Ra^{+}	2842.8		3433.9	3404(2) [44, 45]		0.9

In Table 3.5, we present the magnetic HFS constant of alkali metal atoms singly charged alkaline earth metal atoms using Z-vector method. We also present the experimental results and the

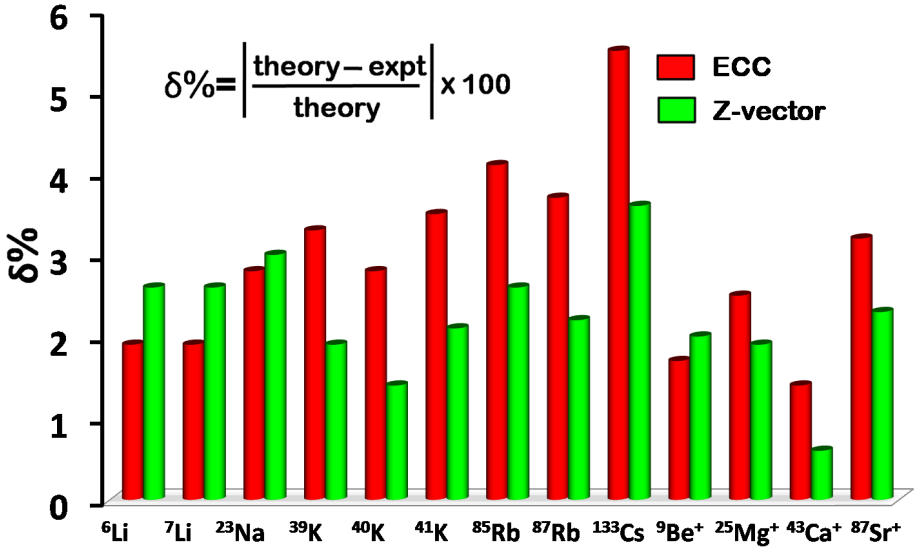

Figure 3.3: Comparison of relative deviations between Z-vector and ECC values of magnetic HFS constant of atoms.

values calculated using ECC method [32]. The deviation of the Z-vector values from the experimental values are presented as $\delta\%$ in the same table. From the table, it is clear that the deviation of Z-vector results from the experiments are well within 3% except for the ^{133}Cs atom, where it is 3.6%. The Z-vector results are quite impressive, especially for the heavy atoms. The deviations of ECC and Z-vector values from the experimental values are presented in Figure 3.3. From the figure, it is clear that Z-vector results are far better than the ECC results except for three small atoms like Li, Na and Be^+. So, the above results show that the Z-vector method can produce far better wavefunction in the nuclear region than the ECC method and it is quite impressive for the heavy atoms also.

3.6 Conclusion

We have successfully implemented the Z-vector method in the relativistic coupled cluster framework to calculate the first order energy derivatives. We applied this method to calculate the molecular dipole moment and parallel magnetic HFS constant of SrF molecule. We have also calculated the magnetic HFS constant of alkali metal atoms and mono-positive alkaline earth metal atoms.

The results from our calculations are in good agreement with the experimental values. As the magnetic HFS constant and the molecular dipole moment demand the wavefunction to be accurate in the near nuclear region and the region away from nucleus, respectively, we can conclude that the Z-vector method in the relativistic framework can produce an accurate wavefunction in the near nuclear region as well as far from the nucleus. In the Z-vector method, the equation of the cluster amplitudes of excitation operators are decoupled from the deexcitation operators and thus, those equation converges much faster than the ECC method. This makes the Z-vector method more feasible than the ECC method from a computational point of view.

References

[1] J. Čížek, Journal of Chemical Physics **45**, 4256 (1966).

[2] J. Čížek, *On the Use of the Cluster Expansion and the Technique of Diagrams in Calculations of Correlation Effects in Atoms and Molecules* (John Wiley & Sons, Inc., 2007), pp. 35–89.

[3] R. J. Bartlett and G. D. Purvis, International Journal of Quantum Chemistry **14**, 561 (1978).

[4] R. J. Bartlett and M. Musiał, Reviews of Modern Physics **79**, 291 (2007).

[5] D. Mukherjee and S. Pal, Advances in Quantum Chemistry **20**, 291 (1989).

[6] W. Kutzelnigg, Theoretica chimica acta **80**, 349 (1991).

[7] H. J. Monkhorst, Int. J. Quantum Chem. **12**, 421 (1977).

[8] G. Fitzgerald, R. J. Harrison, and R. J. Bartlett, Journal of Chemical Physics **85**, 5143 (1986).

[9] N. C. Handy and H. F. Schaefer, Journal of Chemical Physics **81**, 5031 (1984).

[10] E. A. Salter, G. W. Trucks, and R. J. Bartlett, Journal of Chemical Physics **90**, 1752 (1989).

[11] C. Trefzger, C. Menotti, B. Capogrosso-Sansone, and M. Lewenstein, Journal of Physics B: Atomic, Molecular and Optical Physics **44**, 193001 (2011).

[12] E. S. Shuman, J. F. Barry, and D. DeMille, Nature **467**, 820 (2010).

[13] S. Mathavan, C. Meinema, J. van den Berg, H. Bethlem, and S. Hoekstra, Deceleration, cooling and trapping of srf molecules for precision spectroscopy, in *46th Conference of the European Groups on Atomic Systems*, p. 54, 2014.

[14] J. van den Berg *et al.*, Journal of Molecular Spectroscopy **300**, 22 (2014).

[15] J. v. d. Berg, K. Jungmann, C. Meinema, A. v. d. Poel, and S. Hoekstra, Verhandlungen der Deutschen Physikalischen Gesellschaft (2012).

[16] I. Shavitt and R. J. Bartlett, *Many-body methods in chemistry and physics: MBPT and coupled-cluster theory* (Cambridge university press, 2009).

[17] DIRAC, a relativistic ab initio electronic structure program, Release DIRAC10 (2010), written by T. Saue, L. Visscher and H. J. Aa. Jensen, with contributions from R. Bast, K. G. Dyall, U. Ekström, E. Eliav, T. Enevoldsen, T. Fleig, A. S. P. Gomes, J. Henriksson, M. Iliaš, Ch. R. Jacob, S. Knecht, H. S. Nataraj, P. Norman, J. Olsen, M. Pernpointner, K. Ruud, B. Schimmelpfennig, J. Sikkema, A. Thorvaldsen, J. Thyssen, S. Villaume, and S. Yamamoto (see http://www.diracprogram.org).

[18] L. Visscher and K. Dyall, Atomic Data and Nuclear Data Tables **67**, 207 (1997).

[19] K. Faegri Jr and K. G. Dyall, *Introduction to relativistic quantum chemistry* (Oxford University Press, USA, 2007).

[20] T. H. Dunning, Journal of Chemical Physics **90**, 1007 (1989).

[21] K. G. Dyall, The Journal of Physical Chemistry A **113**, 12638 (2009).

[22] S. A. Kucharski and R. J. Bartlett, Theoretica chimica acta **80**, 387 (1991).

[23] K. Huber and G. Herzberg, *Constants of Diatomic Molecules, Vol. 4, Molecular Spectra and Molecular Structure* (Van Nostrand Reinhold, New York, 1979).

[24] W. Ernst, J. Kändler, S. Kindt, and T. Törring, Chemical physics letters **113**, 351 (1985).

[25] T. Törring, W. Ernst, and S. Kindt, Journal of Chemical Physics **81**, 4614 (1984).

[26] S. R. Langhoff, C. W. Bauschlicher Jr, H. Partridge, and R. Ahlrichs, Journal of Chemical Physics **84**, 5025 (1986).

[27] J. Mestdagh and J. Visticot, Chemical physics **155**, 79 (1991).

[28] J. Kobus, D. Moncrieff, and S. Wilson, Physical Review A **62**, 062503 (2000).

[29] V. Prasannaa, M. Abe, and B. Das, Physical Review A **90**, 052507 (2014).

[30] W.Weltner, *Magnetic Atoms and Molecules* (Dover, New York, 1983).

[31] Y. Azuma, W. Childs, G. Goodman, and T. Steimle, Journal of Chemical Physics **93**, 5533 (1990).

[32] S. Sasmal, H. Pathak, M. K. Nayak, N. Vaval, and S. Pal, Phys. Rev. A **91**, 022512 (2015).

[33] A. Beckmann, K. Böklen, and D. Elke, Zeitschrift für Physik **270**, 173 (1974).

[34] J. Eisinger, B. Bederson, and B. Feld, Physical Review **86**, 73 (1952).

[35] J. Vanier, J.-F. Simard, and J.-S. Boulanger, Physical Review A **9**, 1031 (1974).

[36] L. Essen, E. Hope, and D. Sutcliffe, Nature **189**, 298 (1961).

[37] E. Arimondo, M. Inguscio, and P. Violino, Reviews of Modern Physics **49**, 31 (1977).

[38] J. E. Sansonetti, Journal of physical and chemical reference data **36**, 497 (2007).

[39] D. Wineland, J. Bollinger, and W. M. Itano, Physical Review Letters **50**, 628 (1983).

[40] W. M. Itano and D. Wineland, Physical Review A **24**, 1364 (1981).

[41] F. Arbes, M. Benzing, T. Gudjons, F. Kurth, and G. Werth, Zeitschrift für Physik D Atoms, Molecules and Clusters **31**, 27 (1994).

[42] F. Buchinger *et al.*, Physical Review C **41**, 2883 (1990).

[43] S. Trapp *et al.*, Hyperfine Interactions **127**, 57 (2000).

[44] K. Wendt *et al.*, Zeitschrift für Physik D Atoms, Molecules and Clusters **4**, 227 (1987).

[45] W. Neu *et al.*, Zeitschrift für Physik D Atoms, Molecules and Clusters **11**, 105 (1989).

CHAPTER 4

$\mathcal{P},\mathcal{T}$-odd Interaction Constants of RaF

> Knowledge isn't life changing. The application of knowledge is.
>
> Todd Stocker

As we have found a suitable method namely, the Z-vector method, which can generate accurate wavefunction in the nuclear region of the heavy nucleus, in this chapter, we have applied the method to calculate the $\mathcal{P},\mathcal{T}$-odd interaction constants of one of the relevant molecule, RaF. So, we have employed both the Z-vector method and the expectation-value approach in the relativistic coupled-cluster framework to calculate the effective electric field (E_{eff}) experienced by the unpaired electron and the scalar-pseudoscalar (S-PS) $\mathcal{P},\mathcal{T}$-odd interaction constant (W_{s}) in the ground electronic state of RaF. As the experimental magnetic HFS constants of RaF are not available, we have calculated the magnetic HFS constants of $^{223}Ra^{+}$ and compared with the experimental values. The outcome shows that the Z-vector method is superior to the expectation-value approach. The Z-vector calculation shows that RaF has a high E_{eff} (52.5 GV/cm) and W_{s} (141.2 kHz). This makes it a potential candidate for the eEDM experiment.

4.1 Introduction

The ongoing accelerator based experiments in the search for new physics can solve some of the unanswered problems of the fundamental physics like matter-antimatter asymmetry. A complementary to these high energy experiments is the search for violation in spatial inversion ($\mathcal{P}$) and time reversal ($\mathcal{T}$) symmetries in nuclei, atoms or molecules in the low energy domain using non-accelerator experiments [1–7]. One of such $\mathcal{P},\mathcal{T}$-violating interaction results into the electric dipole moment of electron (eEDM) [8–11]. The eEDM predicted by the standard model (SM) of elementary particle physics is too small ($< 10^{-38}$ e cm) [12] to be observed by the today's experiment. However, many extensions of the SM predict the value of eEDM to be in the range of $10^{-26} - 10^{-29}$ e cm [13] and the sensitivity of the modern eEDM experiment also lies in the same range. Till date, the experiment done by ACME collaboration [11] using ThO yields the best upper bound limit of eEDM. The high sensitivity of modern eEDM experiment is mainly due to the fact that heavy paramagnetic diatomic molecules offer a very high internal effective electric field (E_{eff}), which enhances the eEDM effects [14, 15]. So, it is very important to search for new paramagnetic diatomic molecules which offers high enhancement of eEDM effects. In the experiment, both eEDM and the coupling interaction between the scalar-hadronic current and the pseudoscalar electronic current contribute to the $\mathcal{P},\mathcal{T}$-odd frequency shift. Therefore, it is impossible to decouple the individual contribution from these two effects in a single experiment. However, it is possible to untwine these two contributions from each other and an independent limit on the value of eEDM (d_e) and scalar-pseudoscalar (S-PS) coupling constant (k_s) can be obtained by using data from two different experiments as suggested by Dzuba *et al* [16]. It is, therefore, an accurate value of the E_{eff} and the scalar-pseudoscalar (S-PS) $\mathcal{P},\mathcal{T}$-odd interaction constant (W_{s}) are needed since these two quantities cannot be measured by means of any experiment. Therefore, one has to rely on an accurate *ab initio* theory that can simultaneously take care of the effects of relativity and electron correlation for the calculation of these quantities.

The best way to include the effects of special relativity in the electronic structure calculations is to solve the Dirac-Hartree-Fock (DHF) equation in the four-component framework. The DHF method considers an average electron-electron interaction and thus misses the correlation between electrons having same spin. On the other hand, the single reference coupled-cluster (SRCC)

method is the most preferred many-body theory to incorporate the dynamic part of the electron correlation. The calculation of property in the SRCC framework can be done either numerically or analytically. In numerical method (also known as the finite-field (FF) method), the coupled-cluster amplitudes are functions of the external field parameters [17] and thus, for the calculations of each of the property, separate set of CC calculation is needed. The error associated with the FF method is also dependent on the method of calculation, i.e., the number of data points considered for the numerical differentiation. On the contrary, in the analytical method, the CC amplitudes are independent of the external field of perturbation and therefore, one needs to solve only one set of CC equation for the calculations of any number of properties. Normal CC (NCC) method being non-variational, does not satisfy the generalized Hellmann-Feynman (GHF) theorem and thus, the expectation value and the energy derivative approach are two different formalisms for the calculation of first order property. However, the energy derivative in NCC framework is the corresponding expectation value plus some additional terms which make it closer to the property value obtained in the full configuration interaction (FCI) method. Thus, the property value obtained in the energy derivative method is much more reliable than the corresponding expectation value method. Another disadvantage of the expectation value method is that it leads to a non-terminating series and any truncation further introduces an additional error. The Z-vector method [18, 19] (an energy derivative method), on the other hand, leads to a naturally terminating series at any level of approximation. The higher order derivative in the NCC framework can be calculated by using the Lagrange multiplier method [20] and for the first order energy derivative, it leads to the identical equations as of Z-vector method. It is worth to note that there are alternative options like expectation value CC (XCC) [21, 22], unitary CC (UCC) [23, 24], and extended CC (ECC) [25–27] to solve the SRCC equation. All these methods are known in the literature as the variational coupled-cluster (VCC) method [28]. These VCC methods are well established in the non-relativistic framework but are not that much popular in the relativistic domain, a few are documented in the literature like relativistic UCC by Sur *et al.* [29, 30], applicable only for the purpose of atomic calculations. Recently, we implemented ECC in the four-component relativistic domain to calculate the magnetic hyperfine structure (HFS) constants of both atoms and molecules in their open-shell ground state configuration [31]. The ECC method being variational satisfies the

GHF theorem, therefore, expectation value and the energy derivative approach are identical to each other. However, in ECC method amplitude equations for the excitation and de-excitation operators are coupled to each other, whereas, in Z-vector method, the amplitude equations of excitation operator are decoupled from the amplitude equations of the de-excitation operator. This accelerates the convergence in the Z-vector method with a lesser computational cost as compared to the ECC.

In the previous chapter we have shown that the Z-vector method in the relativistic CC framework [32] is computationally feasible and yields accurate wavefunction in the nuclear region of heavy nucleus. So, in this chapter, we have calculated the E_{eff} and W_{s} of RaF in its ground electronic ($^2\Sigma$) state using Z-vector method in the CC framework. We also calculated these properties in the expectation value method to show the superiority of the Z-vector method over the expectation value method.

4.2 Importance of RaF as a candidate for eEDM experiment

We have chosen the RaF molecule for the following reasons: This molecule has been proposed for the $\mathcal{P}$-odd and $\mathcal{P},\mathcal{T}$-odd experiment [33–35] due to its high Schiff moment, E_{eff} and W_{s}. The E_{eff} of $^2\Sigma$ state of RaF is even higher than the ground state ($^2\Sigma$) of YbF. Therefore, the more precise value of E_{eff} and W_{s} and their ratio are very important for the eEDM experiment using this molecule. RaF can be directly laser cooled as it has high diagonal Franck-Condon matrix element between the ground and first excited electronic state and the corresponding transition frequency lies in the visible region with a reasonable lifetime [33]. However, the experiment with radioactive molecules like RaF demands special facility. The TRIμP facility at the Kernfysisch Versneller Instituut (KVI) of the University of Groningen was approved in 2007 to test the fundamental symmetries of physics by doing precision experiments these radioactive isotopes [36].

4.3 Expectation value method in the coupled cluster framework

In this chapter, we have calculated the E_{eff} and W_{s} of RaF using both the Z-vector and the expectation value method. The details of the Z-vector method in the relativistic CC framework is given in the Section 3.3 of Chapter 3. Computationally, expectation value method in the CC framework is a two step process. The first step is the calculation of the NCC cluster amplitudes, which is given in Section 1.14 of Chapter 1. Next step is the calculation of the property of interest by using the NCC cluster amplitudes. The expectation value of any property operator, $\langle O_N \rangle$, can be calculated by the following expression [37, 38],

$$\langle O_N \rangle = \frac{\langle \Psi_{cc} | O_N | \Psi_{cc} \rangle}{\langle \Psi_{cc} | \Psi_{cc} \rangle} = \frac{\langle \Phi_0 e^{T^\dagger} | O_N | e^T \Phi_0 \rangle}{\langle \Phi_0 | e^{T^\dagger} e^T | \Phi_0 \rangle} = \langle \Phi_0 | (e^{T^\dagger} O_N e^T)_c | \Phi_0 \rangle. \tag{4.1}$$

The above series is a non-terminating series. Since, the dominant contribution comes from the linear terms, therefore, linear approximation is the most favored choice. The detailed diagrammatic

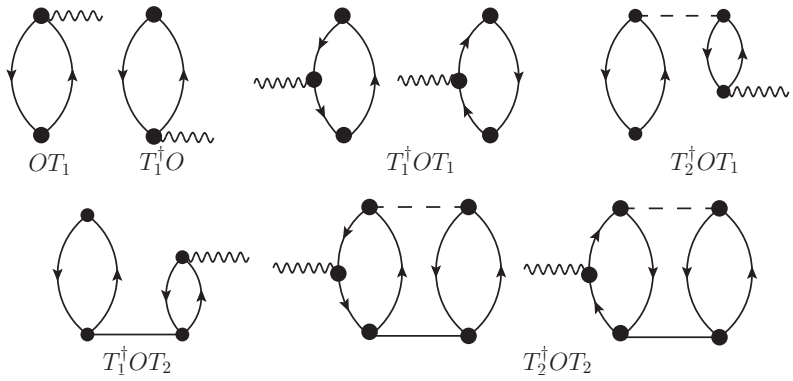

Figure 4.1: Diagrams for expectation value approach using linear truncation scheme

expression considering only linear terms within the CCSD approximation is given in Figure 4.1 and the corresponding algebraic equation is given as in Eq. 4.2.

$$\begin{aligned} \langle O \rangle &= O(i,a) \cdot t_i^a + t_a^i \cdot O(a,i) + t_a^i \cdot O(a,b) \cdot t_i^b - t_a^i \cdot O(j,i) \cdot t_j^a + t_{ab}^{ij} \cdot O(b,j) \cdot t_i^a \\ &\quad + t_a^i \cdot O(j,b) \cdot t_{ij}^{ab} - \frac{1}{2} t_{ab}^{ij} \cdot O(k,j) \cdot t_{ik}^{ab} + \frac{1}{2} t_{ab}^{ij} \cdot O(b,c) \cdot t_{ij}^{ac}. \end{aligned} \tag{4.2}$$

We have used Einstein summation convention, i.e., the repeated indices are summed over in the expression. The t amplitudes with particle(hole) indices at the subscript(superscript) are the corresponding amplitudes of the $T^\dagger$ operator. It is interesting to note that there is no possible diagrams (as well as algebraic expression) of the kind $T_2^\dagger O$ or OT_2, since closed connected diagrams can not be constructed by these two expressions.

4.4 Computational details

The locally modified version of DIRAC10 [39] program package is used to solve the DHF equation and to construct the one-body, two-body matrix elements and the one electron property integrals of interest. Finite size of nucleus with Gaussian charge distribution is considered as the nuclear model where the nuclear parameters [40] are taken as default values of DIRAC10. Small component basis functions are generated from the large component by applying restricted kinetic balance (RKB) [41] condition. The basis functions are represented in scalar basis and unphysical solutions are removed by means of the diagonalization of free particle Hamiltonian. This generates the electronic and positronic solution in 1:1 manner. In our calculations, we have used the following uncontracted basis sets: triple zeta (TZ) basis: dyall.cv3z [42] for Ra and cc-pCVTZ [43] for F; quadruple zeta (QZ) basis: dyall.cv4z [42] basis for Ra and cc-pCVQZ [43] basis for F. In TZ basis, three calculations are done for the magnetic HFS constant of Ra^+ by using 51, 69 and 87 number of correlated electrons and these are denoted by A, B and C, respectively. In QZ basis, three more calculations are done by using 51, 69 and 87 number of correlated electrons and these are denoted by D, E and F, respectively. The properties of RaF are calculated using two different basis. In TZ basis, three calculations are done by using 61, 79 and 97 correlated electrons and those are denoted by G, H and I, respectively and similarly in QZ basis, the calculations using 61, 79 and 97 correlated electrons are denoted by J, K and L, respectively. The bond length of RaF is taken as $4.23a_0$ (2.24 Å) [35] in all our calculation.

4.5 Results and discussion

The aim of the present study is to exploit RaF molecule for the eEDM experiment and to provide more accurate value of the P,T-odd interaction constants of RaF. Since, there are no experimental analogue of the P,T-odd interaction constants like E_{eff} and W_{s}, the accuracy of these theoretically obtained quantities can be assessed by comparing the theoretically obtained HFS values with the corresponding experimental values. Unfortunately, the experimental HFS results of Ra in RaF are not available. Therefore, we compare the experimental HFS value of $^{223}Ra^{+}$ [44, 45] with the value obtained by theory using the same basis of Ra as used for the calculation of RaF.

Table 4.1: Cutoff used and correlation energy of the ground state of Ra^{+} and RaF in different basis sets

	Basis			Cutoff (a.u.)		Spinor		Correlation Energy (a.u.)	
Name	Nature	Ra	F	Occupied	Virtual	Occupied	Virtual	MBPT(2)	CCSD
Ra^{+}									
A	TZ	dyall.cv3z		-30	500	51	323	-1.74841495	-1.57235409
B	TZ	dyall.cv3z		-130	500	69	323	-2.42790147	-2.20700361
C	TZ	dyall.cv3z			500	87	323	-2.78897499	-2.55468917
D	QZ	dyall.cv4z		-30	20	51	349	-1.43221422	-1.31515023
E	QZ	dyall.cv4z		-130	20	69	349	-1.49747209	-1.37242346
F	QZ	dyall.cv4z			20	87	349	-1.50382815	-1.37827038
RaF									
G	TZ	dyall.cv3z	cc-pCVTZ	-30	500	61	415	-2.09671991	-1.91684123
H	TZ	dyall.cv3z	cc-pCVTZ	-130	500	79	415	-2.77624243	-2.55153111
I	TZ	dyall.cv3z	cc-pCVTZ		500	97	415	-3.13733209	-2.89923481
J	QZ	dyall.cv4z	cc-pCVQZ	-30	20	61	449	-1.76368821	-1.63988444
K	QZ	dyall.cv4z	cc-pCVQZ	-130	20	79	449	-1.82908547	-1.69728677
L	QZ	dyall.cv4z	cc-pCVQZ		20	97	449	-1.83544557	-1.70314714

In Table 4.1, we present the information regarding the employed basis-sets, cutoff used for occupied and virtual orbitals and the the number of active spinor for the correlation calculation. We also compiled the correlation energy obtained from second-order many-body perturbation theory (MBPT(2)) and CCSD method in the same table.

In Table 4.2, we present the ground state (^{2}S) magnetic HFS constant value of $^{223}Ra^{+}$ using both expectation value and Z-vector method. Our results are compared with the available experimental value [44, 45]. The deviations of Z-vector and expectation values from the experiment are presented in Figure 4.2. It is clear that the deviations of expectation value method are always greater than those of Z-vector method. This is expected because Z-vector is a better method than

Table 4.2: Magnetic hyperfine coupling constant (in MHz) of $^{223}Ra^{+}$

Basis	Expectation	Z-vector	Expt. [44, 45]
A	3458	3418	
B	3504	3464	
C	3547	3506	3404(2)
D	3434	3394	
E	3448	3409	
F	3453	3414	

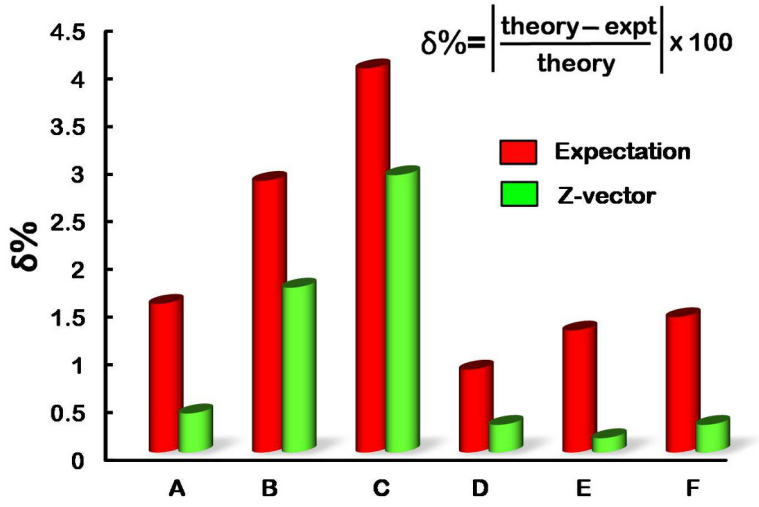

Figure 4.2: Comparison of relative deviations between expectation value and Z-vector results of the magnetic HFS constant of $^{223}Ra^{+}$

the expectation value method for the ground state property; in fact, the Z-vector value is the corresponding expectation value plus some additional terms which make it closer to the FCI property value. It is interesting to note that when we go from TZ to QZ basis with same number of correlated electrons (i.e., from A to D, B to E, and C to F), the relative deviation of both Z-vector and expectation value decreases. This is because QZ, in comparison to TZ, further improves the configuration space by adding one higher angular momentum basis function. It is also interesting to see that in TZ basis, if we go from A to B and B to C, the addition of 18 electrons (4s+3d+4p and 1s-3p) changes the Z-vector HFS constant by 46 MHz and 42 MHz. Similarly in QZ basis, as we go from D to E and E to F, the addition of 18 electrons changes the Z-vector HFS constant

by 15 MHz and 5 MHz. From this observation, we can comment that the core polarization plays a definite role in the correlation contribution of HFS constant and the effect is severe for lower basis sets. Further, the enlargement of basis set and addition of core electrons have opposite effects in the calculated HFS value of Ra^+. However, The magnetic HFS constant obtained in all electron Z-vector calculation using QZ basis (basis F) is very close to the experimental value ($\delta\%$ = 0.29).

The properties like E_{eff}, W_{s} and magnetic HFS constants are strongly dependent on the electronic configuration of the given (heavy) atom and are also known as "atom in compound (AIC)" properties [46]. The accuracy of the theoretically calculated AIC properties depends on the accurate evaluation of the electron density near the atomic core region. From the accuracy of our calculated HFS constant of Ra^+ ($\delta\%$ = 0.29), we can comment that the all electron Z-vector calculation produces an accurate wavefunction in the vicinity of Ra nucleus and we also expect the same kind of accuracy for RaF molecule.

Table 4.3: Molecular dipole moment (μ) and magnetic HFS constants of ^{223}Ra in RaF

Basis	μ (D)		$A_\perp$ (MHz)		$A_\parallel$ (MHz)	
	Expect.	Z-vector	Expect.	Z-vector	Expect.	Z-vector
G	3.7059	3.7220	2031	1987	2123	2078
H	3.7028	3.7207	2059	2014	2152	2107
I	3.7017	3.7201	2084	2038	2178	2132
J	3.8404	3.8474	2029	1982	2119	2072
K	3.8375	3.8459	2037	1991	2128	2082
L	3.8374	3.8459	2040	1993	2131	2085

We have calculated the molecular-frame dipole moment (μ) of RaF, perpendicular ($A_\perp$) and parallel ($A_\parallel$) magnetic HFS constants of ^{223}Ra in RaF using both expectation value and Z-vector method. The results are compiled in Table 4.3. From this table, it is clear that inclusion of more core electrons decreases the value of μ but increases the value of magnetic HFS constants of ^{223}Ra in RaF. On the other hand, if we go from TZ to QZ basis, the μ value is increased but the magnetic HFS values are decreased. This observation shows that the increase of correlation space either by the addition of core electrons or higher angular momentum wavefunctions have opposite effect on the near nuclear and outer region part of the molecular wavefunction of RaF. We can also comment that the enlargement of basis set and core electrons have opposite effects in the properties of RaF.

Table 4.4: P,T-odd interaction constants and their ratio of RaF

Basis	$W_{\rm s}$ (kHz)		$E_{\rm eff}$ (GV/cm)		R (10^{18}/e cm)	
	Expect.	Z-vector	Expect.	Z-vector	Expect.	Z-vector
G	144.7	143.6	53.9	53.5	90.1	90.1
H	147.4	146.3	54.9	54.5	90.1	90.1
I	149.3	148.1	55.6	55.1	90.0	90.0
J	141.2	140.4	52.6	52.3	90.1	90.1
K	141.9	141.1	52.8	52.5	90.0	90.0
L	142.0	141.2	52.8	52.5	89.9	89.9

In Table 4.4, we present the two P,T-odd interaction constant, namely $E_{\rm eff}$ and $W_{\rm s}$. The $E_{\rm eff}$ value of RaF in QZ basis using all electron Z-vector calculation (basis L) is 52.5 GV/cm. This $E_{\rm eff}$ value of RaF is even higher than the $E_{\rm eff}$ value of YbF in its ground state [47–52]. The $W_{\rm s}$ value of RaF using Z-vector method in the same basis (QZ, all electron) is 141.2 kHz. This high value of $W_{\rm s}$ suggests that the S-PS interaction will also be responsible for significant change in the P,T-odd frequency shift in the eEDM experiment. These results reveal the possibility of using RaF in future eEDM experiment. The ratio (R) of $E_{\rm eff}$ to $W_{\rm s}$ is also calculated as this is a very important quantity to obtain the independent limit of $\rm d_e$ and $\rm k_s$ by using two independent experiments. Our calculated value of R using all electron Z-vector method in QZ (L) basis is 89.9 in units of 10^{18}/e cm. Using this ratio, the relation of independent $\rm d_e$ and $\rm k_s$ with experimentally determined $\rm d_e^{expt}$ becomes (for more details see Section 1.8 of Chapter 1 and Ref. [53])

$$d_e + 5.56 \times 10^{-21} k_s = d_e^{expt}|_{k_s=0}, \tag{4.3}$$

where, $d_e^{expt}|_{k_s=0}$ is the eEDM limit derived from the experimentally measured P,T-odd frequency shift at the limit $\rm k_s = 0$.

The possible sources of error in our calculations are mainly from four sources: (i) higher order relativistic effects (especially Breit/Gaunt interaction) and non-adiabatic effects, (ii) incompleteness of basis set, (iii) higher order correlation effects, and (iv) cutoff used for the virtual orbitals. Now, the AIC properties described here are mainly dependent on the electron density of the valence electron in the nuclear region and thus these types of properties are not very sensitive to the retardation and magnetic effects described by the Breit interaction [54, 55]. The error associated

with the non-adiabatic effects is also insignificant as the properties of a heavy diatomic molecule are calculated here. The error associated with incompleteness of basis sets can be accessed by comparing our TZ and QZ results. The difference of all electron correlation results of $E_{\rm eff}$ and $W_{\rm s}$ in TZ and QZ basis is about 5%. The proper way to estimate the error associated with missing correlation is to compare our results with the FCI or CCSD with partial triples (CCSD(T)) values. However, these types of calculations are very much expensive and beyond the scope of our present study. From our experience, we can comment that the error associated with the missing higher order correlation effects is about 3.5%. Therefore, considering all other sources of error it can be assumed that the overall uncertainty in our final results is less than 10%.

Table 4.5: Comparison of magnetic HFS constant (^{223}Ra), $W_{\rm s}$ and $E_{\rm eff}$ of RaF

Method	$A_\perp$ (MHz)	$A_\parallel$ (MHz)	$W_{\rm s}$ kHz	$E_{\rm eff}$ (GV/cm)
ZORA-GHF [34]	1860	1900	150	45.5
SODCI [35]	1720	1790	131	49.6
FS-RCC [35]	2020	2110	139	52.9
This work (QZ basis,	all electron)			
Expect.	2040	2131	142.0	52.8
Z-vector	1993	2085	141.2	52.5

We have compared our calculated results with other theoretically obtained values in table 4.5. The first *ab initio* calculation of $W_{\rm s}$ of RaF was performed by Isaev *et al.* [34]. They employed two-component zeroth-order regular approximation (ZORA) generalized Hartree-Fock (GHF) method and obtained the value of $W_{\rm s}$ as 150 kHz. They also obtained the value of $E_{\rm eff}$ as 45.5 GV/cm by using ZORA-GHF value of $W_{\rm s}$ and the approximate ratio between $E_{\rm eff}$ and $W_{\rm s}$. Kudashov *et al.* [35] employed two different methods to incorporate relativistic and electron correlation effects: (i) spin-orbit direct configuration interaction (SODCI) method and (ii) relativistic two-component Fock-space coupled cluster approach (FS-RCC) within single- and double- excitation approximation. However, it is worth to remember that truncated CI is not size extensive and thus cannot treat electron correlation properly, specially, for the heavy electronic system like RaF where the number of electron is so large. In their FS-RCC method, Kudashov *et al.* [35] calculated the properties of RaF using the finite field method, which is a numerical technique. They corrected

the error associated with their calculation considering higher order correlation effect and basis set with the addition of partial triple in the CCSD model (CCSD(T)) and using enlarged basis set, respectively. On the other hand, we have calculated the property values of RaF via two analytical methods (expectation value and Z-vector method) in the relativistic coupled-cluster framework within four-component formalism. We also calculated the E_{eff} and W_{s} values directly by using Eqs. 1.15 and 1.17, respectively.

4.6 Conclusion

In conclusion, we have applied both Z-vector and expectation value method in the relativistic coupled-cluster framework to calculate parallel and perpendicular magnetic HFS constant of ^{223}Ra in RaF, E_{eff} and W_{s} of RaF. We have also calculated the magnetic HFS constant of $^{223}Ra^{+}$ to show the reliability of our results. Our most reliable value of E_{eff} and W_{s} of RaF are 52.5 GV/cm and 141.2 kHz, respectively, with an estimated uncertainty of less than 10%. This shows that RaF can be a potential candidate for the eEDM experiment. We also showed that core electrons play significant role and the effect is severe for lower basis sets. Our results also show that the Z-vector, being an energy derivative method, is much more reliable than the expectation value method.

References

[1] J. Ginges and V. Flambaum, Physics Reports **397**, 63 (2004).

[2] P. Sandars, Physics Letters **14**, 194 (1965).

[3] P. G. H. Sandars, Phys. Rev. Lett. **19**, 1396 (1967).

[4] L. N. Labzovskii, Sov. Phys. JETP **48**, 434 (1978).

[5] L. M. Barkov, M. S. Zolotorev, and I. B. Khriplovich, Soviet Physics Uspekhi **23**, 713 (1980).

[6] F. L. Shapiro, Soviet Physics Uspekhi **11**, 345 (1968).

[7] M. Pospelov and A. Ritz, Annals of physics **318**, 119 (2005).

[8] W. Bernreuther and M. Suzuki, Rev. Mod. Phys. **63**, 313 (1991).

[9] B. C. Regan, E. D. Commins, C. J. Schmidt, and D. DeMille, Phys. Rev. Lett. **88**, 071805 (2002).

[10] J. Hudson *et al.*, Nature **473**, 493 (2011).

[11] J. Baron *et al.*, Science **343**, 269 (2014).

[12] I. B. Khriplovich and S. K. Lamoreaux, *CP Violation without Strangeness: The Electric Dipole Moments of Particles, Atoms, and Molecules* (Springer, London, 2011).

[13] E. D. Commins, Advances In Atomic, Molecular, and Optical Physics **40**, 1 (1999).

[14] O. Sushkov and V. Flambaum, Journal of Experimental and Theoretical Physics **48**, 608 (1978).

[15] V. V. Flambaum, Sov. J. Nucl. Phys. **24**, 199 (1976).

[16] V. A. Dzuba, V. V. Flambaum, and C. Harabati, Phys. Rev. A **84**, 052108 (2011).

[17] H. J. Monkhorst, Int. J. Quantum Chem. **12**, 421 (1977).

[18] N. C. Handy and H. F. Schaefer, Journal of Chemical Physics **81**, 5031 (1984).

[19] E. A. Salter, G. W. Trucks, and R. J. Bartlett, Journal of Chemical Physics **90**, 1752 (1989).

[20] H. Koch *et al.*, Journal of Chemical Physics **92**, 4924 (1990).

[21] R. J. Bartlett and J. Noga, Chemical physics letters **150**, 29 (1988).

[22] S. Pal, Theoretica chimica acta **66**, 151 (1984).

[23] R. J. Bartlett, S. A. Kucharski, and J. Noga, Chemical physics letters **155**, 133 (1989).

[24] S. Pal, Theoretica chimica acta **66**, 207 (1984).

[25] J. Arponen, Annals of Physics **151**, 311 (1983).

[26] R. Bishop, J. Arponen, and P. Pajanne, *Aspects of Many-body Effects in Molecules and Extended Systems, Lecture Notes in Chemistry Vol. 50* (Springer-Verlag, Berlin, 1989).

[27] S. Pal, Phys. Rev. A **34**, 2682 (1986).

[28] P. G. Szalay, M. Nooijen, and R. J. Bartlett, Journal of Chemical Physics **103**, 281 (1995).

[29] C. Sur, R. K. Chaudhuri, B. K. Sahoo, B. P. Das, and D. Mukherjee, Journal of Physics B: Atomic, Molecular and Optical Physics **41**, 065001 (2008).

[30] C. Sur and R. K. Chaudhuri, Phys. Rev. A **76**, 032503 (2007).

[31] S. Sasmal, H. Pathak, M. K. Nayak, N. Vaval, and S. Pal, Phys. Rev. A **91**, 022512 (2015).

[32] S. Sasmal, H. Pathak, M. K. Nayak, N. Vaval, and S. Pal, Phys. Rev. A **91**, 030503 (2015).

[33] T. A. Isaev, S. Hoekstra, and R. Berger, Phys. Rev. A **82**, 052521 (2010).

[34] T. Isaev and R. Berger, arXiv preprint arXiv:1302.5682 (2013).

[35] A. D. Kudashov *et al.*, Phys. Rev. A **90**, 052513 (2014).

[36] E. Traykov *et al.*, Nuclear Instruments and Methods in Physics Research Section B: Beam Interactions with Materials and Atoms **266**, 4532 (2008).

[37] J. Cizek, *Advances in Chemical Physics: Correlation Effects in Atoms and Molecules* (Wiley, Hoboken, NJ, 1967).

[38] S. Pal, M. D. Prasad, and D. Mukherjee, Theoretica chimica acta **62**, 523 (1983).

[39] DIRAC, a relativistic ab initio electronic structure program, Release DIRAC10 (2010), written by T. Saue, L. Visscher and H. J. Aa. Jensen, with contributions from R. Bast, K. G. Dyall, U. Ekström, E. Eliav, T. Enevoldsen, T. Fleig, A. S. P. Gomes, J. Henriksson, M. Iliaš, Ch. R. Jacob, S. Knecht, H. S. Nataraj, P. Norman,

J. Olsen, M. Pernpointner, K. Ruud, B. Schimmelpfennig, J. Sikkema, A. Thorvaldsen, J. Thyssen, S. Villaume, and S. Yamamoto (see http://www.diracprogram.org).

[40] L. Visscher and K. Dyall, Atomic Data and Nuclear Data Tables **67**, 207 (1997).

[41] K. Faegri Jr and K. G. Dyall, *Introduction to relativistic quantum chemistry* (Oxford University Press, USA, 2007).

[42] K. G. Dyall, The Journal of Physical Chemistry A **113**, 12638 (2009).

[43] T. H. Dunning, Journal of Chemical Physics **90**, 1007 (1989).

[44] K. Wendt *et al.*, Zeitschrift für Physik D Atoms, Molecules and Clusters **4**, 227 (1987).

[45] W. Neu *et al.*, Zeitschrift für Physik D Atoms, Molecules and Clusters **11**, 105 (1989).

[46] A. V. Titov, Y. V. Lomachuk, and L. V. Skripnikov, Phys. Rev. A **90**, 052522 (2014).

[47] M. G. Kozlov and V. F. Ezhov, Phys. Rev. A **49**, 4502 (1994).

[48] M. Kozlov, Journal of Physics B: Atomic, Molecular and Optical Physics **30**, L607 (1997).

[49] A. V. Titov, N. S. Mosyagin, and V. F. Ezhov, Phys. Rev. Lett. **77**, 5346 (1996).

[50] H. Quiney, H. Skaane, and I. Grant, Journal of Physics B: Atomic, Molecular and Optical Physics **31**, L85 (1998).

[51] F. A. Parpia, Journal of Physics B: Atomic, Molecular and Optical Physics **31**, 1409 (1998).

[52] N. Mosyagin, M. Kozlov, and A. Titov, Journal of Physics B: Atomic, Molecular and Optical Physics **31**, L763 (1998).

[53] S. Sasmal, H. Pathak, M. K. Nayak, N. Vaval, and S. Pal, Journal of Chemical Physics **144**, 124307 (2016).

[54] H. M. Quiney, J. K. Laerdahl, K. Fægri Jr, and T. Saue, Physical Review A **57**, 920 (1998).

[55] E. Lindroth, B. Lynn, and P. Sandars, Journal of Physics B: Atomic, Molecular and Optical Physics **22**, 559 (1989).

CHAPTER 5

$\mathcal{P}, \mathcal{T}$-violating Interactions in PbF

> An ounce of practice is generally worth more than a ton of theory.
>
> Ernst F. Schumacher

The chapter considers the calculation of E_{eff} and parallel component of HFS constant ($A_{\parallel}$) of PbF as it has some interesting characteristics, which make it a strong candidate in the search of electron EDM. We have achieved a very accurate wavefunction in the near nuclear region which is evident from our $A_{\parallel}$ values. This shows that our calculated E_{eff} value (38.1 GV/cm) is the most reliable one. The outcome of our calculations also clearly suggests that the core electrons have significant contribution to the "atom in compound" properties.

5.1 Introduction

The well established model of the interaction of elementary particles, the Standard Model (SM), is incomplete as it cannot explain some of the well known phenomena of fundamental physics. One such phenomenon is the dominance of matter over antimatter in our universe, although the SM treats matter and antimatter exactly in the same way [1]. The violation of two fundamental symmetries: inversion symmetry ($\mathcal{P}$) and charge conjugation ($\mathcal{C}$), is one of the several conditions that can explain the matter antimatter asymmetry [2]. The $\mathcal{CP}$ violation within the SM originating from the complex quark mixing Kobayashi-Maskawa matrix is too weak to explain such an asymmetry. Therefore, the search for an extra $\mathcal{CP}$ violation (flavour-diagonal $\mathcal{CP}$ violation), which is absent in the SM is needed to explore new physics beyond the conventional SM [3, 4]. Another fundamental symmetry is the time-reversal ($\mathcal{T}$) symmetry, which is also violated with the violation of $\mathcal{CP}$ symmetry though a direct observation of the violation of $\mathcal{T}$ symmetry is yet to observe [5].

The electric dipole moment (EDM) of any elementary particle is a consequence of violation of both $\mathcal{T}$ and $\mathcal{P}$ as dipole moment is odd under $\mathcal{P}$ and even under $\mathcal{T}$ but spin is even under $\mathcal{P}$ and odd under $\mathcal{T}$ [6]. According to SM, the electron EDM is too small (less than 10^{-38}) to observe experimentally [7]. Therefore, a measurable non zero EDM of electron would be the proof of an extra $\mathcal{CP}$ violation and the first direct observation of $\mathcal{T}$ violation [8]. However, the intensive search for the electron EDM over the period of half a century have not drawn any conclusion to the final value of electron EDM, which would have out-turned in the upper bound limit of the electron EDM for different quantum systems. Till date, the best limit of electron EDM in an atomic system is achieved from the Tl atom experiment ($|d_e| < 1.6 \times 10^{-27}$ e cm) [9]. However, the discovery of Sandars [10] reveals that the effective internal electric field experienced by an electron is profoundly enhanced in heavy-atom containing polar molecule which makes these polar diatomics very promising candidate in the search of the $\mathcal{P}$- and $\mathcal{P}, \mathcal{T}$ -violating experiments and creates a dimension to explore new physics. The latest best upper limit of electron EDM is set from the ThO experiment ($|d_e| < 8.7 \times 10^{-29}$ e cm) by ACME collaboration [11]. This limit is one order lower in magnitude than the previous best limit ($|d_e| < 10.5 \times 10^{-28}$ e cm), which is obtained from the molecular YbF experiment [12].

Another advantage of using diatomic molecules in the search of electron EDM is the Ω doublet

structure of the ground and metastable state of such polar diatomic molecules, which gives an additional enhancement and due to this reason different molecules having $^2\Sigma_{\frac{1}{2}}$ ground state (YbF [12–16], HgF [17] , HgH, BaF [18]), $^2\Pi_{\frac{1}{2}}$ ground state (PbF [19–21]), $^3\Delta_1$ metastable state (ThO [11, 22–24], ThF^+ [25–27], HfH^+ [28], PtH^+ [28], WC [29, 30]) et cetera have been proposed. Among these molecules, PbF has some interesting characteristics, which make it a strong candidate in the search of electron EDM. Pb is neither a lanthanide or actinide f element nor a transition d element and PbF has a $^2\Pi_{\frac{1}{2}}$ ground state, which means the unpaired electron is in the π orbital while in most of the other molecules, the unpaired electron is in the σ orbital in their ground state. PbF, being a $^2\Pi_{\frac{1}{2}}$ ground state molecule, the spin angular momentum of the unpaired electron contributing to the magnetic moment almost cancels the orbital angular momentum contribution to the magnetic moment. This leads to a smaller g-factor in the $^2\Pi_{\frac{1}{2}}$ state of PbF. The smaller g-factor [31, 32] makes it very insensitive to the background magnetic field and this leads to reduction in some systematic errors in the experimental observation of electron EDM [33]. The other molecules having small g-factor like PbF are ThO, ThF^+, HfH^+, PtH^+, WC, et cetera but that is in their metastable $^3\Delta_1$ state. On the other hand, $^2\Pi_{\frac{1}{2}}$ state of PbF is a ground state, which is easy to synthesize experimentally as compared to the metastable states. The energy shifts of the levels of opposite parity in the ground rotational state of ^{207}PbF due to the Ω doubling is canceled by the magnetic hyperfine interaction as a repercussion the gap between two opposite parity levels is very small (almost degenerate) [19]. Therefore, the molecule can be polarized very easily with the application of a weak electric field and opposite sign of the Ω doublet component leads to the cancellation of some systematic error.

The effective electric field (E_{eff}) experienced by the electron in an atom or a molecule, which is equally known as P,T-odd interaction constant ($W_d = E_{\text{eff}}/|\Omega|$) is a non-measurable quantity. On the other hand, it is very important to set the upper bound limit in the search of electric dipole moment of electron. Therefore, one has to rely on a very accurate theoretical method to calculate E_{eff}, precisely.

we have chosen Z-vector method in the coupled-cluster single- and double- excitation approximation (CCSD) for the calculation of effective electric field, E_{eff}, experienced by the unpaired electron in the ground state of PbF molecule. The parallel magnetic hyperfine structure (HFS)

constant of ^{207}Pb in PbF molecule is also calculated to judge the accuracy in the calculated $E_{\rm eff}$ values, since both of these properties need an accurate wavefunction in the near nuclear region. Further, we have calculated molecular dipole moment of PbF molecule and both the calculated HFS constant and molecular dipole moment are compared with the experimental value and all these results are compared with the values calculated by means of other theoretical methods.

5.2 Computational details

The locally modified DIRAC10 [34] program package is used to construct one electron spinors, two-body matrix elements and one-electron property integrals. Gaussian charge distribution is considered to take care of the finite size of the nucleus where the nuclear parameters [35] are taken as default value of DIRAC10. Restricted kinetic balance (RKB) [36] is used to construct small component basis functions from large component basis. In RKB, the basis functions are represented in scalar basis and unphysical solutions are removed by diagonalizing free particle Hamiltonian. The positive and negative energy solutions are generated in 1:1 manner by this formalism. We have done five different calculations (A-E) by varying basis function and number of correlated electrons. For Pb, dyall.cv3z [37] and for F, cc-pCVTZ [38] basis is used and two different calculations are done by using 55 and 73 number of correlated electrons and these are denoted by A and B, respectively. We have done three more calculations by using 55, 73 and 91 (all electron) correlated electrons where dyall.cv4z [37] and cc-pCVQZ [38] are used for Pb and F, respectively and these calculations are denoted as C, D and E, respectively. The cutoff used for A, B, C, D and E calculations are 3500 a.u., 1000 a.u., 70 a.u., 70 a.u., and 70 a.u., respectively. We have used the experimental bond length (3.89 a.u.) [39] for the calculation of properties of PbF in its ground state.

5.3 Results and discussion

In Table 5.1, we present the molecular dipole moment (μ), parallel component of magnetic hyperfine structure constant ($A_{\parallel}$) of ^{207}Pb and effective electric field ($E_{\rm eff}$) experienced by the unpaired electron of PbF. From Table 5.1, it is clear that our dipole moment values are in good agreement

Table 5.1: Dipole moment, parallel magnetic HFS of ^{207}Pb and effective electric field of PbF

	μ (D)		$A_{\parallel}$ (MHz)		E_{eff}(GV/cm)
Basis	Z-vector	Expt. [31]	Z-vector	Expt. [20, 31]	Z-vector
A	3.71		9865		36.6
B	3.72		9962		37.5
C	3.82	3.5±0.3	9968	10147	37.2
D	3.82		10043		37.9
E	3.83		10121		38.1

with the experimental value [31]. We got values in the range from 3.71 D (basis A) to 3.83 D (basis E) due to different basis and number of correlated electrons but this range fits well within experimental limit (3.5±0.3 D).

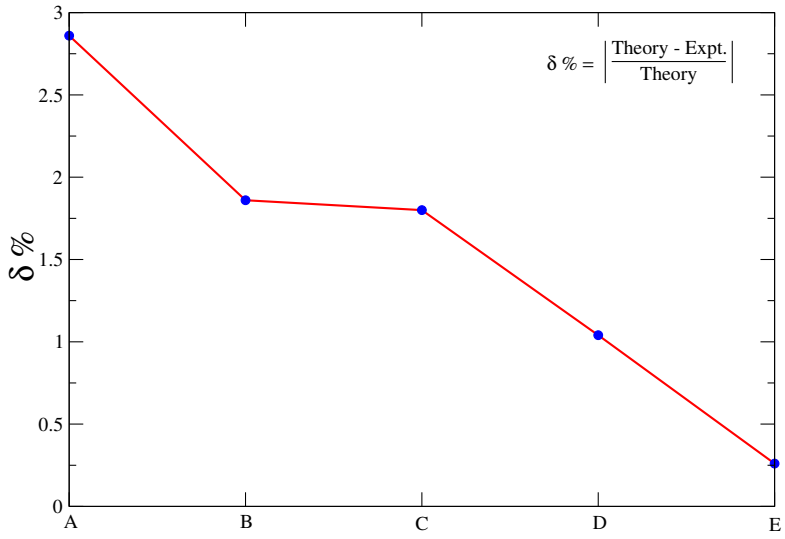

Figure 5.1: Relative deviations between Z-vector and Expt. values of parallel magnetic HFS values.

The calculated parallel component of magnetic HFS constant of ^{207}Pb in PbF shows an excellent agreement with the experiment [20, 31]; specially for E basis where the absolute difference between theory and experiment is only 26 MHz. The relative error of the parallel magnetic HFS constant in five different calculations (A-E) is shown in Figure 5.1. The highest and lowest deviations of Z-vector value from experiment are for basis A (2.86%) and basis E (0.26%), respectively.

This trend in the deviations (expressed in $\delta\%$) is expected. When we go from triple zeta (TZ) basis to quadruple zeta (QZ) basis with same number of correlated electrons (from A to C and B to D where number of correlated electrons are 55 and 73, respectively) the $\delta\%$ decreases as QZ improves the configuration space more by including one higher angular momentum basis function than TZ. On the other hand, for same basis, if we include more electrons in correlation calculation (for TZ, from A to B and for QZ, from C to E), the $\delta\%$ decreases as the more number of correlated electrons includes more orthogonal space to Dirac-Hartree-Fock space and thus includes more correlation contribution to the property value. It is also interesting to see that in TZ basis, when we go from A to B, the addition of 18 electrons (i.e., 4s+3d+4p core electrons of Pb) improves the parallel magnetic HFS constant by 97 MHz. In QZ basis, as we go from C to D and D to E, the addition of 18 electrons (i.e., 4s+3d+4p and 1s-3p core electrons of Pb, respectively) improves the $A_{\parallel}$ value by 75 MHz and 78 MHz, respectively. From this observation we can conclude that the core electrons have significant role in the correlation contribution of parallel magnetic HFS value.

In Table 5.1, we present our Z-vector results of E_{eff} of PbF in five different calculations where the value ranges from 36.6 GV/cm to 38.1 GV/cm. We believe that the value in E basis (38.1 GV/cm) is the most reliable value of E_{eff} of PbF system as its corresponding parallel magnetic HFS value has the closest agreement with experiment. In E basis, the Z-vector magnetic HFS value has a uncertainty of 0.26%. So, considering basis set and other higher order correlation and relativistic effects, we can conclude that the E_{eff} of PbF is 38.1 GV/cm with 4% uncertainty.

Table 5.2: Comparison of molecular dipole moment, magnetic HFS constant and E_{eff} of PbF

Method	μ (Debye)	$A_{\parallel}$ (^{207}Pb) (MHz)	E_{eff} (GV/cm)
SODCI(13e) [40]	4.26	9727	33
SODCI(13e)+OC [41]	5.00	10262	37
2c-CCSD(31e) [21]	3.97	10265	41
2c-CCSD(T)(31e) [21]	3.87	9942	40
4c-Z-vector(QZ, all electron)	3.83	10121	38.1
Experiment [20, 31]	3.5 ± 0.3	10147	

We compared our Z-vector results with other theoretically obtained values. From Table 5.2, it is clear that our all electron value in QZ basis for both dipole moment and parallel magnetic HFS

of ^{207}Pb in PbF has the best agreement with experiment among all the other theoretical values. Baklanov *et al* did two calculations with 13 correlated electrons in spin-orbit direct CI (SODCI) methods – one without outer core (OC) [40] correlation correction and the other with OC correlation correction [41]. The SODCI with OC correction [41] calculation gives better value for $A_{\parallel}$ of ^{207}Pb but gives poorer value of molecular dipole moment. It is worth to remember that CI is not size extensive and thus does not scale properly with number of electrons. So, CI is not a reliable method for the system with a reasonable number of electrons, especially with heavy atom containing systems. Recently, Skripnikov *et al* [21] have done two two-component (2c) coupled cluster calculations – one with single and double approximation (CCSD) and the other with CCSD with perturbative triples (CCSD(T)) correction. In their calculations, Skripnikov *et al* have included only 31 correlated electrons and removed 60 electrons (1s-4f inner-core electrons of Pb) by using "valence" semilocal version of the GRECP scheme [42, 43]. In valence semilocal version of GRECP, the components were constructed for nodal valence pseudospinors by interpolating the potential in the neighbor of pseudospinor node to avoid the singularity in the potential. The problem of valence GRECP approximation is that it can lead to "non-negligible" errors for valence electronic states due to the improper reproduction of nuclear screening [42]. Although the molecular GRECP calculations are two-component ones, the proper four-component wave function near the nucleus is restored at the nonvariational restoration stage that can lead to small errors. On the other hand our all-electron calculations are four-component at all the stages of calculations. Although the authors in Ref. [21] claim that the "contemporary full-electron studies have not yet been able to unambiguously surpass our approach when it comes to AIC and spectroscopic properties of interest", we believe that the explicit treatment of core electrons is necessary for this types of "atom in coumpound " (AIC) [44] properties where the polarization of the inner core electrons plays an important role, which is evident from our calculated parallel magnetic HFS constant value.

5.4 Conclusions

In conclusion, we have applied Z-vector method in the coupled cluster framework to calculate $E_{\rm eff}$ experienced by the electron in the ground state of PbF molecule. The calculated molecular dipole

moment and $A_{\parallel}$ of ^{207}Pb are in excellent agreement with the experimental values. As the calculated HFS constant is in very good agreement with experiment, we can say that our calculated E_{eff} = 38.1 GV/cm is most reliable as both require accurate wave function near the nucleus and expectation value of their operator are similar in structure. The core electrons have significant contribution in the calculated values, which is evident from our calculated results. Therefore, it is desirable to treat all the electrons explicitly to have much more accurate and reliable result.

References

[1] M. Dine and A. Kusenko, Reviews of Modern Physics **76**, 1 (2003).

[2] A. D. Sakharov, JETP lett. **5**, 24 (1967).

[3] M. Pospelov and A. Ritz, Annals of physics **318**, 119 (2005).

[4] N. Fortson, P. Sandars, and S. Barr, Physics Today **56**, 33 (2003).

[5] R. F. Streater and A. S. Wightman, *PCT, spin and statistics, and all that* (Princeton University Press, 2000).

[6] W. Bernreuther and M. Suzuki, Rev. Mod. Phys. **63**, 313 (1991).

[7] I. B. Khriplovich and S. K. Lamoreaux, *CP Violation without Strangeness: The Electric Dipole Moments of Particles, Atoms, and Molecules* (Springer, London, 2011).

[8] R. G. Sachs, *The Physics of Time Reversal* (University of Chicago Press, Chicago, London, 1987).

[9] B. C. Regan, E. D. Commins, C. J. Schmidt, and D. DeMille, Phys. Rev. Lett. **88**, 071805 (2002).

[10] P. G. H. Sandars, Phys. Rev. Lett. **19**, 1396 (1967).

[11] J. Baron *et al.*, Science **343**, 269 (2014).

[12] J. Hudson *et al.*, Nature **473**, 493 (2011).

[13] N. Mosyagin, M. Kozlov, and A. Titov, Journal of Physics B: Atomic, Molecular and Optical Physics **31**, L763 (1998).

[14] H. Quiney, H. Skaane, and I. Grant, Journal of Physics B: Atomic, Molecular and Optical Physics **31**, L85 (1998).

[15] F. A. Parpia, Journal of Physics B: Atomic, Molecular and Optical Physics **31**, 1409 (1998).

[16] M. Kozlov, Journal of Physics B: Atomic, Molecular and Optical Physics **30**, L607 (1997).

[17] Y. Y. Dmitriev *et al.*, Physics Letters A **167**, 280 (1992).

[18] M. Kozlov, A. Titov, N. Mosyagin, and P. Souchko, Physical Review A **56**, R3326 (1997).

[19] C. P. McRaven, P. Sivakumar, and N. E. Shafer-Ray, Phys. Rev. A **78**, 054502 (2008).

[20] A. Petrov, L. Skripnikov, A. Titov, and R. Mawhorter, Physical Review A **88**, 010501 (2013).

[21] L. Skripnikov, A. Kudashov, A. Petrov, and A. Titov, Physical Review A **90**, 064501 (2014).

[22] E. R. Meyer and J. L. Bohn, Physical Review A **78**, 010502 (2008).

[23] L. Skripnikov, A. Petrov, and A. Titov, Journal of Chemical Physics **139**, 221103 (2013).

[24] T. Fleig and M. K. Nayak, Journal of Molecular Spectroscopy **300**, 16 (2014).

[25] H. Loh *et al.*, Science **342**, 1220 (2013).

[26] L. Skripnikov and A. Titov, Physical Review A **91**, 042504 (2015).

[27] M. Denis *et al.*, New Journal of Physics **17**, 043005 (2015).

[28] E. R. Meyer, J. L. Bohn, and M. P. Deskevich, Physical Review A **73**, 062108 (2006).

[29] J. Lee, E. Meyer, R. Paudel, J. Bohn, and A. Leanhardt, Journal of Modern Optics **56**, 2005 (2009).

[30] J. Lee *et al.*, Physical Review A **87**, 022516 (2013).

[31] R. J. Mawhorter *et al.*, Physical Review A **84**, 022508 (2011).

[32] L. V. Skripnikov *et al.*, Phys. Rev. A **92**, 032508 (2015).

[33] N. E. Shafer-Ray, Physical Review A **73**, 034102 (2006).

[34] DIRAC, a relativistic ab initio electronic structure program, Release DIRAC10 (2010), written by T. Saue, L. Visscher and H. J. Aa. Jensen, with contributions from R. Bast, K. G. Dyall, U. Ekström, E. Eliav, T. Enevoldsen, T. Fleig, A. S. P. Gomes, J. Henriksson, M. Iliaš, Ch. R. Jacob, S. Knecht, H. S. Nataraj, P. Norman, J. Olsen, M. Pernpointner, K. Ruud, B. Schimmelpfennig, J. Sikkema, A. Thorvaldsen, J. Thyssen, S. Villaume, and S. Yamamoto (see http://www.diracprogram.org).

[35] L. Visscher and K. Dyall, Atomic Data and Nuclear Data Tables **67**, 207 (1997).

[36] K. Faegri Jr and K. G. Dyall, *Introduction to relativistic quantum chemistry* (Oxford University Press, USA, 2007).

[37] K. G. Dyall, Theoretical Chemistry Accounts **115**, 441 (2006).

[38] T. H. Dunning, Journal of Chemical Physics **90**, 1007 (1989).

[39] K. Huber and G. Herzberg, *Constants of Diatomic Molecules, Vol. 4, Molecular Spectra and Molecular Structure* (Van Nostrand Reinhold, New York, 1979).

[40] K. Baklanov, A. Petrov, A. Titov, and M. Kozlov, Physical Review A **82**, 060501 (2010).

[41] K. I. Baklanov, Masters thesis, Department of Physics, Saint Petersburg State University, Saint Petersburg, Petrodvoretz, Russia, 2012.

[42] N. S. Mosyagin, A. Zaitsevskii, and A. V. Titov, International Review of Atomic and Molecular Physics **1**, 63 (2010).

[43] A. Titov and N. Mosyagin, International journal of quantum chemistry **71**, 359 (1999).

[44] A. V. Titov, Y. V. Lomachuk, and L. V. Skripnikov, Phys. Rev. A **90**, 052522 (2014).

CHAPTER 6

A Potential Candidate for the eEDM Experiment: HgH

> There are two possible outcomes: if the result confirms the hypothesis, then you've made a measurement. If the result is contrary to the hypothesis, then you've made a discovery.
>
> Enrico Fermi

Here, we have applied the Z-vector method in the relativistic coupled-cluster framework to calculate various $\mathcal{P},\mathcal{T}$-odd interaction constants of HgH and found that it has a very large E_{eff} (123.2 GV/cm) and W_{s} (284.2 kHz). This makes HgH a potential candidate for the next generation eEDM experiment. Our calculated parallel and perpendicular magnetic HFS constants of HgH are also in good agreement with the experiment. This shows the reliability of our final E_{eff} and W_{s} values. Further, We have derived the relationship between these quantities and the ratio which will help us to get model independent value of eEDM and S-PS interaction constant.

6.1 Introduction

In the quest of new physics, there have been an extensive search in order to observe the violation of parity ($\mathcal{P}$) and time reversal ($\mathcal{T}$) symmetries [1]. An accurate measurement of electric dipole moment of an electron (eEDM) [2, 3], which arises due to the violation of both $\mathcal{P}$ and $\mathcal{T}$ is the most promising way to explore in this direction. Although, the intensive search over the past half a century did not conclude in any final value of eEDM, however, it leads to achieve a tremendous increase in the experimental sensitivity, and an upper bound limit of eEDM [4]. The enhancement of eEDM effects in heavy polar diatomic molecules is the main reason for the higher sensitivity of modern eEDM experiment [5, 6]. The sensitivity of the eEDM experiment using a heavy polar diatomic molecule depends on the molecule's permanent molecular EDM [7, 8]. There are two main sources of permanent molecular EDM of a paramagnetic molecule; the eEDM and the coupling interaction between the scalar-hadronic current and the pseudoscalar electronic current. However, in most of the calculation either eEDM or the scalar-pseudoscalar (S-PS) interaction is considered as the only possible source of permanent molecular EDM. For example, the best upper bound limit of eEDM (d_e) and S-PS interaction constant (k_s) is obtained from the ThO experiment by ACME collaboration [4] where they have used the theoretically calculated value of effective electric field (E_{eff}) and S-PS P,T-odd interaction constant (W_{s}) [9, 10]. In the calculation of d_e, the S-PS coupling constant k_s, is assumed to be zero and vice versa, although both of these contribute to the P,T-odd frequency shift in the experiment. However, it is possible to get independent limit of d_e and k_s by using the results from two different experiments [11] and for this the accurate value of E_{eff}, W_{s} and their ratio are very important. Since, E_{eff} and W_{s} cannot be measured by any experimental technique, therefore, these quantities have to be calculated by means of an accurate theoretical method, which can incorporate both the effects of relativity and electron correlation in an intertwined manner.

In this article, we focus on HgH molecule as it offers very high value of E_{eff} and W_{s} in its ground electronic state ($^2\Sigma$), which makes it a potential candidate for the future eEDM experiments. The Z-vector method [12–14] in the relativistic coupled-cluster formalism is used to calculate E_{eff} and W_{s} as it is the most reliable method for the calculation of ground state properties. However, high values of E_{eff} and W_{s} are not the only requirement for the precise measurement of

eEDM, but the molecule must be fully polarized with a low external electric field to fully utilize the $E_{\rm eff}$. The large rotational constant and small dipole moment of HgH suggest that one needs to apply a much higher electric field to polarize HgH in a spectroscopic experiment. However, Kozlov and Derevianko have suggested that it can be polarized easily in the matrix isolated solid state non-spectroscopic experiment [15], which also offers 2-3 orders of higher sensitivity than the current limit. Therefore, the detailed investigation of $E_{\rm eff}$ and $W_{\rm s}$ of HgH and their inter-relation is very important for the eEDM experiment based on HgH moecule.

6.2 Computational details

The locally modified version of DIRAC10 program package [16] is used to solve the Dirac-Hartree-Fock equation where the Dirac-Coulomb Hamiltonian is used. On the other hand, the Z-vector method in the CCSD framework is used for the correlation treatment. The wavefunction is four-component in nature and the small-component functions are linked to the large-components by the restricted kinetic balance (RKB) condition [17]. Finite nucleus size is considered and the nuclear potential is calculated considering Gaussian charge distribution [18]. We have done two calculations - one with triple zeta (TZ) basis (dyall.cv3z for Hg [19] and cc-pCVTZ for H [20]) and the other with quadruple zeta (QZ) basis (dyall.cv4z for Hg [19] and cc-pCVQZ for H [20]). As the higher energy virtual orbitals contribute very less in the correlation calculations, the virtual orbitals whose energy exceeds 500 a.u. are removed from our calculations. None of the occupied orbitals are frozen in our correlation calculation as the core polarization effect plays a vital role for the type of properties of interest [14]. The experimental bond length of HgH (1.766 Å) [21] is used to calculate the properties in its ground state ($^2\Sigma_{1/2}$).

6.3 Results and discussion

The accuracy of the $\mathcal{P},\mathcal{T}$-odd properties like $E_{\rm eff}$ and $W_{\rm s}$ can be determined by comparing the theoretically obtained magnetic HFS constants with the experimental values since all these matrix elements require an accurate wavefunction in the near nuclear region of the heavy nucleus. The parallel ($A_{\parallel}$) and perpendicular ($A_{\perp}$) magnetic HFS constant values of ^{199}Hg and ^{201}Hg in HgH

Table 6.1: Dipole Moment (μ) (in Debye) and Magnetic HFS constants of HgH (in MHz)

		^{199}Hg		^{201}Hg	
Basis	μ	$A_{\parallel}$	$A_{\perp}$	$A_{\parallel}$	$A_{\perp}$
TZ	0.25	8371	6483	-3090	-2392
QZ	0.27	8440	6575	-3116	-2427
Expt.	0.47	7780(5)[a]	6200(3)[a]	$-2875(15)$[a]	$-2275(10)$[a]
		8200(60)[b]	6500(50)[b]	$-2980(40)$[b]	$-2380(30)$[b]

[a]measured in Ne matrices, [b]measured in Ar matrices.

are presented in Table 6.1. The experimental values are taken from Ref. [22], where Stowe *et al* measured the magnetic HFS constant of HgH trapped in neon and argon matrices at 4K by electron spin resonance study. The agreement of our calculated $A_{\parallel}$ and $A_{\perp}$ results with the experimental values shows that the wavefunction evaluated in Z-vector method is very accurate in the near nuclear region and thus it also shows the reliability of our calculated $E_{\rm eff}$ and $W_{\rm s}$ values. Further, we have calculated molecular-frame dipole moment (μ) of the HgH molecule using same Z-vector method. The obtained (μ) values are 0.25 D and 0.27 D in TZ and QZ basis, respectively. These results are also compiled in the same table and compared with the available experimental value [23]. However, the experimental μ value of HgH reported in Ref. [23] was measured with an unusual and indirect way and the value is also given without any experimental uncertainty.

Table 6.2: $E_{\rm eff}$ (in GV/cm), $W_{\rm s}$ (in kHz) and the ratio of them (R = $E_{\rm eff}$/$W_{\rm s}$ in units of 10^{18}/e cm) of HgH.

Basis	$E_{\rm eff}$		$W_{\rm s}$		R	
	SCF	Z-vector	SCF	Z-vector	SCF	Z-vector
TZ	106.8	123.3	241.2	284.3	107.1	104.9
QZ	106.9	123.2	241.7	284.2	106.9	104.8

In Table 6.2, we present the $E_{\rm eff}$ and $W_{\rm s}$ values of our calculation. The $E_{\rm eff}$ value of HgH obtained in QZ basis is 123.2 GV/cm. This result shows that HgH is one of those diatomic molecules which have the largest effective electric field. Previously, Kozlov calculated the $E_{\rm eff}$ of HgH by using a semiempirical method and the value found to be 79 GV/cm. On the other hand, we have used an *ab initio* (Z-vector method in the relativistic CCSD framework) method with sufficiently large

basis sets (TZ and QZ) to calculate the properties of HgH which makes our calculated values more reliable. Our calculated $W_{\rm s}$ value in QZ basis is 284.2 kHz. This large value of $W_{\rm s}$ suggests that the S-PS interaction can contribute a significant amount to the permanent molecular EDM. These characteristics of HgH make it an important player in the field of eEDM search. The ratio (R) of $E_{\rm eff}$ to $W_{\rm s}$ is also calculated as this is a very important quantity to obtain the model independent limit of d_e and k_s as suggested by Dzuba *et al* [11]. They suggest that this ratio would be constant for a particular heavy nucleus for the following reasons: (i) these types of property mainly depend on the core (near nuclear region) electronic wavefunction and in this short distance the one electron Dirac equation becomes identical for all single-electron states with the given angular momenta; (ii) the main contribution of these types of properties comes from the $s_{_{1/2}}$-$p_{_{1/2}}$ matrix elements and thus the many-body effects like core polarization has a very little effect on the ratio R. Our calculated values of R in QZ basis are 106.9 and 104.8 in units of 10^{18}/e cm in the SCF and in the Z-vector calculations, respectively. These results support the previous argument as the correlation treatment changes the value of R only by 2 units. These values are very close to the value obtained by Dzuba *et al* (112.5 in the same unit) [11] where they used an analytic expression to evaluate this ratio. By putting the value of R in Eq.1.20, we can get the following relation (for details see Section 1.8 of Chapter 1)

$$d_e + 4.77 \times 10^{-21} k_s = d_e^{\rm expt}\big|_{k_s=0}, \tag{6.1}$$

where $d_e^{\rm expt}\big|_{k_s=0}$ is the eEDM limit derived from the $\mathcal{P},\mathcal{T}$-odd energy shift of HgH experiment at the limit of k_s = 0.

There are three main possible sources of error associated with our calculation - (i) basis set incompleteness, (ii) cutoff used for virtual orbitals in the correlation calculations and (iii) higher order correlation effect. The error associated with the incompleteness of the basis set can be estimated by comparing TZ and QZ basis calculations. The difference between the results calculated in TZ and QZ basis for both $E_{\rm eff}$ and $W_{\rm s}$ is less than 0.1%. We have done a series of calculations (compiled in Table 6.3) to estimate the error associated with the restriction of correlation space by neglecting higher energy virtual orbitals. In this calculation, the $E_{\rm eff}$ and $W_{\rm s}$ values are calculated by employing double zeta (DZ) basis (dyall.cv2z for Hg [19] and cc-pCVDZ for H [20]) in the Z-vector method with different cutoff of virtual orbitals. The difference of calculated values using

Table 6.3: Convergence pattern of $A_{\parallel}$ of ^{199}Hg in HgH, μ, $E_{\rm eff}$ and $W_{\rm s}$ of HgH as a function of virtual orbitals

Cutoff (a.u.)	Virtual spinor	μ (D)	$A_{\parallel}$ (MHz)	$E_{\rm eff}$ (GV/cm)	$W_{\rm s}$ (kHz)
100	175	0.168	7911	115.6	260.5
200	199	0.169	7918	115.7	260.6
400	207	0.169	7977	116.8	263.0
500	231	0.170	7980	116.8	263.1
1000	239	0.170	8015	117.5	264.6
no cutoff	355	0.170	8069	118.5	266.9

500 a.u. cutoff for virtual orbitals and using all virtual orbitals in correlation calculation are 1.7 GV/cm and 3.8 kHz for $E_{\rm eff}$ and $W_{\rm s}$, respectively. Therefore, if we use 500 a.u. as cutoff for the virtual orbitals, then the associated errors in both $E_{\rm eff}$ and $W_{\rm s}$ values are about 1.4%. The effect of higher order correlation terms can be estimated by comparing our CCSD results with CCSD with partial triples (CCSD(T)) or with full configuration interaction (FCI) calculations. These types of calculations are very expensive and beyond the scope of the present study. However, from our experience we can comment that the error associated with this effect will be within 3.5%. Although these three effects are intertwined in nature, assuming linearity, we estimate our results are correct within 5% uncertainty. It is worth to mention that our results are free from the error associated with the effect of core polarization since all the electrons are correlated in our calculation. From Table 6.1, 6.2 and 6.3, we can see that the HFS constants, $E_{\rm eff}$ and $W_{\rm s}$ values are following the same trend and thus, we can comment that the calculated $E_{\rm eff}$ and $W_{\rm s}$ values are very accurate.

The above results suggest that HgH can be a potential candidate for the future eEDM experiment. However, there are other factors that need to be considered for an eEDM experiment. The ground state of HgH is a $^2\Sigma$ state. It has no orbital angular momentum contribution to the magnetic moment and thus it cannot cancels the unpaired electron's spin angular momentum contribution to the magnetic moment unlike PbF and ThO. For this reason the $^2\Sigma$ state of HgH has a higher g-factor compared to $^2\Pi_{1/2}$ state of PbF [24] or $^3\Delta_1$ state of ThO [25, 26]. Thus, it can give a significant magnetic noise in the spectroscopic eEDM experiment. Being a $^2\Sigma$ state, there are no Ω-doublets [27] available for the ground state of HgH which can be used as a comagnetometer

state [26, 28, 29] that can suppress some systematic errors though it is possible to find the sets of "internal comagnetometer" states with the proper combinations of different rotational states [30]. Even though HgH has a high $E_{\rm eff}$, one needs to fully polarize the molecule in an external laboratory electric field for the maximal utilization of $E_{\rm eff}$. But the large rotational constant [31] and small molecular dipole moment [23] of HgH suggest that enormous amount of external electric field is required to fully polarize the HgH molecule. On the contrary, as suggested by Kozlov *et al* [15], HgH can be polarized easily in the matrix isolated solid state non-spectroscopic experiment. They also argued that in this method, it is possible to improve the eEDM limit by 2-3 orders higher than the current limit. Therefore, considering these facts, we can comment that HgH can be a potential candidate for eEDM experiment and the solid state non-spectroscopic experimental technique would be best suitable for it.

6.4 Conclusion

In summary, we have performed the precise calculation of $E_{\rm eff}$ and $W_{\rm s}$ of HgH molecule in its open-shell ground state using the most reliable Z-vector method in the relativistic coupled-cluster framework. The outcome of our study reveals that HgH has one of the highest $E_{\rm eff}$ and $W_{\rm s}$ known for the polar diatomic molecule. On the other hand, HgH can be polarized easily using a solid state non-spectroscopic technique. Thus, the combination makes HgH a very important candidate for the next generation eEDM experiment.

References

[1] J. Ginges and V. Flambaum, Physics Reports **397**, 63 (2004).

[2] W. Bernreuther and M. Suzuki, Rev. Mod. Phys. **63**, 313 (1991).

[3] E. D. Commins, Advances In Atomic, Molecular, and Optical Physics **40**, 1 (1999).

[4] J. Baron *et al.*, Science **343**, 269 (2014).

[5] O. Sushkov and V. Flambaum, Journal of Experimental and Theoretical Physics **48**, 608 (1978).

[6] V. V. Flambaum, Sov. J. Nucl. Phys. **24**, 199 (1976).

[7] The EDM of a polar diatomics due to the different number of proton in two nucleus and uneven distribution of electron density is not really be called as permanent molecular EDM. This is because the Stark shift induced by

this EDM in an external laboratory field does not increase linearly rather quadratically with the electric field in the weak field limit. Thus strictly speaking, a polar diatomic molecule cannot have a permanent molecular EDM unless there is a violation of both P and T. [8].

[8] L. R. Hunter, Science **252**, 73 (1991).

[9] L. Skripnikov, A. Petrov, and A. Titov, Journal of Chemical Physics **139**, 221103 (2013).

[10] L. Skripnikov and A. Titov, Journal of Chemical Physics **142**, 024301 (2015).

[11] V. A. Dzuba, V. V. Flambaum, and C. Harabati, Phys. Rev. A **84**, 052108 (2011).

[12] E. A. Salter, G. W. Trucks, and R. J. Bartlett, Journal of Chemical Physics **90**, 1752 (1989).

[13] S. Sasmal, H. Pathak, M. K. Nayak, N. Vaval, and S. Pal, Phys. Rev. A **91**, 030503 (2015).

[14] S. Sasmal, H. Pathak, M. K. Nayak, N. Vaval, and S. Pal, Journal of Chemical Physics **143**, 084119 (2015).

[15] M. G. Kozlov and A. Derevianko, Phys. Rev. Lett. **97**, 063001 (2006).

[16] DIRAC, a relativistic ab initio electronic structure program, Release DIRAC10 (2010), written by T. Saue, L. Visscher and H. J. Aa. Jensen, with contributions from R. Bast, K. G. Dyall, U. Ekström, E. Eliav, T. Enevoldsen, T. Fleig, A. S. P. Gomes, J. Henriksson, M. Iliaš, Ch. R. Jacob, S. Knecht, H. S. Nataraj, P. Norman, J. Olsen, M. Pernpointner, K. Ruud, B. Schimmelpfennig, J. Sikkema, A. Thorvaldsen, J. Thyssen, S. Villaume, and S. Yamamoto (see http://www.diracprogram.org).

[17] K. Faegri Jr and K. G. Dyall, *Introduction to relativistic quantum chemistry* (Oxford University Press, USA, 2007).

[18] L. Visscher and K. Dyall, Atomic Data and Nuclear Data Tables **67**, 207 (1997).

[19] K. G. Dyall, Theoretical Chemistry Accounts **112**, 403 (2004).

[20] T. H. Dunning, Journal of Chemical Physics **90**, 1007 (1989).

[21] K. Huber and G. Herzberg, *Constants of Diatomic Molecules, Vol. 4, Molecular Spectra and Molecular Structure* (Van Nostrand Reinhold, New York, 1979).

[22] A. C. Stowe and L. B. Knight Jr, Molecular Physics **100**, 353 (2002).

[23] O. Nedelec, B. Majournat, and J. Dufayard, Chemical Physics **134**, 137 (1989).

[24] L. V. Skripnikov *et al.*, Phys. Rev. A **92**, 032508 (2015).

[25] A. C. Vutha *et al.*, Journal of Physics B: Atomic, Molecular and Optical Physics **43**, 074007 (2010).

[26] A. Petrov *et al.*, Physical Review A **89**, 062505 (2014).

[27] G. Herzberg, *Molecular Spectra and Molecular Structure, Vol. 1, Spectra of Diatomic Molecules* (Van Nostrand Reinhold, New York, 1950).

[28] The comagnetometer state [26, 29] means two states that have comparable magnetic moment but opposite polarizibility. In spectroscopic eEDM experiment, the existance of a comagnetometer state is very important because it allows one to reverse the E_{eff} spectroscopically (i.e., by populating the molecules in different comagnetometer state), without reversing the external laboratory electric field, which is used to polarize the molecule.

[29] D. DeMille *et al.*, Physical Review A **61**, 052507 (2000).

[30] V. S. Prasannaa, A. C. Vutha, M. Abe, and B. P. Das, Phys. Rev. Lett. **114**, 183001 (2015).

[31] L. Veseth, Journal of Molecular Spectroscopy **44**, 251 (1972).

CHAPTER 7

Summary and Future Scope of the Thesis

> Reasoning draws a conclusion, but does not make the conclusion certain, unless the mind discovers it by the path of experience.
>
> Roger Bacon

7.1 Summary

The main aim of this thesis was to develop an *ab initio* method that can generate precise wavefunction in the nuclear region of the heavy nucleus of the atomic and molecular systems and to apply the method to obtain various parity ($\mathcal{P}$) and time reversal ($\mathcal{T}$) violating interaction constants of relevant systems. These $\mathcal{P},\mathcal{T}$-odd interaction constants are very important quantities in the electron's electric dipole moment (eEDM) experiment, which has the potential to solve some well known mysteries of physics. The simultaneous inclusion of relativistic and electron correlation effects is the key for the precise calculation of these properties. The Dirac-Hartree-Fock (DHF) method in the four-component formalism is used to include the effect of special relativity where the Coulomb approximation is used to treat the electron-electron interaction term in the Hamiltonian.

At the first attempt of correlation treatment, we have implemented the extended coupled-cluster (ECC) method, where the coupled-cluster equation is solved in a variational way. The implemented method is applied to calculate the magnetic hyperfine structure (HFS) constant of some atoms and

diatomic molecules. Although we have achieved good results, the generated wavefunction in the nuclear region is not good enough for the $\mathcal{P},\mathcal{T}$-odd properties. Computationally, the ECC is a very expensive method and thus, the calculation of $\mathcal{P},\mathcal{T}$-odd interaction constants of the relevant heavy diatomic molecules in a reasonable basis is almost impossible.

Next, we have solved the CC more traditionally, i.e., non-variationally. The property values have been obtained using the Z-vector method. The implemented Z-vector method in the CC framework is applied to calculate the dipole moment and the parallel component of magnetic HFS constant of SrF. The results show that the Z-vector method can generate very good wavefunction not only in the nuclear region but in the outer region also. We have also compared the Z-vector and the ECC results of the magnetic HFS constant of alkali metal atoms and mono-positive alkaline earth metal atoms, and the comparison shows that the Z-vector method can produce far better results than the ECC method. And computationally, the Z-vector method is more feasible than the ECC method.

Next, we have applied the Z-vector method in the CC framework to calculate the effective electric field ($E_{\rm eff}$) experienced by the unpaired electron and the electron-nucleus scalar-pseudoscalar (S-PS) interaction constant ($W_{\rm s}$) of RaF, PbF and HgH. We have showed that the core polarization can play a vital role for the calculation of these types "atom in compound" (AIC) properties and thus it is desirable to treat all the electrons explicitly in the correlation calculation. The most reliable value of $E_{\rm eff}$ of RaF, PbF and HgH are 52.5, 38.1 and 123.2 GV/cm, respectively. The most reliable value of $W_{\rm s}$ of RaF and HgH are 141.2 and 284.2 kHz, respectively. The ratio of $E_{\rm eff}$ to $W_{\rm s}$ and the interrelation between the value of eEDM (d_e) and the $\mathcal{P},\mathcal{T}$-odd S-PS constant (k_s) are obtained in the respective chapters as these are important to set independent limit on d_e and k_s.

In conclusion, the thesis identifies three important players for the next generation eEDM experiment and provides the most reliable values of $E_{\rm eff}$ and $W_{\rm s}$ of these systems which cannot be obtained experimentally.

7.2 Further scope

We have found an unusual behavior in the TlH^+ system. Previously, we have found that the $E_{\rm eff}$ and $W_{\rm s}$ of HgH are very high. Although TlH^+ is an iso-electronic to HgH, the $E_{\rm eff}$ and $W_{\rm s}$ of TlH^+ are surprisingly low (more than 20 times lower). So, we want to understand why these are so low for the TlH^+ system.

So far, we have calculated the $E_{\rm eff}$ and $W_{\rm s}$ of various systems in their ground electronic state. Next, we want to calculate the properties of the excited state as there are very promising candidate like ThO, ThF^+, HfH^+, PtH^+, WC, etc., which offers very high eEDM effects in their metastable excited ($^3\Delta$) state.

Appendices

APPENDIX A

Algebraic expression of ECC energy and cluster amplitude equation

The zeroth order ECC energy functional within the approximation stated in the thesis is

$$\begin{aligned} E^{(0)} =&\langle\Phi_0|\Big[vt_2^{(0)} + s_2^{(0)}v + s_1^{(0)}ft_1^{(0)} + s_2^{(0)}ft_2^{(0)} + s_1^{(0)}vt_1^{(0)} + s_2^{(0)}vt_2^{(0)} + s_2^{(0)}vt_1^{(0)} \\ &+ s_1^{(0)}vt_2^{(0)} + \frac{1}{2!}vt_1^{(0)}t_1^{(0)} + \frac{1}{2!}s_1^{(0)}s_1^{(0)}v + \frac{1}{2!}s_1^{(0)}vt_1^{(0)}t_1^{(0)} + \frac{1}{2!}s_1^{(0)}s_1^{(0)}vt_1^{(0)} \\ &+ s_1^{(0)}vt_1^{(0)}t_2^{(0)} + s_2^{(0)}vt_1^{(0)}t_2^{(0)} + \frac{1}{2!}s_2^{(0)}vt_2^{(0)}t_2^{(0)} + s_1^{(0)}s_2^{(0)}vt_2^{(0)} + \frac{1}{3!}s_2^{(0)}v(t_1^{(0)})^3 \\ &+ \frac{1}{2!}s_2^{(0)}vt_2^{(0)}(t_1^{(0)})^2 + \frac{1}{4!}s_2^{(0)}v(t_1^{(0)})^4 + \frac{1}{3!}(s_1^{(0)})^3vt_2^{(0)} + ft_1^{(0)} + s_1^{(0)}f \\ &+ \frac{1}{2!}s_1^{(0)}f(t_1^{(0)})^2 + s_2^{(0)}ft_1^{(0)}t_2^{(0)} + \frac{1}{3!}s_1^{(0)}v(t_1^{(0)})^3\Big]|\Phi_0\rangle. \end{aligned} \tag{A.1}$$

Equation for $s_1^{(0)}[\delta E^{(0)}/\delta t_1^{(0)} = 0]$ is given by

$$\begin{aligned} \langle\Phi_0|\Big[&vt_1^{(0)} + s_1^{(0)}(f+v) + s_2^{(0)}v + s_1^{(0)}vt_1^{(0)} + s_1^{(0)}vt_2^{(0)} + s_2^{(0)}vt_1^{(0)} + s_2^{(0)}vt_2^{(0)} \\ &+ \frac{1}{2!}s_1^{(0)}s_1^{(0)}v + s_2^{(0)}vt_2^{(0)}t_1^{(0)} + \frac{1}{2!}s_2^{(0)}vt_1^{(0)}t_1^{(0)} + \frac{1}{3!}s_2^{(0)}v(t_1^{(0)})^3 + f \\ &+ s_1^{(0)}ft_1^{(0)} + s_2^{(0)}ft_2^{(0)} + \frac{1}{2!}s_1^{(0)}vt_1^{(0)}t_1^{(0)}\Big]|\Phi_i^a\rangle = 0. \end{aligned} \tag{A.2}$$

Equation for $s_2^{(0)}[\delta E^{(0)}/\delta t_2^{(0)} = 0]$ is given by

$$\begin{aligned} \langle\Phi_0|\Big[&v + s_1^{(0)}v + s_2^{(0)}(f+v) + \frac{1}{2!}s_1^{(0)}s_1^{(0)}v + s_1^{(0)}s_2^{(0)}v + s_1^{(0)}vt_1^{(0)} + s_2^{(0)}vt_1^{(0)} \\ &+ s_2^{(0)}vt_2^{(0)} + \frac{1}{2!}s_2^{(0)}vt_1^{(0)}t_1^{(0)} + \frac{1}{3!}(s_1^{(0)})^3v + s_2^{(0)}ft_1^{(0)}\Big]|\Phi_{ij}^{ab}\rangle = 0. \end{aligned} \tag{A.3}$$

Equation for $t_1^{(0)}[\delta E^{(0)}/\delta s_1^{(0)} = 0]$ is given by

$$\begin{aligned}\langle\Phi_i^a|\Big[(f+v)t_1^{(0)} + vt_2^{(0)} + \frac{1}{2!}vt_1^{(0)}t_1^{(0)} + vt_1^{(0)}t_2^{(0)} + s_1^{(0)}v + s_1^{(0)}vt_1^{(0)} + s_1^{(0)}vt_2^{(0)} \\ + s_2^{(0)}vt_2^{(0)} + s_1^{(0)}s_1^{(0)}vt_2^{(0)} + f + \frac{1}{2!}ft_1^{(0)}t_1^{(0)} + \frac{1}{3!}v(t_1^{(0)})^3\Big]|\Phi_0\rangle = 0.\end{aligned} \tag{A.4}$$

Equation for $t_2^{(0)}[\delta E^{(0)}/\delta s_2^{(0)} = 0]$ is given by

$$\begin{aligned}\langle\Phi_{ij}^{ab}|\Big[v + vt_1^{(0)} + (f+v)t_2^{(0)} + \frac{1}{2!}vt_1^{(0)}t_1^{(0)} + vt_1^{(0)}t_2^{(0)} + \frac{1}{2!}vt_2^{(0)}t_2^{(0)} + \frac{1}{2!}vt_2^{(0)}t_1^{(0)}t_1^{(0)} \\ + \frac{1}{3!}v(t_1^{(0)})^3 + \frac{1}{4!}v(t_1^{(0)})^4 + ft_1^{(0)}t_2^{(0)} + s_1^{(0)}vt_2^{(0)}\Big]|\Phi_0\rangle = 0.\end{aligned} \tag{A.5}$$

Equation for $E^{(1)}$ is given by

$$E^{(1)} = \langle\Phi_0|\Big[Ot_1^{(0)} + s_1^{(0)}O + s_1^{(0)}Ot_1^{(0)} + s_2^{(0)}Ot_2^{(0)} + \frac{1}{2!}s_1^{(0)}Ot_1^{(0)}t_1^{(0)} + s_2^{(0)}Ot_1^{(0)}t_2^{(0)}\Big]|\Phi_0\rangle. \tag{A.6}$$

APPENDIX B

Diagrammatic of amplitude equation and energy derivative of ECC

In Figure B.1, Figure B.2, Figure B.3 and Figure B.4, we present all the necessary diagrams required to construct the equations for s_1, s_2, t_1 and t_2 amplitudes respectively. The diagrams required for first order energy derivative ($E^{(1)}$) are given in Figure B.5.

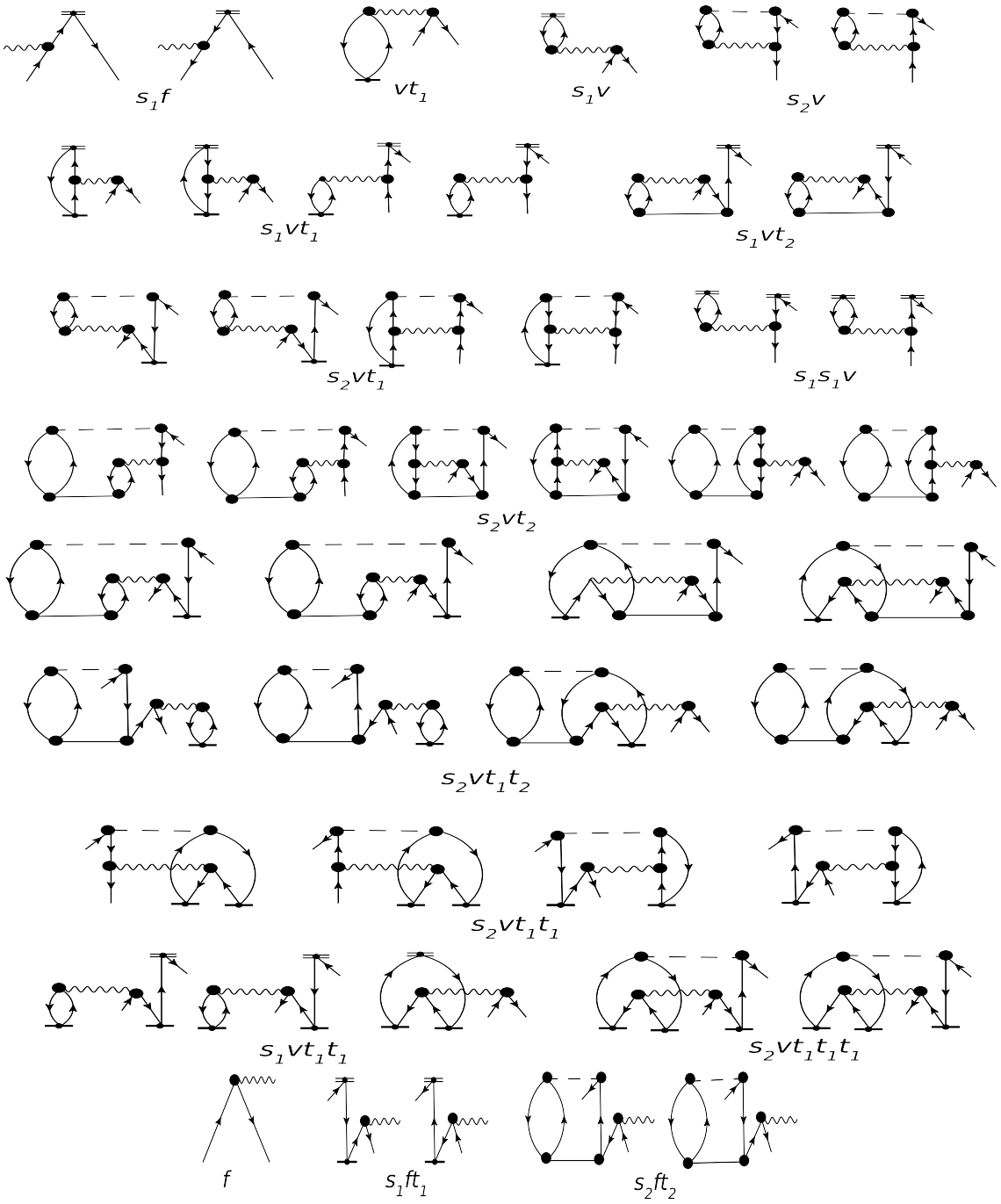

Figure B.1: Diagrams for s_1 amplitude

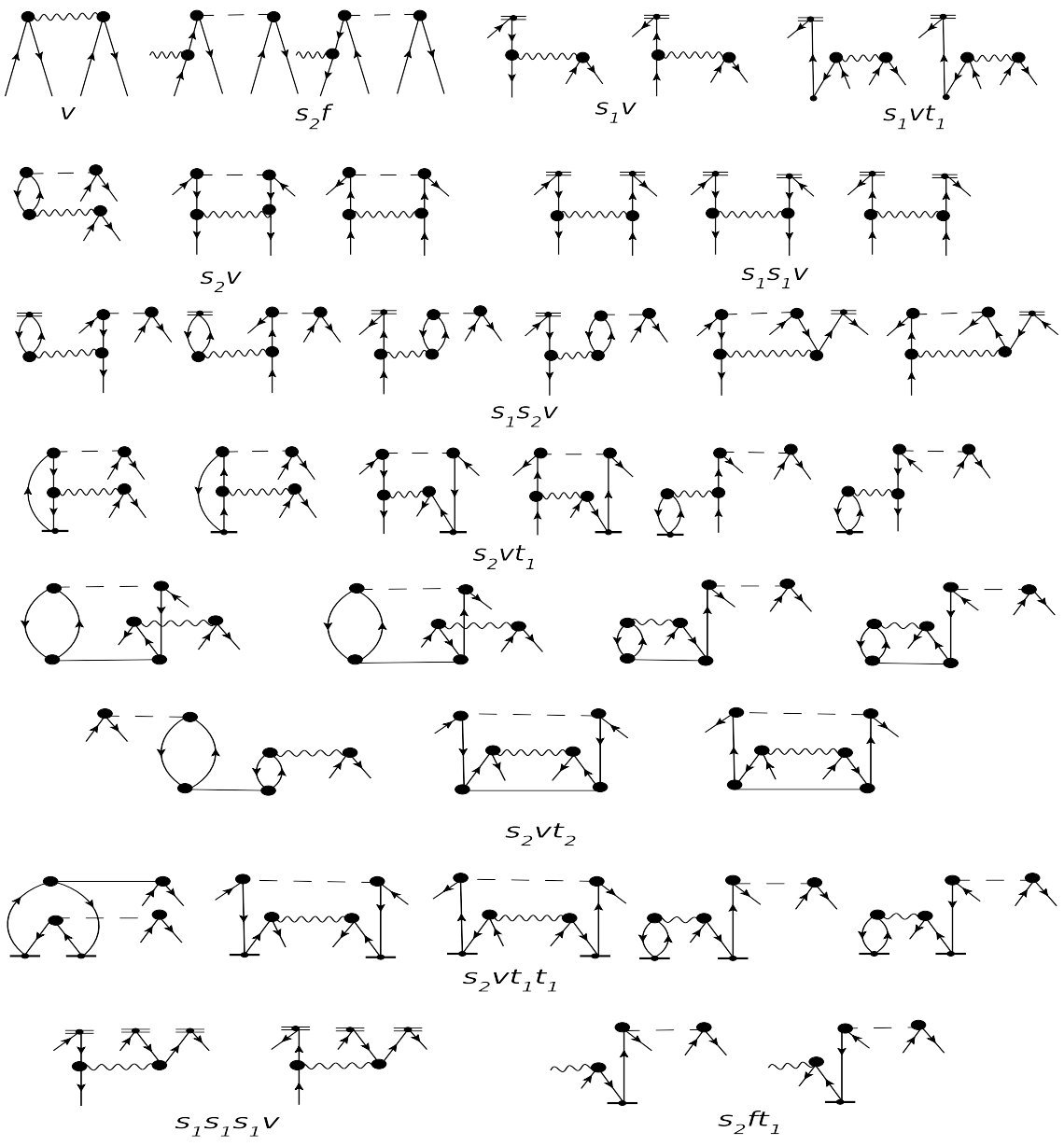

Figure B.2: Diagrams for s_2 amplitude

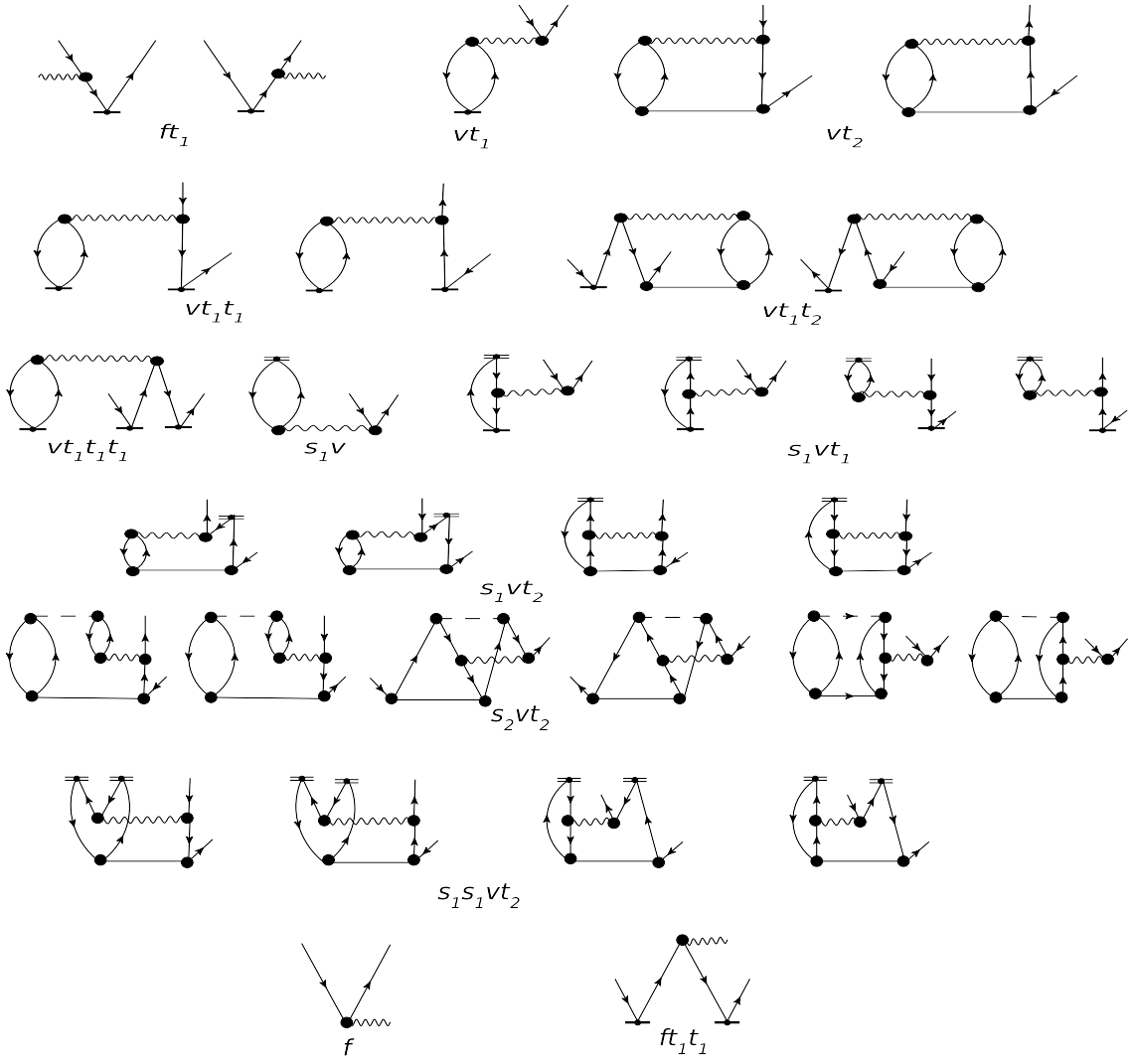

Figure B.3: Diagrams for t_1 amplitude

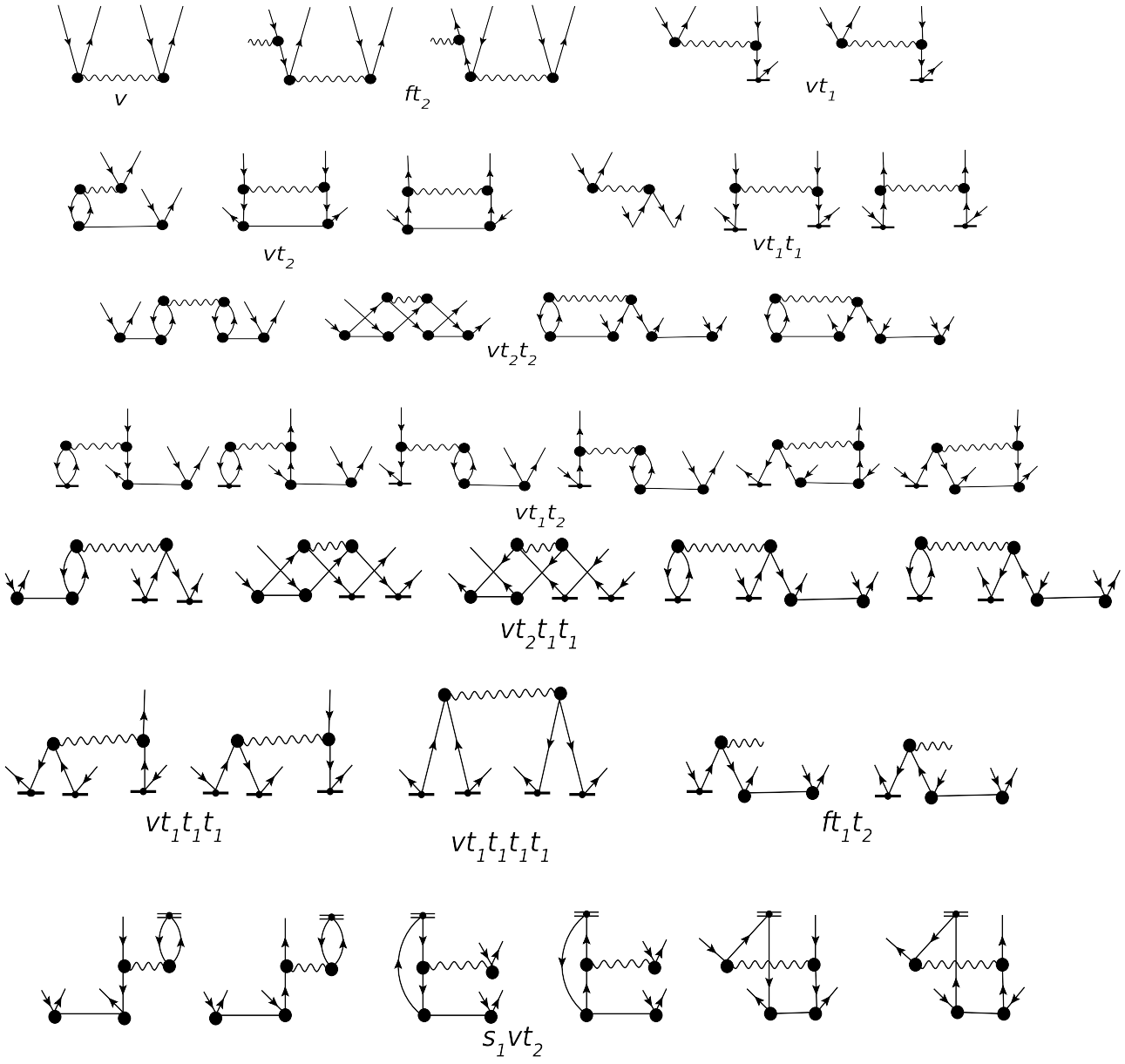

Figure B.4: Diagrams for t_2 amplitude

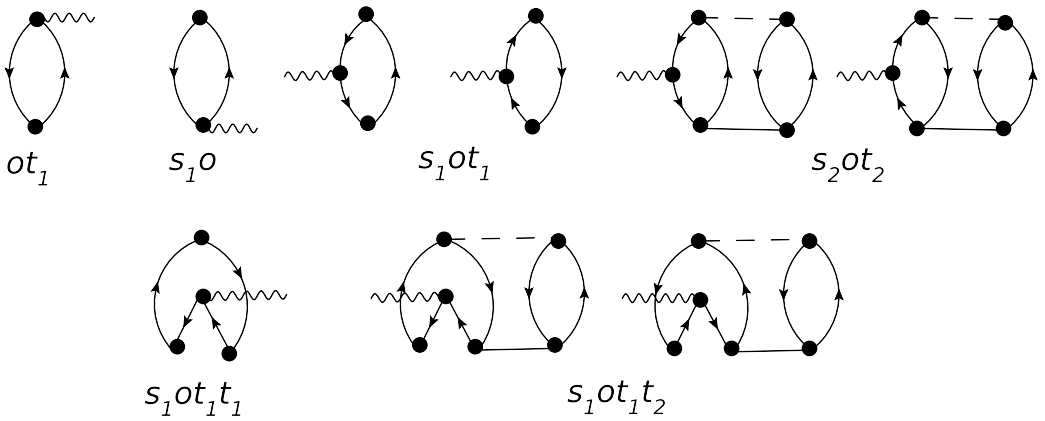

Figure B.5: Diagrams for first order energy derivative ($E^{(1)}$)